

---

Doctoral Dissertations

Student Theses and Dissertations

---

Summer 2024

# Integrated Study of Heat Transfer and Local Gas Dynamics in a Pebble Bed Very High Temperature Nuclear Reactor using Advance Measurement Techniques

Muhna N. Alshammari

*Missouri University of Science and Technology*

Follow this and additional works at: [https://scholarsmine.mst.edu/doctoral\\_dissertations](https://scholarsmine.mst.edu/doctoral_dissertations)



Part of the [Nuclear Engineering Commons](#)

Department: Nuclear Engineering and Radiation Science

---

## Recommended Citation

Alshammari, Muhna N., "Integrated Study of Heat Transfer and Local Gas Dynamics in a Pebble Bed Very High Temperature Nuclear Reactor using Advance Measurement Techniques" (2024). *Doctoral Dissertations*. 3311.

[https://scholarsmine.mst.edu/doctoral\\_dissertations/3311](https://scholarsmine.mst.edu/doctoral_dissertations/3311)

This thesis is brought to you by Scholars' Mine, a service of the Missouri S&T Library and Learning Resources. This work is protected by U. S. Copyright Law. Unauthorized use including reproduction for redistribution requires the permission of the copyright holder. For more information, please contact [scholarsmine@mst.edu](mailto:scholarsmine@mst.edu).

INTEGRATED STUDY OF HEAT TRANSFER AND LOCAL GAS DYNAMICS IN A  
PEBBLE BED VERY HIGH TEMPERATURE NUCLEAR REACTOR USING  
ADVANCE MEASUREMENT TECHNIQUES

by

MUHNA NAZAL ALSHAMMARI

A DISSERTATION

Presented to the Faculty of the Graduate School of the  
MISSOURI UNIVERSITY OF SCIENCE AND TECHNOLOGY

In Partial Fulfillment of the Requirements for the Degree

DOCTOR OF PHILOSOPHY

in

NUCLEAR ENGINEERING

2023

Approved by:

Muthanna. H AI-Dahhan, Advisor  
Shoaib Usman,  
Carlos H. Castano  
Ayodeji B. Alajo  
Kelly Homan

© 2023

Muhna N Alshammari

All Rights Reserved

### **PUBLICATION DISSERTATION OPTION**

This dissertation has been prepared in the form of three papers for publication as follows:

Paper I: Pages 11-55 intended for submission

Paper II: Pages 56-102 intended for submission.

Paper III: Pages 103-154 intended for submission.

## ABSTRACT

The aim of this study, pebbles of diameter of 5 *cm* and a pebble-to-diameter ratio (aspect ratio) of 6 were used. In part I, the local gas velocities were studied at different radial and axial locations in the pebble bed using a sophisticated hot wire anemometry (HWA) technique, which was supported with a novel probe-protector case to protect the fragile probe, allowing the measurements to be taken between the pebbles for the first time. The local gas velocities were found to be significantly higher in the near wall region due to the higher void fractions in the near-wall region, compared to the center. In the part II, the local convective heat transfer coefficients were studied using a cartridge heated probe pebble, a microfoil heat flux sensor and a thermocouple at various radial locations, axial locations, and angular orientations and under different superficial inlet gas velocities that correspond to both laminar and turbulent flow conditions. The obtained results showed that the local heat transfer coefficients are higher in the near-wall region compared to the center of the bed, which is the same pattern as that observed for the local gas velocities. In part III, new heat transfer coefficients measurements were conducted by changing the orientation of the probe pebble and the location of the thermocouple, accordingly. This allowed us to confirm the reproducibility of the local heat transfer measurements using our measurement technique as well as to confirm the patterns of the variation of the local heat transfer coefficients along the diameter of the pebble bed. Data from all the parts of this study were compared with correlations from the literature and new correlations were developed for the predictions of the local gas velocity and local heat transfer coefficients within the experimental range of our study.

## ACKNOWLEDGMENTS

First and foremost, I sincerely thank and praise the almighty Allah. The completion of my dissertation would not have been possible without His guidance and blessings. Furthermore, I would like to express my sincere gratitude to my advisor Dr. Muthanna Al-Dahhan for his continuous support and the motivation he gave me during my years of Ph.D. I am deeply grateful for the great knowledge that I gained from him. I would like to extend my gratitude to the Nuclear Engineering department at Missouri S&T. In addition, I would like to extend special thanks to my country Kingdom of Saudi Arabia, and my employer KACST for the scholarship to complete my higher education and cover all my study expenses.

My genuine thanks and prayers to my father, who unfortunately passed away before seeing my graduation, for his unlimited confidence and support when I decided to pursue my higher education.

Likewise, I want to express my limitless appreciation, love, and gratitude to my family, especially my wonderful mom, my wife, and my kids (Abdulkarim, Ritaj, Sana, Anas, Leen, and Faiz), for everything they did to help me until I reached this stage. Moreover, I appreciate my friends' help and support during this journey to overcome all stress. Finally, I would like to thank the beautiful people at Rolla city for creating a friendly environment around my family and me during our years there.

## TABLE OF CONTENTS

	Page
PUBLICATION DISSERTATION OPTION .....	iii
ABSTRACT.....	iv
ACKNOWLEDGMENTS .....	v
LIST OF ILLUSTRATIONS.....	x
LIST OF TABLES.....	xv
 SECTION	
1. INTRODUCTION .....	1
1.1. OVERVIEW .....	1
1.2. PEBBLE BED REACTOR (PBR).....	4
1.3. THE EFFICIENCY OF PBR.....	7
1.4. PBR ADVANTAGES AND DISADVANTAGES .....	8
2. SCOPE AND OBJECTIVES .....	9
 PAPER	
I. EXPERIMENTAL INVESTIGATION OF THE VARIATION OF THE LOCAL GAS VELOCITIES IN A COLD FLOW PEBBLE BED REACTOR (PBR) USING A HOT WIRE ANEMOMETRY TECHNIQUE .....	11
ABSTRACT.....	11
1. INTRODUCTION .....	12
2. MEASUREMENT TECHNIQUE .....	18
2.1. HOT WIRE ANEMOMETRY (HWA) FOR GAS VELOCITY MEASUREMENT.....	18

2.2. A NEW PROBE-PROTECTOR OF HWA FOR IMPLEMENTING IN THE COLD FLOW PEBBLE BED REACTOR .....	24
3. EXPERIMENTAL SETUP .....	28
4. EXPERIMENTAL PROCEDURE .....	32
5. RESULTS AND DISCUSSION .....	33
5.1. RADIAL PROFILES OF THE GAS VELOCITY .....	33
5.2. CORRELATION DEVELOPMENT FOR THE LOCAL GAS VELOCITY USING POLYNOMIAL REGRESSION.....	39
5.2.1. Validation of the Second Order Polynomial Regression Correlation .....	41
5.2.2. Test of Significance of the Input Features in the Correlation .....	45
6. CONCLUSION .....	47
NOMENCLATURE.....	49
REFERENCES.....	50
II. INVESTIGATION OF CONVECTIVE HEAT TRANSFER IN A COLD FLOW PEBBLE BED NUCLEAR REACTOR .....	56
ABSTRACT .....	56
1. INTRODUCTION .....	57
2. EXPERIMENTAL WORK.....	65
2.1. EXPERIMENTAL SETUP.....	65
2.2. HEAT TRANSFER COEFFICIENT MEASUREMENT TECHNIQUE .....	67
2.3. EXPERIMENTAL CONDITIONS .....	68
3. DATA COLLECTION AND ANALYSIS .....	70
4. RESULT AND DISCUSSION .....	73



5. COMPARISON WITH CORRELATIONS REPORTED IN THE LITERATURE .....	88
6. NEW CORRELATION DEVELOPMENT .....	93
7. CONCLUDING REMARKS .....	96
NOMENCLATURE.....	98
REFERENCES.....	99
III. EXPERIMENTAL INVESTIGATION OF THE CONVECTIVE HEAT TRANSFER COEFFICIENT AT DIFFERENT ANGULAR ORIENTATIONS INSIDE THE VOID IN A COLD FLOW PEBBLE BED REACTOR USING A NON-INVASIVE PEBBLE PROBE.....	103
ABSTRACT.....	103
1. INTRODUCTION.....	104
2. EXPERIMENTAL SETUP .....	110
3. MEASUREMENT TECHNIQUES .....	113
3.1. NONINVASIVE HEAT TRANSFER PROBE PEBBLE WITH MICRO-FOIL SENSOR AND A THERMOCOUPLE .....	113
3.2. DATA ACQUISITION .....	115
4. EXPERIMENTAL PROCEDURES .....	118
5. RESULTS AND DISCUSSION. ....	122
5.1. EFFECT OF THE GAS FLOW AND LOCATION INSIDE THE PBR'S CORE ON THE HEAT TRANSFER .....	122
5.2. COMPARISON OF THE OVERALL HEAT TRANSFER INSIDE THE PBR WITH THE EMPIRICAL CORRELATIONS AVAILABLE IN THE LITERATURE. ....	135
5.3. MODELING OF THE LOCAL HEAT TRANSFER COEFFICIENT IN A PBR.....	139
6. CONCLUSION .....	147

NOMENCLATURE.....	148
REFERENCES.....	150
SECTION	
3.CONCLUSIONS.....	155
BIBLIOGRAPHY.....	157
VITA.....	159

## LIST OF ILLUSTRATIONS

SECTION	Page
Figure 1.1. Share of electricity generation from power technology. ....	2
Figure 1.2. Schematic diagram of the pebble-bed nuclear reactor . ....	6
Figure 1.3. TRISO fuel in pebble bed reactor.....	7
 PAPER I	
Figure 1. Comparison between PIV, LDA, and HWA output signals . ....	19
Figure 2. Hot wire anemometer components . ....	20
Figure 3. HWA data acquisition system .....	23
Figure 4. HWA predetermined pebble arrangement probe-protector case design components .....	27
Figure 5. Assembly of the designed probe-protector case.....	28
Figure 6. Experimental setup for the PBR.....	30
Figure 7. Schematic illustration showing a)- axial levels ( $H/D = 0.72$ , $H/D = 1.48$ , $H/D = 2.88$ ) and b)- radial positions where the measurements were taken.....	31
Figure 8. Local radial velocity profiles at different Reynolds number (993.78 to 7950.24) at three axial locations in the column.....	37
Figure 9. The variation of the local gas velocity based on Reynolds number in the center of the test column ( $r/R = 0$ ) and the in the near-wall region ( $r/R = 0.9$ ) at three axial locations.....	38
Figure 10. Radial profiles of the local gas velocity at the top ( $H/D = 0.72$ ), middle ( $H/D = 1.48$ ) and bottom ( $H/D = 2.88$ ) of the column under four superficial inlet gas velocities.....	39
Figure 11. Residuals by normal quantile plot. ....	43
Figure 12. Goodness of fit plot. ....	44

Figure 13. Contour plots showing the variation of the local gas velocity as a function of the radial and axial position in the experimental column at a)- $Re = 993.78$ , b)- $Re = 2318.82$ , and c)- $Re = 7950.24$ . .....	46
---	----

## PAPER II

Figure 1. Illustration of the heat transfer mechanisms inside the pebble bed reactor.....	64
Figure 2. (a) Schematic diagram of the cold flow pebble bed experimental setup, (b) plenum cone shape, (c) distributor plate, and (d) setup picture.....	66
Figure 3. Picture of the heat transfer pebble probe technique and schematic of the pebble probe. ....	68
Figure 4. (a) Schematic showing the three axial levels $H1\ HD = 0.72$ , $H2\ HD = 1.48$ , and $H3\ HD = 2.88$ , (b) Schematic of measurement locations at different radial and angular positions for each axial level. ....	70
Figure 5. Time series of the difference between the temperatures of the bulk and the surface of the copper pebble probe.....	72
Figure 6. The stability of the heat transfer coefficients as function of the sampling time.	73
Figure 7. Local heat transfer coefficients at the top axial level of the bed ( $H/D = 0.72$ ) at three different superficial inlet gas velocities .....	76
Figure 8. Local heat transfer coefficients in the middle axial level of the bed ( $H/D = 1.48$ ) at three different superficial inlet gas velocities.....	77
Figure 9. Local heat transfer coefficients at the bottom axial level of the bed ( $H/D = 2.88$ ) at three different superficial inlet gas velocities.....	78
Figure 10. Diameter profiles of the local heat transfer at a superficial inlet gas velocity of 0.3 m/s at three different axial levels. ....	79
Figure 11. Diameter profiles of the local heat transfer at a superficial inlet gas velocity of 1.2 m/s at three different axial levels. ....	80
Figure 12. Diameter profiles of the local heat transfer at a superficial inlet gas velocity of 2 m/s at three different axial levels .....	81

Figure 13. Diameter profiles of angularly averaged heat transfer coefficients for each radial location of Y, X, Z, and L diameter lines using various superficial inlet gas velocities from $U_g = 0.3$ m/s to $U_g = 2.0$ m/s at three axial positions.....	85
Figure 14. Diameter profiles of angularly averaged heat transfer coefficients for the three axial levels (Top ( $H/D = 0.72$ ), Middle ( $H/D = 1.48$ ), & Bottom ( $H/D = 2.88$ )) at the lowest and highest superficial inlet gas velocity .....	87
Figure 15. Comparison of the empirical correlations with the measured overall convective heat-transfer at the superficial inlet gas velocities studied (0.3 m/s to 2 m/s). .....	91
Figure 16. Goodness-of-fit plot of the Pseudo-3D model prediction against experimental data.....	95
 PAPER III	
Figure 1. Experimental setup.....	112
Figure 2. Micro-foil heat flux sensor. ....	114
Figure 3. Solid copper sphere with a micro-foil sensor and cartridge heater. ....	115
Figure 4. Cartridge heater. ....	115
Figure 5. Steady-state time series with different temperatures between the bulk temperature and the surface temperature. ....	117
Figure 6. The stability of heat transfer coefficients as a function of the sampling time. ....	118
Figure 7. Schematic illustration showing a) axial levels and, b) radial positions where the measurements were taken. ....	120
Figure 8. Schematic representation of the position of the three angular orientations of the copper probe pebble in the void. ....	121
Figure 9. The variation of heat transfer coefficient depending on the radial position and the velocity of the flowing gas when the thermocouple probe is placed at three different positions in the void, at the top level of the bed ( $H/D = 0.72$ ). ....	128

Figure 10. The variation of heat transfer coefficient depending on the radial position and the velocity of the flowing gas when the thermocouple probe is placed at three different positions in the void, at the middle level of the bed ( $H/D = 1.48$ ). .....	129
Figure 11. The variation of heat transfer coefficient depending on the radial position and the velocity of the flowing gas when the thermocouple probe is placed at three different positions in the void, at the lower level of the bed ( $H/D = 2.88$ ). .....	130
Figure 12. The variation of the local heat transfer coefficients as a function of the superficial inlet gas velocity at the three axial positions (Top ( $H/D = 0.72$ ), Middle ( $H/D = 1.48$ ), Bottom ( $H/D = 2.88$ )) in the center of the void at a)- $r/R = 0$ and b)- $r/R = 0.9$ .....	131
Figure 13. The variation of the heat transfer coefficients as a function of the superficial inlet gas velocity at the top axial level ( $H/D = 0.72$ ) of the column for three different angular orientation of the pebble in the void at a)- $r/R = 0$ and b)- $r/R = 0.9$ .....	131
Figure 14. The variation of the heat transfer coefficients as a function of the superficial inlet gas velocity at the middle axial level ( $H/D = 1.48$ ) of the column for three different angular orientation of the pebble in the void at a)- $r/R = 0$ and b)- $r/R = 0.9$ .....	132
Figure 15. The variation of the heat transfer coefficients as a function of the superficial inlet gas velocity at the bottom axial level ( $H/D = 2.88$ ) of the column for three different angular orientation of the pebble in the void at a)- $r/R = 0$ and b)- $r/R = 0.9$ .....	132
Figure 16. Comparison between the heat transfer coefficients in the center of the void and the average heat transfer coefficients in the void in the center ( $r/R = 0$ ) and the near-wall region ( $r/R = 0.9$ ) at a)- Top level ( $H/D = 0.72$ ), b)- Middle level ( $H/D = 1.48$ ), c)- Bottom level ( $H/D = 2.88$ ).....	133
Figure 17. Comparison between the heat transfer coefficients in the center of the void and the average heat transfer coefficients in the void in the center ( $r/R = 0$ ) and the near-wall region ( $r/R = 0.9$ ) at Top level ( $H/D = 0.72$ ), b)- Middle level ( $H/D = 1.48$ ), c)- Bottom level ( $H/D = 2.88$ ). .....	134
Figure 18. Comparison of the empirical correlations with the measured overall convective heat-transfer at the superficial inlet gas velocities studied (0.3 m/s to 2 m/s). .....	139
Figure 19. Goodness of fit plot. ....	143

Figure 20. Contour plots showing the variation of Nusselt's number ( $Nu$ ) as a function of the axial level ( $Z/H$ ) and the radial position ( $r/R$ ) at: a)-  $Re=993.78$  and b)-  $Re=6625.2$ . ..... 145

## LIST OF TABLES

SECTION	Page
Table 1.1. The Next Generation Nuclear Plant (NGNP) or called Generation IV Reactors .....	4
PAPER I	
Table 1. Advantages and disadvantages of various wire supports (prongs) fabrication materials. ....	21
Table 2. Input features and their range of variation.....	41
Table 3. The results of the validation tests of the polynomial model. ....	42
Table 4. The results of student's t-test. ....	47
PAPER III	
Table 1. Empirical correlations for the overall convective heat transfer coefficient.....	136
Table 2. Parameters and their experimental range.....	141
Table 3. The results of student's t-test. ....	144



# 1. INTRODUCTION

## 1.1. OVERVIEW

The significant growth of the world's population has led and continues to lead to a high increase in the energy demand worldwide. Therefore, providing a sufficient energy supply to respond to the increasing demand has become a challenge, especially with the environmental considerations and with the depletion of conventional sources of energy. For electricity generation for example, unclean conventional sources of energy such as coal, and fossil fuels, which emit global warming gases and pollute the environment, are still dominantly used because of their safety of operation and cost-efficiency. However, renewable energy such as wind and solar and geothermal energy is on the rise and becoming an important source of electricity. But, the current supply of renewable energy is still insufficient and not cost-efficient, as the plants take a lot of investment to build, while the conversion is not sufficient. Another source of clean energy is nuclear energy, which provides the advantageous of being eco-friendly as well as being cost-efficient. However, the main problem with nuclear energy is the safety of operation, as the failure of one of the reactors can result in severe consequences.

Figure 1.1, which was published by the international energy agency (IEA) elucidates the variation of the share of electricity produced by different sources of energy, which are coal, oil, natural gas, nuclear energy, and renewables, over the last 48 years (from 1971 to 2019). From Figure 1.1, it is clear that there is still reliance on coal for electricity productions, which takes a share of about 37 – 42%, while oil has almost no longer used for the generation of electricity. On the other hand, relatively clean sources,

such as natural gas, and clean energy sources such as renewables become an important source of electrical energy, with both being responsible in total for around 50% of the total share of electricity production. However, nuclear energy is only responsible for 10% of the total electricity production.

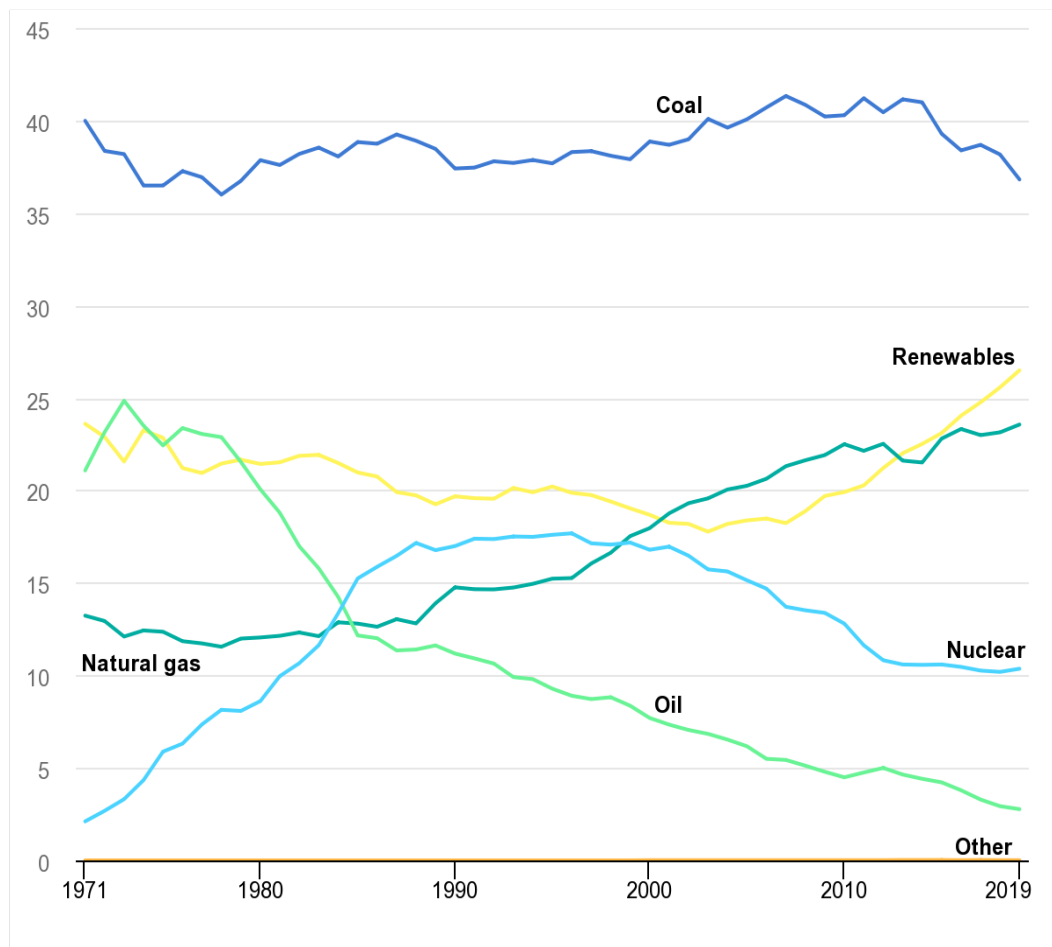


Figure 1.1. Share of electricity generation from power technology (The International Energy Agency (IEA)).

Despite many of the proposed solutions and initiatives to respond to the increasing energy demand and the to counter the pollution and emission of carbon, it is still a big

challenge that requires more research and investment. Most of the solutions to provide the energy for the next generations focus on two main important requirements:

- Clean energy.
- High-output energy with high thermal efficiency.

Nuclear energy one of the sources that can conform with the two conditions (clean and can produce a high megawatt of power which is good for industrial use too). Nuclear energy has been one of the most important energy sources in many countries over the last fifty years. Nuclear energy technology has passed through three generations so far, which saw major productivity developments and safety improvements (DoE 2002). In 2000, the office of nuclear energy under the U.S., Department of energy, met with senior governments from around nine countries to discuss the next nuclear reactors generation or generation four GIV.

The discussion took around a year of study and inspection from more than 100 scientists from different countries and they selected six reactors out of around 100 concepts to be the promise generation (The Generation IV International Forum (GIF), 2002). These selected fourth generation reactors are as follows:

- Very-high-temperature reactor (VHTR).
- Molten salt reactor (MSR).
- Gas-cooled fast reactor (GFR).
- Lead-cooled fast reactor (LFR)
- Supercritical-water-cooled reactor (SCWR).
- Sodium-cooled fast reactor (SFR).

Table 1.1 shows a summary of the general characteristics of the fourth-generation reactors. The VHTR will be described in the next Section 1.2, which will be focused on the pebble bed reactor (PBR), which is the system that will be studied in this work.

Table 1.1. The Next Generation Nuclear Plant (NGNP) or called Generation IV Reactors.

<b>Reactor Name</b>	<b>Neutron Spectrum Type</b>	<b>Coolant System</b>	<b>Temperature (C°)</b>	<b>(MWe)</b>	<b>Fuel Cycle</b>
VHTR	Thermal	Helium	900-1000	250-300	Open
MSR	Thermal/Fast	Fluoride Salts	700-800	1000	Closed
GFR	Fast	Helium	850	1200	Closed
LFR	Fast	Lead	480-570	20-180 300-1200 600-1000	Closed
SCWR	Thermal/Fast	Water	510-625	300-700 1000-1500	Closed/Open
SFR	Fast	Sodium	500-550	50-150 300-1500 600-1500	Closed

## 1.2. PEBBLE BED REACTOR (PBR)

The pebble-bed nuclear reactor (PBR) is one of two types of nuclear reactors which are called very-high temperature reactors (VHTR); the other is called the prismatic modeler reactor (Koster, Matzner, and Nicholsi 2003). This research is interested in the PBR type only. The pebble-bed nuclear reactor was created in Germany in the middle of the 20th century. Currently, South Africa's PBR is in the last phase of construction. Many features of these reactors motivated the investment in PBR in these countries, but the most important feature is the high temperature produced by the reactor, which can reach up to

1000° C. The very high temperatures generated are not only important for energy production but have become important in many fields such as industrial treatment, which has increased the importance of these reactors in the last decade. Due to the increasing importance of these reactors, they have attracted the attention of researchers and investors to studying and developing VHTRs. The name pebble bed reactor (PBR) comes from the type of fuel used in the reactor which consists of spherical fuel elements called pebbles. The PBR core is designed from steel and lined with bricks made of graphite to control the heat (Figure 1.2). The core of the reactor is packed with thousands (around 360,000 uranium-fueled pebbles (Kadak 2005)) of fuel and graphite spheres. The core is separated into two regions depending on the sphere types, where the center contains the graphite spheres and is surrounded by fuel spheres. The graphite spheres work as a moderator and help with the structure inside the core. Thousands of pebbles or fuel spheres with a diameter of 6cm are randomly packed inside the reactor.

A single sphere contains triple-coated isotropic or Tristructural-isotropic (TRISO) fuel particles. The TRISO name is derived from using three isotropic materials that are coating the fuel sphere in four layers. TRISO is in the center of the fuel kernel such as UOX, UC, or UCO, coated by a layer made of carbon followed by a dense layer of pyrolytic carbon (PyC) and then by a ceramic layer of SiC, which helps retaining the fission products during high temperatures. To create a strong structure, the last layer is dense PyC (Figure 1.3).

To transfer the heat from the reactor a gas (Helium) that does not react with the fuel pebbles is injected through the inlet of the reactor core at 500°-550°C and departs the

reactor at a temperature of around  $900^{\circ}\text{C}$ - $1000^{\circ}\text{C}$ . Helium was chosen because it is chemically and radiologically inert and because of its excellent ability to exchange heat.

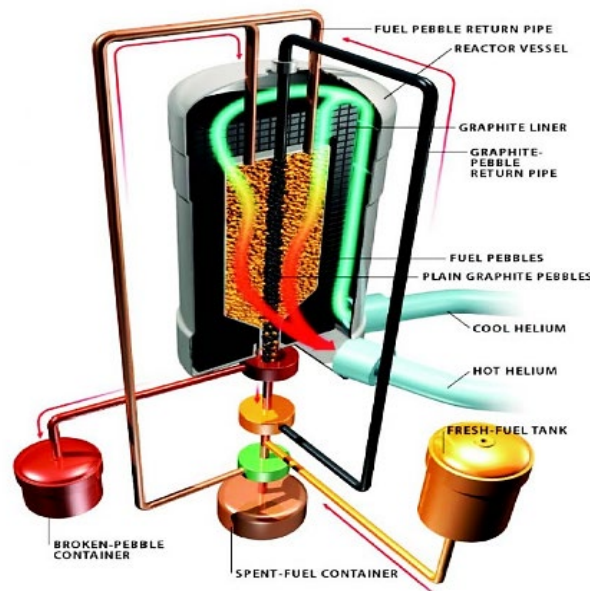


Figure 1.2. Schematic diagram of the pebble-bed nuclear reactor (Rycroft 2007).

To transfer the heat from the reactor a gas (Helium) that does not react with the fuel pebbles is injected through the inlet of the reactor core at  $500^{\circ}\text{C}$ - $550^{\circ}\text{C}$  and departs the reactor at a temperature of around  $900^{\circ}\text{C}$ - $1000^{\circ}\text{C}$ . Helium was chosen because it is chemically and radiologically inert and because of its excellent ability to exchange heat. The gas also acts as a coolant that lowers the temperature inside the core of the reactor (Huda and Obara 2008). Passive safety methods are used in this type of reactor to control the very high temperatures during the accident scenario. Passive safety is a feature included in the reactor design that works naturally (such as gravity) without any action required from an operator or auto electrical mechanism to lead the reactor to shut down safely during

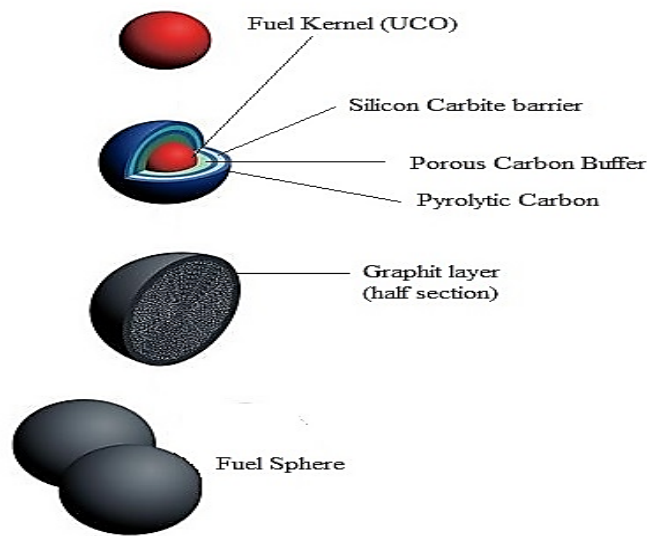


Figure 1.3. TRISO fuel in pebble bed reactor.

emergencies. The distribution of fuel pebbles inside the reactor core affects the gas fluid flow and the removal of heat from the reactor. Therefore, the helium is pumped from the top of the reactors and flows in a downward direction from the top to the bottom along the core of the PPBR, which helps to limit the reactor power density and stop the bed levitation problems (Claxton 1966).

### 1.3. THE EFFICIENCY OF PBR

To measure or evaluate the quality of any power source system, two important points are considered; the economic profit and the amount of energy produced. The feature of continuous refueling in pebble bed reactors distinguishes it from many other reactors. Other reactors require shutdown to refuel, which stops energy production and affects the total production per year and revenue. The second point to consider for evaluating a power system is the efficiency of the energy produced. The average reactor efficiency is between

30% to 35% with the remainder transferred as heat. The PBR production is preferable because it can reach up to 40% and 45% efficiency with the possibility to reach greater efficiency with advancing development.

#### **1.4. PBR ADVANTAGES AND DISADVANTAGES**

The PBR system like any system has advantages and disadvantages. The most prevalent advantages are as follows:

- Passive safety is one of the most important features of this system working during accident scenarios.
- The basic core design allows the use of different fuels without changing a structure.
- Refueling, fuel replacement, or checking the uranium can be done online without shutting down the reactor.
- PBR produces less contamination than the reactor using the liquid coolant.
- The very high temperature produced by the PBR is very useful for industrial requirements such as material treatment.

All the disadvantages of the PBR revolve around complexity, such as the complicated flow structure with the randomly packed pebbles, In addition to the challenges of increasing the safety of the reactor operation that produces high temperatures.



## 2. SCOPE AND OBJECTIVES

The objective of this dissertation is to investigate the variation of the gas dynamics and the local convective heat transfer coefficients inside the pebble bed core at various flow conditions, corresponding to laminar and turbulent flow conditions. This investigation will allow us to find and quantify the relation between the variation of the local gas velocity and the variations in the local heat transfer coefficients in the pebble bed, which are directly related to the bed structure and the void fractions in the bed. To achieve these objectives, the study was conducted in three parts:

- I. Measuring the local actual gas velocities at different radial locations in the pebble bed, from the center of the bed to the region near the wall ( $r/R=0, 0.33, 0.67, \text{ and } 0.9$ ) using a sophisticated hot wire anemometry (HWA) technique, with the incorporation of a probe protector case that protects the probe from contact with pebbles and which allows the measurement of the gas velocity in the center of the bed for the first time ever.
- II. Measuring the local convective heat transfer coefficients using an inhouse developed technique which consists of a microfilm heat flux sensor, a cartridge heated probe pebble, and a thermocouple that are moved around inside the pebble bed to obtain the heat transfer coefficients at various radial locations, axial locations, and angular orientations and under several superficial inlet gas velocities that correspond to both laminar and turbulent flow conditions.
- III. Measuring the local heat transfer coefficients at various locations in the void using the same technique with different angular orientation of the probe pebble along the height of the void, while the thermocouple is moved accordingly to

be facing the heat flux sensor. These measurements are taken at different radial and axial locations in the pebble bed and under different laminar and turbulent flow conditions.

## PAPER

### I. EXPERIMENTAL INVESTIGATION OF THE VARIATION OF THE LOCAL GAS VELOCITIES IN A COLD FLOW PEBBLE BED REACTOR (PBR) USING A HOT WIRE ANEMOMETRY TECHNIQUE

Muhna Alshammari [1,3], Ahmed Alalou [2,5], Hayder A. Alhameedi [2], Muthanna H  
Al-Dahhan [1,2,4]\*

- [<sup>1</sup>] Nuclear Engineering and Radiation Science Department, Missouri University of  
Science and Technology, Rolla, MO 65409, USA.
- [<sup>2</sup>] Linda and Bipin Doshi Chemical and Biochemical Engineering Department, Missouri  
University of Science and Technology, Rolla, MO 65409, USA.
- [<sup>3</sup>] National Center for Nuclear Technology, King Abdulaziz City for Science and  
Technology, Riyadh, Kingdom of Saudi Arabia.
- [<sup>4</sup>] TechCell, Mohammed VI Polytechnic University, Lot 660, Hay Moulay Rachid  
43150, Ben Guerir, Morocco.
- [<sup>5</sup>] Applied Organic Chemistry Labs, Faculty of Sciences and Technologies, Sidi  
Mohammed Ben Abdellah University, B.P. 2202 Fez, Morocco.

## ABSTRACT

Obtaining accurate results and new benchmark data for the local velocity of the gas flowing within the pebble bed reactor (PBR) is a key step for understanding the thermal hydraulics in the PBR core as it significantly affects the design and safety operation of these reactors. Therefore, this work focused on studying the local gas velocities inside a pebble bed using a sophisticated hot wire anemometry (HWA) technique, which was supported with a novel probe-protector case that protected the probe, allowing the measurements to be conducted at various locations in a pebble bed with pebble diameter of 5 cm and an aspect ratio of 6. The measurements were conducted at various superficial

inlet gas velocities ( $0.3 \leq U_g \leq 2.4$  m/s), covering both laminar and turbulent flow conditions ( $993.78 \leq Re \leq 7950.24$ ) at three axial levels and four radial locations ( $r/R = 0, 0.33, 0.67, 0.9$ ). The results highlighted the effect of the wall on the variation of the local gas velocities inside the pebble bed, as higher gas velocities were recorded at the near-wall region, where the void fractions are higher, compared to the center of the bed. Furthermore, a second order polynomial correlation with an  $R^2=94.65\%$  and an AARE equal to 1.64% was developed for the prediction of the local gas velocity at the fully developed region of the bed, within the experimental range of the study. The accurate gas velocity measurements obtained in this study can serve as benchmark data for the validation of CFD simulations coupled with heat transfer calculations.

## 1. INTRODUCTION

Pebble bed reactor (PBR) is regarded as one of the most probable solutions in the effort to respond to the rapidly growing energy demand. As a fourth generation (Gen IV) high temperature gas-cooled reactor (HTGR), the pebble bed reactor is not only efficient and economical but also inherently safe and environmentally acceptable (Jiang et al., 2019; Liu et al., 2021). The high gas outlet temperature, which may reach up to  $1000^\circ C$ , along with other advantages such as their broad applications, their short construction period and the ability for non-stop reloading, make these reactors serious competitors for generation II and generation III reactors and a subject for extensive scientific research (Jiang et al., 2021; Pioro, 2016).

Generally, a PBR-HTGR's core is comprised of fuel spheres that are 6 cm in diameter. Each pebble is a spherical tri-structural isotropic (TRISO) fuel element. A

TRISO particle consists of a microsphere fuel particle of fissile materials. This fuel particle is coated with layers of porous carbon buffer, an inner layer of pyrolytic carbon, a layer of silicon carbide barrier, and finally an outer layer of pyrolytic carbon (Al-Juwaya et al., 2019, 2017). These modern TRISO particles allow for the containment of the fission products at temperatures as high as 1600 °C (Meyer et al., 2007; Nabielek et al., 1990).

The noble gas helium is used as the coolant gas in a PBR because it is chemically and radiologically inert and does not undergo phase change easily (Wu et al., 2002). Helium gas flows downwards in the reactor's core and concurrently with the movement of pebbles to transfer the heat from the pebbles, which is generated due to the fission reaction. The heat transfer from the pebbles to the coolant gas is one of the main criteria for evaluating the performance of a PBR (Koster et al., 2003; Zhang et al., 2016). Many research projects have experimentally investigated the effects of various parameters and factors on the heat transfer coefficients in a PBR-HTGR under different design and operation conditions (Chen et al., 2017; Liu et al., 2018; Meng et al., 2012). There is also a growing effort dedicated to numerical investigation of the heat transfer in a PBR-HTGR by applying computational fluid dynamics (CFD), the discrete element method (DEM) and the other computational methods integrated with heat transfer calculations (Chen et al., 2022; Lee et al., 2007; Li et al., 2009; Wu et al., 2017; Zou et al., 2022). The pressure drop, granular flow, bed structure, pebbles residence time, flow uniformity, stagnation and the design parameters of the reactor have also been given significant attention in research (Abdulmohsin and Al-Dahhan, 2017; Calis et al., 2001; Gui et al., 2014; Hassan and Dominguez-Ontiveros, 2008; Hassan and Kang, 2012; Khane et al., 2016; Al Falahi et al.,

2018; Al Falahi and Al-Dahhan, 2016; Khane et al., 2017; Khane, 2014; Mueller, 2012, 2010, 1992).

During normal operation conditions, forced convective heat transfer from the heated pebbles to the flowing gas is the most dominant form of heat transfer in the reactor's core. One of the factors that affect the convective heat transfer from the pebbles to the flowing coolant gas is the local actual gas velocity inside the reactor's core (Abdulmohsin and Al-Dahhan, 2015). The increase of the local actual velocity of the gas has the same effect as the increase of the superficial inlet gas velocity, which increases the heat transfer coefficients due to the increase of the turbulent flow of the gas (Schröder et al., 2006). *Abdulmohsin and Al-Dahhan, 2015* found that the forced convective heat transfer in the near-wall region was higher compared to the center of a randomly packed pebble bed, with a pebble diameter of 5 cm and a bed diameter to pebble diameter ratio (aspect ratio) of 6. This was attributed to the higher actual velocities of the gas near the wall due to the effect of the wall, which is highlighted due to the large size of the pebbles (5 cm), which approximates the actual size of the pebbles in a real PBR (6 cm) (Abdulmohsin and Al-Dahhan, 2015). The actual velocities vary cross-sectionally of the reactor due to the variation of the void fractions. *Al Falahi et al., 2018; Al Falahi and Al-Dahhan, 2016* experimentally demonstrated that the void fractions in a pebble bed vary through the cross-section of the reactor with higher void near the wall due to the pebbles-wall contact, reaching up to  $\varepsilon = 0.9 - 1.0$ , compared to the center of the reactor where the void fraction was around  $\varepsilon \approx 0.3 - 0.5$ , regardless of the size of the pebbles, which were 1.27 cm, 2.54 cm and 5 cm. However, the fluctuation of the void fractions in the central region ( $r/R = 0 - 0.8$ ) increased with the increase of the size of the pebbles, and hence with

lowering the aspect ratio (bed diameter to pebble diameter) in the packing bed, which had a diameter of 30 *cm* (Al Falahi and Al-Dahhan, 2016). They found as it has been reported in the literature that for high aspect ratios the void fluctuates toward the center of the bed where it becomes uniform. These experimental data agree well with the discrete element method (DEM) simulation developed by *Khane et al., 2017* for the packing of pebble beds with different aspect ratios, as well as the DEM simulation by *Yang et al., 2014*, which was developed for the packing of a real PBR, with a pebble diameter 6 *cm* and an aspect ratio of 30.

Despite the important effect of the void fraction on the local gas velocities and hence, on the local heat transfer coefficients in a PBR, only few studies were conducted for the measurement of the local gas velocities in a PBR. *Hassan, 2008* and *Hassan and Dominguez-Ontiveros, 2008* used Particle Image Velocimetry (PIV) combined with refractive index matching techniques in order to measure the velocity fields of the gas in the gap between the pebbles in the center of a 3x3 *cm* square-shaped test bed. The pebbles consisted of Poly(methyl methacrylate) (PMMA) beads with an average diameter of 4.7 *mm* while tracer particles with a size of 6 microns were mixed with the upwards-flowing fluid. The measurements were only taken at the center of the test section at  $50 \leq Re \leq 500$  with p-cymene as flowing fluid because it has the same refractive index as the PMMA beads. *Lee and Lee, 2009* also used the PIV technique in order to obtain the velocity field in the surroundings of pebbles with a scaled-up size of 12 *cm* in a 17x17 *cm* square-shaped test section under a superficial inlet velocity of the downwards-flowing gas (air) of 1.3 *m/s* (corresponding to  $Re = 2.1614 \times 10^{-4}$ ). The images that were generated by the PIV algorithm showed that the local gas velocities are higher at the locations in the void

that are further from the pebbles. *Hassan, 2019* utilized a similar PIV approach called Time-Resolved Particle Image Velocimetry (TR-PIV) in order to measure the velocity field in a column of  $0.14\text{ m}$  in diameter, packed with  $2.22\text{ cm}$  pebbles, at two flow conditions of the upward flowing p-cymene liquid, corresponding to  $Re = 700$  and  $Re = 1700$ . However, the use of the PIV technique is limited as the flowing liquid and the pebbles should have the same refractory index, which is not the case when air is used as a working fluid. The flow characteristics of the liquid (p-cymene) are very different from gas and hence, these results cannot represent the local gas velocities in a PBR. Besides, the flow of the working liquid in these studies is directed upwards in contrary to the downward flow of the gas in a real PBR. To overcome the inconveniences of the PIV technique, *Amini and Hassan, 2014* used the hot wire anemometry technique in order to measure the local gas velocity in two gaps at the near-wall region in an acrylic column with an outer diameter of  $0.89\text{ m}$ . The pebbles were made of acrylic with diameters of  $3.18\text{ cm}$  and  $3.3\text{ cm}$ , while the two gaps where the measurements were taken had different geometries. The measurement were taken in the two gaps at different flow conditions of the gas (air), which flows downwards in the column at controlled superficial inlet velocities, corresponding to  $2043 \leq Re \leq 6857$  (*Amini and Hassan, 2014*). The local gas velocities were different between the two gaps due to the different void fractions resulting from the disparity in the geometry of the gaps, while the same variation pattern was observed for both gaps, with higher gas velocity near the wall of the test column and lower local gas velocities closer to the surface of the pebbles (*Amini and Hassan, 2014*). Nevertheless, the use of the hot wire anemometry is limited to the near-wall region as the wire is fragile and could not be placed in the center of the reactor in order to measure the fluctuations of the local gas velocity



along the diameter and height of the reactor. Therefore, due to the unavailability of an appropriate technology for measuring the local gas velocity within the pebble bed, CFD simulations were relied upon by *Atmakidis and Kenig, 2009; Das et al., 2017; Reger et al., 2021; Yildiz et al., 2020* for the estimation of the local gas velocity profiles in pebble bed reactors with different aspect ratios and under different inlet flow conditions. These CFD simulations highlighted the effect of the bed porosity on the variation of the local gas velocity along the bed diameter and height.

In order to validate these CFD simulations, an experimental investigation of the local velocity profiles is essential. However, this has never been done before due to the unavailability of a proper technique that can measure the actual gas velocity at various axial and radial locations in a pebble bed reactor. In this study, we at the Multiphase Flows and Reactors Engineering and Education Laboratory (mFREEL) developed and used, for the first time ever, a modified hot wire anemometry technique, which can be utilized at any location in the reactor and not just in the near-wall regions (Alshammari et al., 2020). This modified technique, is considered novel for its implementation in pebble beds. It has been developed in our laboratory and it consists of a Hot Wire Anemometer (HWA) placed inside a probe-protector case of pebbles arrangement that was designed in order to protect the HWA from damage by contact with the pebbles in the reactor. This modification allowed the local measurements of the actual gas velocity in a pebble bed with a pebble diameter of 5 cm and an aspect ratio of 6, at four radial locations ( $r/R = 0, \pm 0.33, \pm 0.67, \pm 0.9$ ) at three axial levels (top, middle and bottom of the reactor) under different superficial inlet gas velocities  $U_g = 0.3, 0.4, 0.54, 0.7, 0.8, 1, 1.08, 1.2, 1.35, 1.5, 1.6, 2.1$  and  $2.4 \text{ m/s}$ , covering both laminar and turbulent flow of the coolant gas in the reactor ( $Re =$

993.78, 1325.04, 1788.80, 2318.82, 2650.08, 3312.60, 3577.61, 3975.12, 4472.001, 4968.9, 5300.16, 6956.46, and 7950.24).

Moreover, a polynomial regression correlation was developed for the prediction of the actual local gas velocity based on the design and operation conditions of the experimental setup used in this work.

The data obtained in this study with the data of *Alshammari et al., 2023* can serve as benchmark data for the validation of the calculations of CFD integrated with heat transfer, which can then be used to predict the performance of pebble bed reactors under the design and operation conditions of the actual PBR-HTGR.

## **2. MEASUREMENT TECHNIQUE**

### **2.1. HOT WIRE ANEMOMETRY (HWA) FOR GAS VELOCITY MEASUREMENT**

Measuring the gas velocity can be carried out by different ways such as Laser Doppler Anemometry (LDA), Particle Image Velocimetry (PIV), and Hot Wire Anemometry (HWA). The main advantage of the last technique, other than being pioneer is that it provides fast frequency continuous signals in contrast to the other techniques as shown in recalibration of the continuous signals in contrast to the other techniques as shown in Figure 1. Moreover, its spatial resolution is very fine and owing to the small wire time constant, it is universally applicable for different fields especially when turbulent flow and rapid velocity variations are present. It is characterized by a good signal-to-noise ratio, high spatial and temporal resolution due to the fine size of the wire, high frequency response and cost efficiency. However, the hot wire anemometer probe is very sensitive

and can be easily broken due to the contact with the pebbles in a pebble bed, therefore, careful handling and protection must be implemented, as shown in the subsequent section. Additionally, the response acquired using HWA is highly affected by the gas stream purity, and to overcome this difficulty, different precautions can be carried out such as installing a filtration gas system, cleaning the sensor with suitable solvents, and recalibration of the wire before each experiment. While this technique is invasive, the very fine size of the wire introduces minimal and negligible flow disturbance.

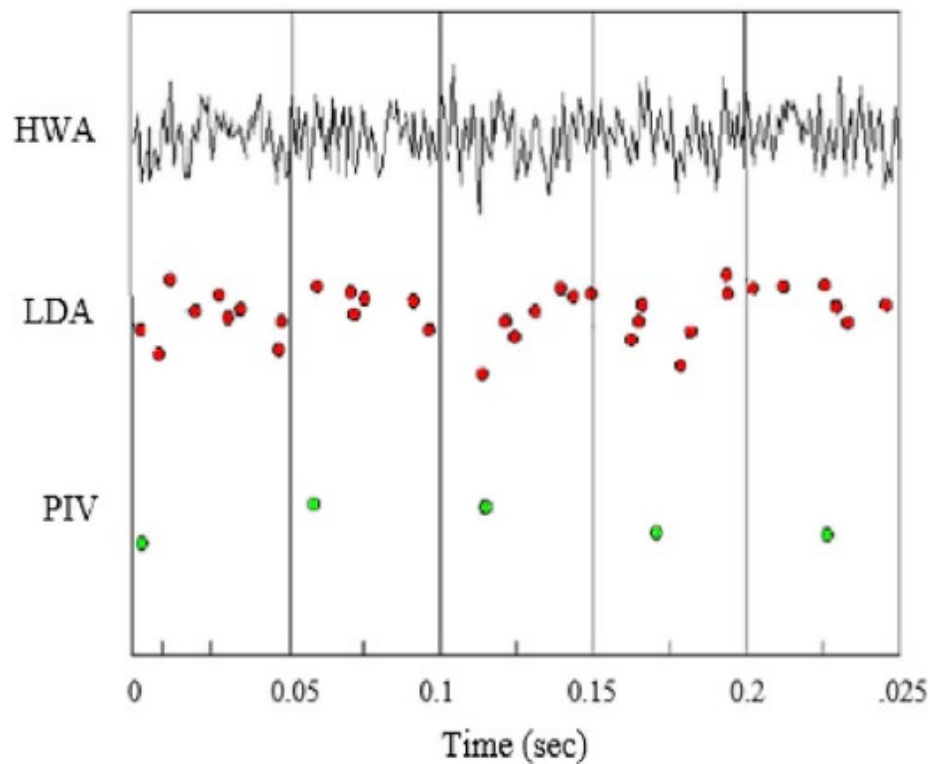


Figure 1. Comparison between PIV, LDA, and HWA output signals (Taha et al., 2019).

Hot wire anemometry is a sophisticated technique for measuring gas velocity. It consists of a simple fine wire with a diameter of few micrometers and length of few

millimeters. This wire is held by supports (prongs) of different materials with various properties as shown in Table 1 and Figure 2. However, hot wire sensors made of Tungsten are the most commonly used due to their low cost. These Tungsten hot wire sensors are coated with a layer of platinum to enhance the oxidation resistance and the resistance temperature coefficient of the hot wire. The stubs are made of gold or copper in order to limit the heat transfer by conduction to the prongs (Taha et al., 2019). The HWA system that was used in this work is the MiniCTA (54 T42 model from Dantec Dynamics). The sensor wire was made of Tungsten, and it was 5  $\mu\text{m}$  in diameter and 0.5 mm in length.

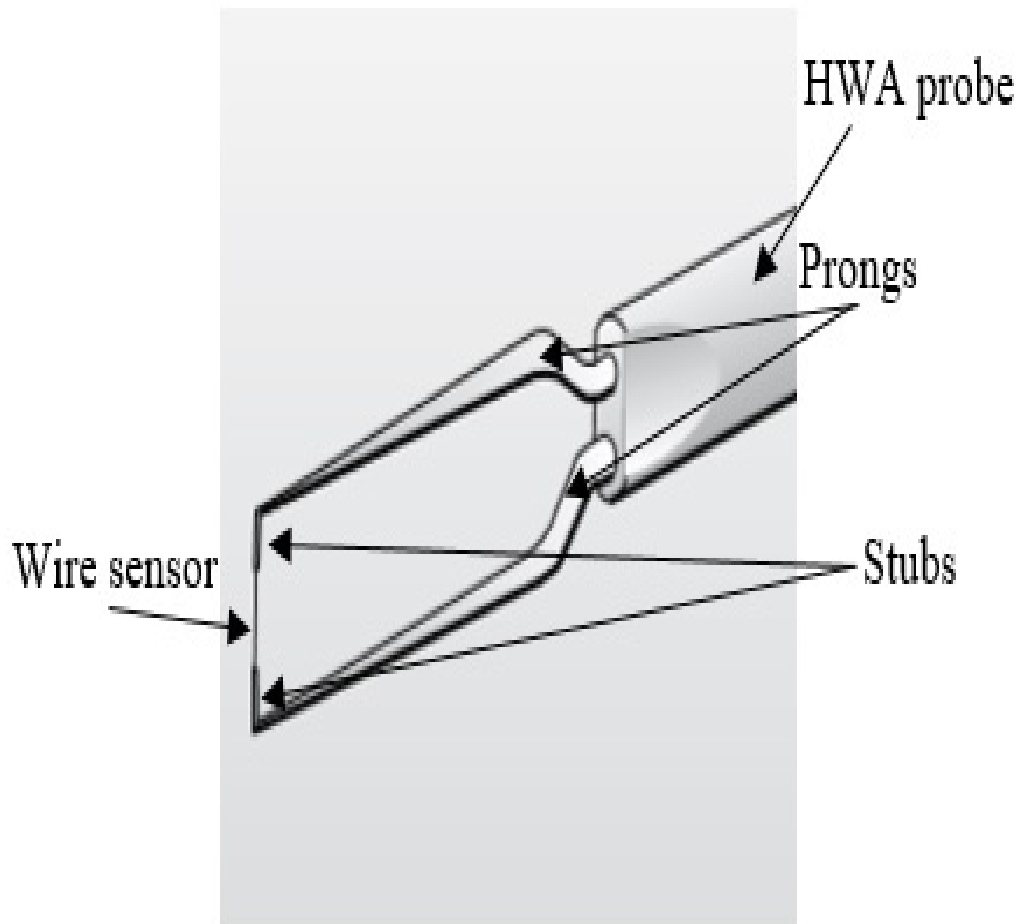


Figure 2. Hot wire anemometer components (Taha et al., 2019).

Table 1. Advantages and disadvantages of various wire supports (prongs) fabrication materials.

Material	Properties	
	Advantages	Disadvantages
Tungsten	High mechanical strength High resistance temperature coefficient ( $0.004/^{\circ}C$ )	Poor resistance to oxidation at high temperatures in many gases.
Platinum	Good oxidation resistance	Mechanically weak
Platinum-iridium alloy	Good oxidation resistance Higher tensile strength than platinum	High resistance temperature coefficient
Platinum-rhodium alloy	High temperature coefficient in comparison to platinum-iridium	Mechanically weaker than platinum-iridium

The heat transfer by convection is the basic operating principle for the hot wire anemometers (HWAs). Heat exchange between the gas flow and the wire by Joule effect takes place based on one of the following principles: i) Maintaining constant current, ii) Maintaining constant temperature. In the first case, as the name indicates, the electric current is kept constant, while the temperature of the wire is allowed to vary. In contrast, at constant temperature, the electric current is varied and controlled in order to maintain the temperature of the wire constant. The main limitation of the constant current mode is the possibility of burning out the wire if the coolant's flow is too low, while inaccurate data will be collected if the flow is too high. Accordingly, constant temperature HWA is used in the current study (Schena et al., 2015). In constant temperature HWAs, the wire temperature is kept constant throughout the operation and this temperature is related to the probe's resistance. Generally, the wire temperature and resistance are directly proportional. When the wire is placed within the gas flow, its temperature changes and so does the

resistance according to the gas velocity, leading to a feedback adjustment in the current passing through the wire to keep the temperature and resistance constant (steady state). This change in the current can be measured and related to the gas velocity which in turn affects the convection heat transfer coefficient, as shown in the following equation (Eq.1):

$$\frac{dE}{dt} = W - H \quad (1)$$

where  $E$  is the thermal energy stored in the wire,  $W$  is the power generated by Joule heating,  $H$  is the amount of heat transferred to the surrounding.

When neglecting the heat losses by radiation and conduction to the prongs at steady state conditions, the heat storage in the wire is equal to zero and then the Joule heating ( $W$ ) is equal to the heat transfer to the surroundings ( $H$ ) as shown below (Eq.2):

$$\frac{dE}{dt} = 0 \quad (2)$$

Therefore,

$$W = H \quad (3)$$

$$I^2 R_w = h_w A (T_w - T_f) \quad (4)$$

where;  $h_w$  is the convection heat transfer coefficient,  $A$  is the heat surface area,  $(T_w - T_f)$  is the difference in temperature between the wire and the fluid,  $I$  is the current passing through the wire,  $R_w$  is the wire's resistance.

Changing the gas velocity will result in changing the heat transfer convection coefficient, as mentioned above, and according to the following equation (Eq.5):

$$h_w = A + B(\rho U)^n \quad (5)$$

where ( $\rho$ ) is the fluid density, ( $U$ ) is the fluid velocity, ( $A$  and  $B$ ) are calibration constants, and the coefficient  $n$  is usually taken to be  $\frac{1}{2}$  (Taha et al., 2019).

In this work, The HWA was operated at a frequency of 0.1 KHz. Before conducting the experiments, to ensure the accuracy of the air velocity measurements, the HWA system was calibrated using an automatic calibrator that is applicable for velocities ranging from a few  $cm/s$  to 300  $m/s$ . The calibrator is connected to the MiniCTA HWA data acquisition system, as well as to a computer via USB (Figure 1). The StreamWare Basic software package is used to control the calibration process.

The uncertainty of the local velocity measurements was estimated to be 0.01, taking in consideration the uncertainties emanating from the calibration, the linearization, and the analogue-to-digital converter ( $A/D$ ) resolution, as per (Eq.6).

$$\text{Measurement uncertainty} = \sqrt{(\text{calibration uncertainty})^2 + (\text{linearization uncertainty})^2 + \left(\frac{A}{D} \text{ uncertainty}\right)^2} \quad (6)$$



Figure 3. HWA data acquisition system: a)- MiniCTA, b)- automatic calibrator.

## **2.2. A NEW PROBE-PROTECTOR OF HWA FOR IMPLEMENTING IN THE COLD FLOW PEBBLE BED REACTOR**

As mentioned above, the HWA provides a superior performance over the other techniques, but this technique suffers from a significant drawback that is due to of the fragility of the top part of the sensors. The tiny wire of the HWA can be easily damaged because of any slight movement during the operation or the installation process (Amini and Hassan, 2014; Taha et al., 2019, 2018). Despite the high performance of HWA, this technique is not widely used to measure the local velocity within narrow regions such as the void between pebbles. Therefore, in order to overcome the inconveniences resulting from the fragility of the HWA, an innovative solution, in the form of a protection case, was designed to protect the tiny wire of the HWA, allowing the use of the HWA at any location in the pebble bed (Alshammari et al., 2020) (Figure 4). The protection case of predetermined pebbles arrangement was designed to have the same structure and shape of the pebbles inside the bed in order to minimize the impact of the protector's body on the mechanism of the fluid flow. Despite the structure being maintained the same as a probe while moving it to various locations in the bed radially and axially, the results obtained are affected by and obtained based on the void structure of the bed directly above it. The bed structure of the random packing of the pebble affects and determines the volumetric flow of the gas flowing to the predetermined pebbles arrangement of the probe-protector case below it and hence the local velocity in the void of the probe-protector case varies with the location of this case of predetermined pebbles arrangement in the bed. These measurements are very important for the validation of the CFD simulations coupled with heat transfer calculations, which will allow these CFD simulations, coupled with DEM simulation for



packing the bed to be used for the prediction of the heat transfer coefficients in the design and operating conditions of a real PBR.

The predetermined pebbles arrangement of the probe-protector case consists of three main parts:

- The sensor holder (Figure 4a)
- The pebbles holder at the top (Figure 4b).
- Four pebbles that are placed at the top of the pebble's holder.

The HWA sensor holder was designed in the shape of coupled spheres, one above the others with the same diameters as the pebbles used for packing the bed. These two parts are cut from the middle to place the probe inside, where it will be protected, as the spheres are tightly bundled together vertically (Figure 4a) (Alshammari et al., 2020). The holder consists of two parts: the first part has a clip and annular rubber to hold the probe pins and eliminate the vibration, while the second part is used as a cover. Each part has hooks at the ends that stick the parts together tightly. The upper part consists of four hemispherical trays, which are used to hold the four pebbles that represent shielding to protect the upper part of the probe from the contact with the packings of the bed. Hence, this part has clips in the center to tightly place in the holder part and the tiny wire sensors can safely exit through the 1 mm diameter hole at the center of the top part, and between the four pebbles, while the sensor cable exits from the bottom of the holder part to the outside the bed (Alshammari et al., 2020).

It is noteworthy that such structure has a limitation of the back-effect on the flow of the gas, particularly if its void structure differs from the void structure of the bed above it and surrounding it. This means that if this case is placed at the top level of the bed, it

would affect the gas flow causing more volumetric flow of the gas to flow toward the location of the probe-protector case resulting in higher local gas velocities. This is because the height of the bed above the probe-protector case is not sufficient to allow for the flow of the gas to equilibrate inside the bed first before flowing into the case to measure the local gas velocity.

Furthermore, the void structure of the probe-protector case represents one configuration of the true void volume of the bed with random packing of the pebbles. However, the configurations of the void structures in a pebble bed vary, which means that the local volume of the void varies affecting the local velocities. In this work, we measure the local gas velocity for such a void configuration relying on the equilibration of the flow of the gas above the probe-protector case. The gas will flow towards the location of the probe-protector case and the obtained measurements will vary depending on the volumetric flow rate of the gas in the region directly above the probe-protector case. Accordingly, such kind of measurements will allow us to obtain qualitative trends for the effect of the local void volume for this configuration of the probe-protector case in the wall region on the local gas velocity compared to inside the bed. Quantitative measurements of the local gas velocity with this void configuration are accurate when there is enough height of the bed of the bed above the probe-protector case to equilibrate the flow of the gas across the cross-section of the bed before reaching the measurement zone. With all this said, the obtained results could be valuable for CFD validation provided that the void structure of the probe-protector case is represented in the bed used for CFD computations.

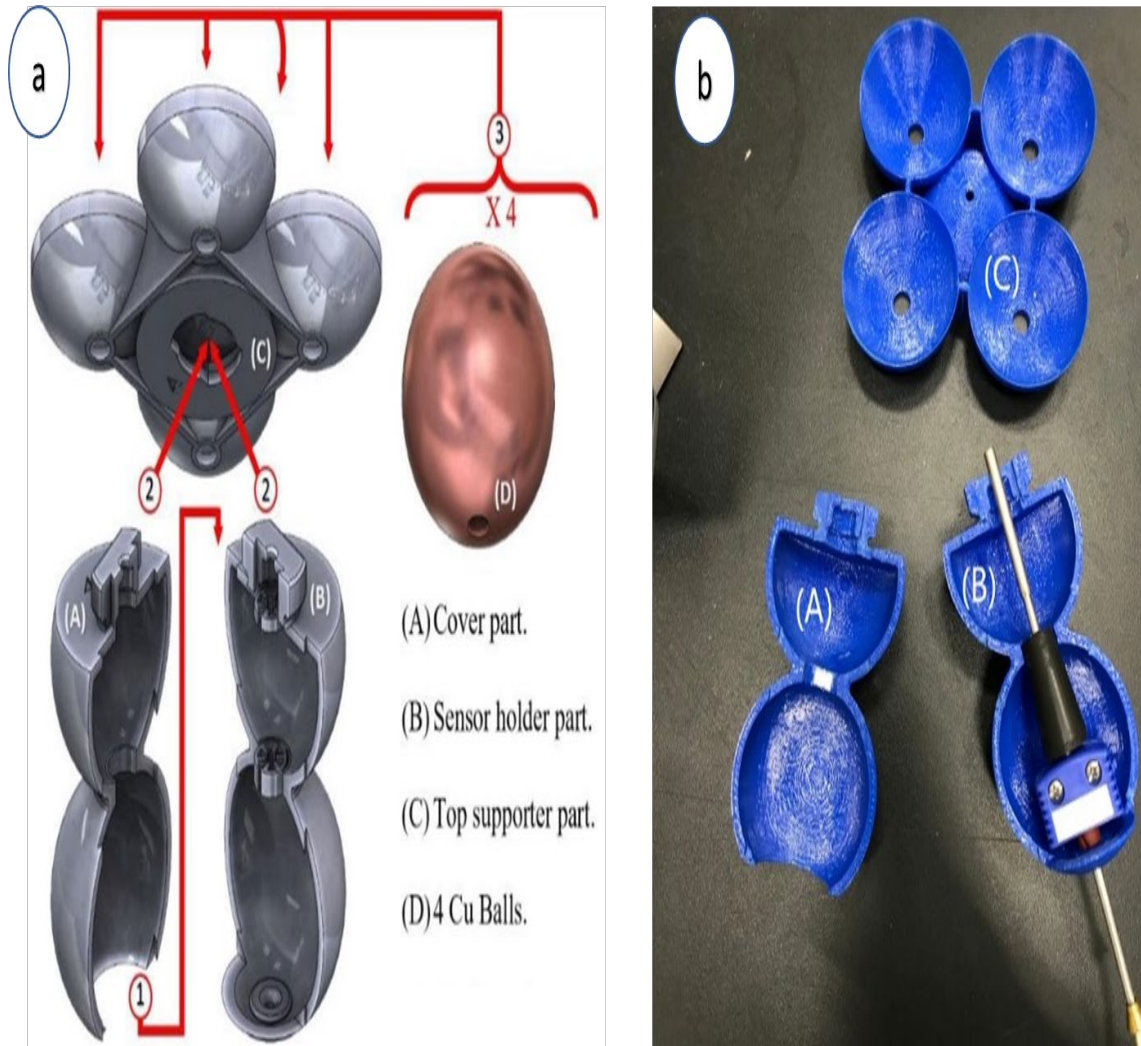


Figure 4. HWA predetermined pebble arrangement probe-protector case design components: a) a 3D design, b) a picture of the actual design of the components.

The probe-protector case was placed at different locations inside the bed, as described in the following section. The same structure of the pebbles and hence, the same void fraction is maintained for all experiments and the difference is observed based on the void fraction above the test area, which varies randomly along the diameter and height of pebble bed and hence, the volumetric flow of the gas through it that flows to the probe-protector case of HWA.

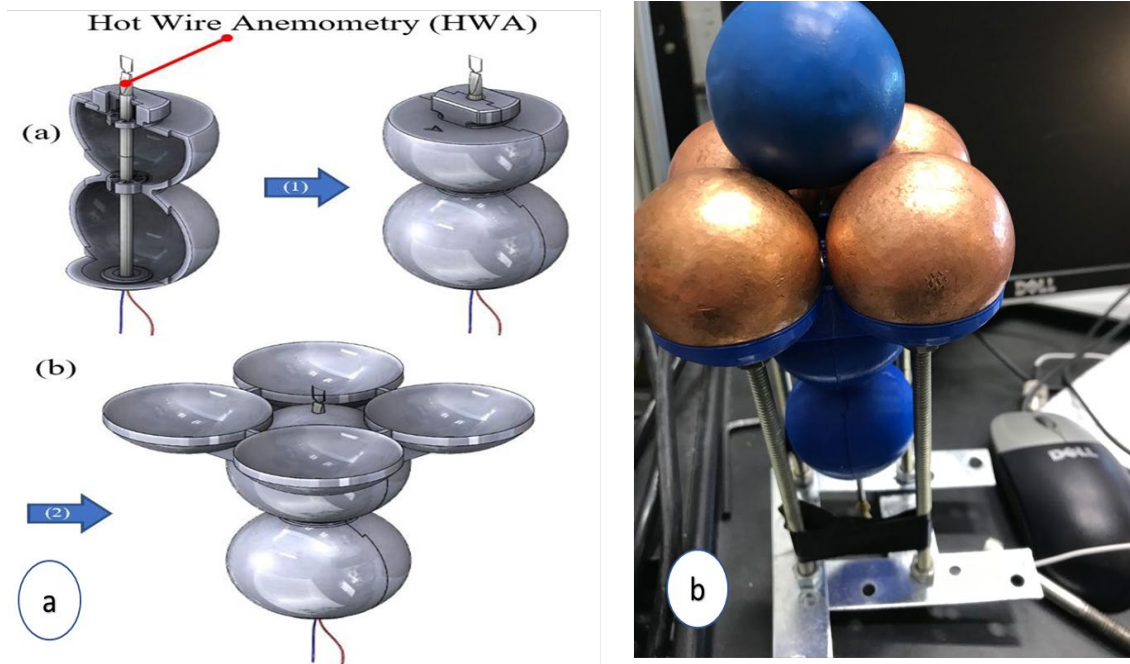


Figure 5. Assembly of the designed probe-protector case: a) a 3D design, b) a picture of the complete assembly.

### 3. EXPERIMENTAL SETUP

The experimental setup used to carry out the experiments was designed in our Multiphase Flows and Reactors Engineering and Education Laboratory (mFReel). The test column is made of plexiglass, its inner diameter is  $0.3\text{ m}$  with a height of  $0.9\text{ m}$  (Figure 6). The top part of the column was covered with a cone shaped plenum with a height of  $0.1\text{ m}$ , which was placed on top of a perforated plate distributor, as shown in Figure 6. The perforated plate distributor contains 140 holes and is used to distribute the coolant air entering the system from the top. Two rotameters (Omega HFL6715A-0045-14) were used to control the air flow rate from the top plenum downwards through the pebble bed and the bottom part of the setup. The bottom part is composed of a plastic cone with a  $30^\circ$  angle,  $0.3\text{ m}$  in diameter,  $0.08\text{ m}$  in height and equipped with a gas outlet vent in the center that

has a diameter of 0.05 *m*, used for the release of the air out of the system. Mono-sized plexiglass pebbles that have a diameter of 5 *cm* were randomly packed in the column, creating a pebble bed with an aspect ratio of 6. Despite the low aspect ratio of the test column, the large size of the pebble, which is close to the size of the pebbles in a real PBR (6 *cm*) allowed us to highlight the wall effect and the fluctuation of the void fraction in the region of the walls and along the diameter and height of the pebble bed. The average bed porosity was calculated using the direct input method and was found to be equal to  $\varepsilon = 0.397$  (Eq. 7).

$$\varepsilon = \frac{V_c - V_p}{V_c} \quad (7)$$

where  $V_c$  is the volume of the column calculated based on the known length and diameter of the column and  $V_p$  is the volume occupied by the pebbles, which is calculated using the number of pebbles in the column and the known diameter of the pebbles, which are considered perfect spheres.

In a real PBR, the pebbles move downwards and leave the reactor via the outlet in order to be tested for burnup and either be returned to the reactor or replaced with a new pebble if the burnup threshold is reached. For our experiments, the pebbles were kept stagnant due to the large disparity in the velocity of the flow of the gas compared to the slow granular flow of the pebbles.

The HWA integrated inside its probe-protection case was placed at four different radial and axial positions in the test column in order to measure the local gas velocity, as shown in Figure 7.

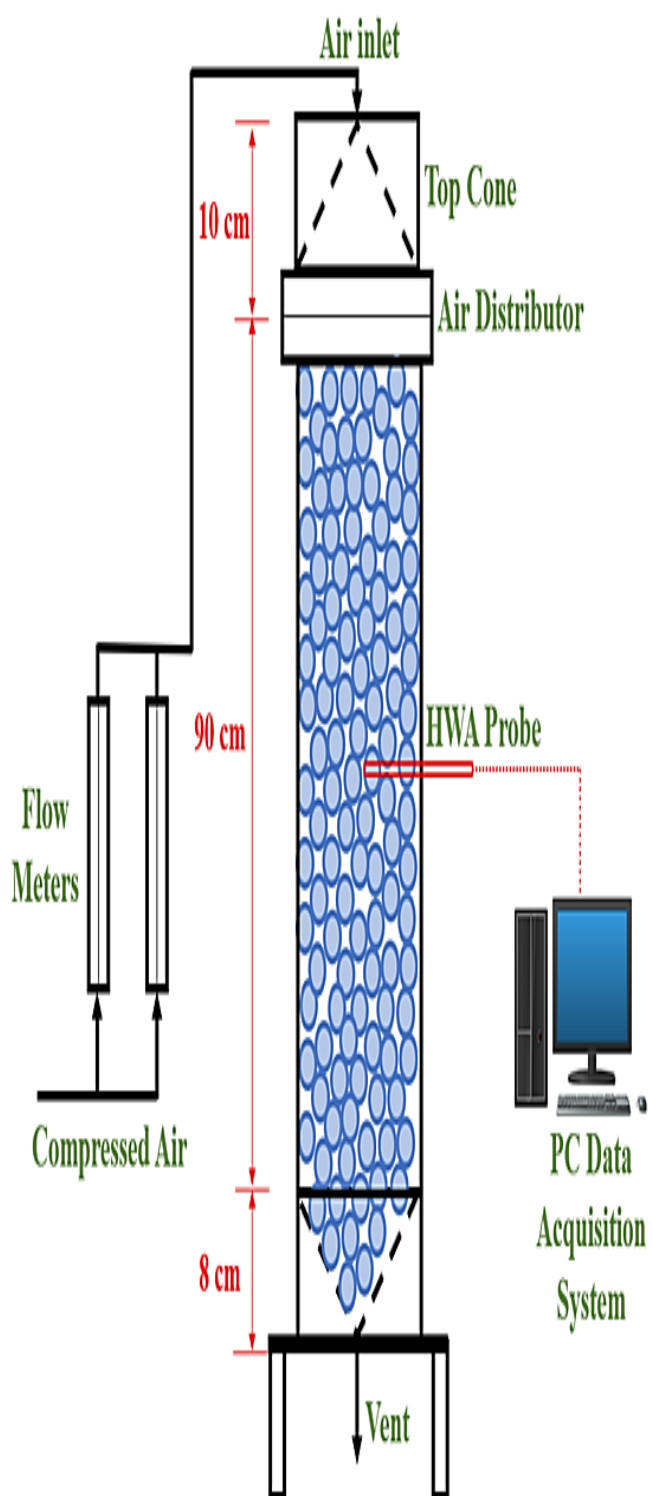


Figure 6. Experimental setup for the PBR: a) schematic diagram with dimensions in cm; b) pictorial representation.

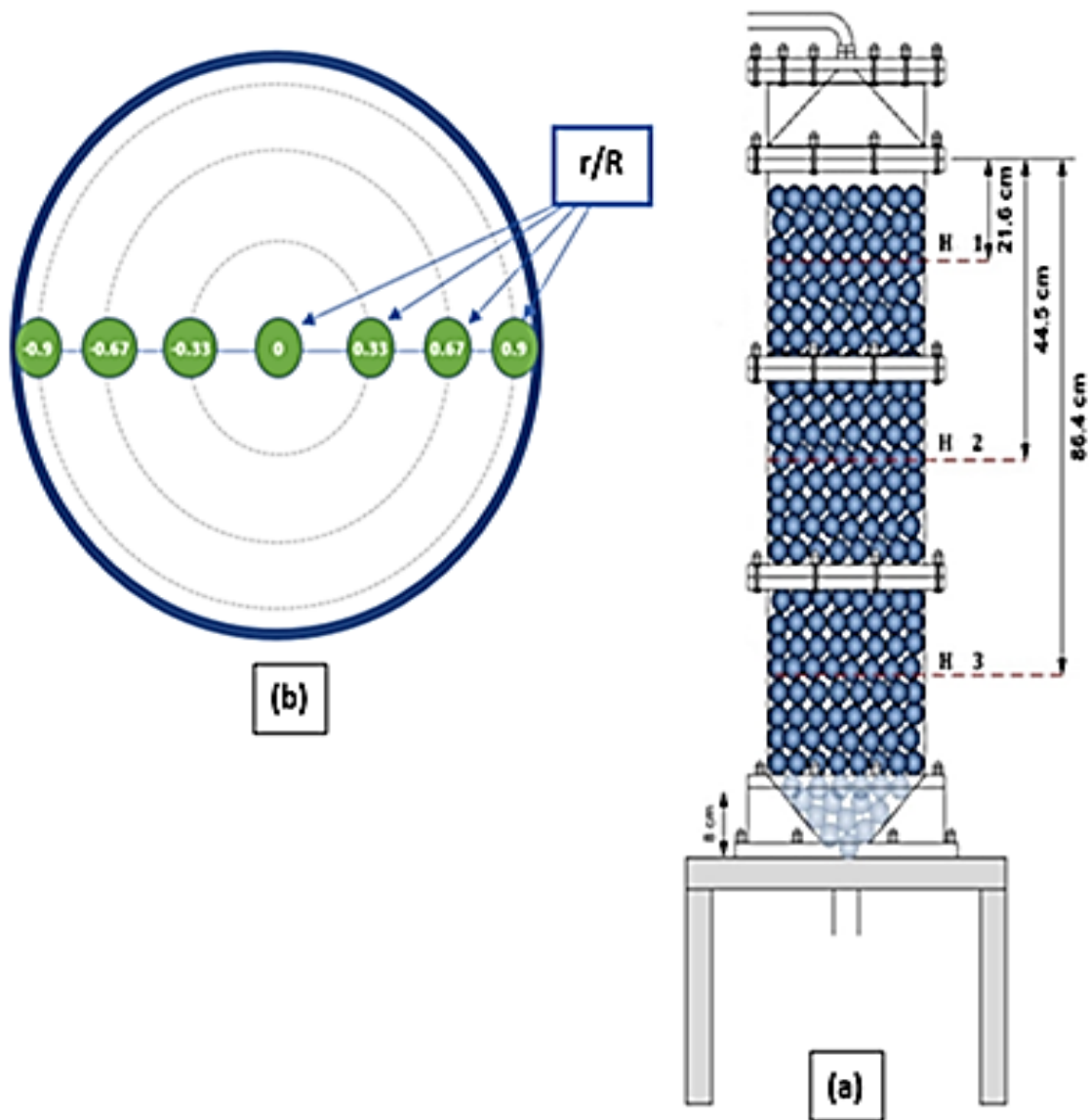


Figure 7. Schematic illustration showing a)- axial levels ( $H/D = 0.72$ ,  $H/D = 1.48$ ,  $H/D = 2.88$ ) and b)- radial positions where the measurements were taken.

Our 1<sup>st</sup> level headings should automatically be single spaced if they are more than one line long. To single-space a 2<sup>nd</sup> level heading, highlight the heading and change to single line spacing. Then, place your cursor at the end of the last line of the heading and add 12 pt of “After” paragraph spacing. Then, use the ruler to make sure your second line is properly aligned under the text of first line.



#### 4. EXPERIMENTAL PROCEDURE

The gas velocities were taken using the HWA integrated in its probe-protector case of predetermined arranged pebbles at three axial levels, which were taken as  $H1 = \left(\left(\frac{H}{D}\right) = 0.72\right)$ ,  $H2 = \left(\left(\frac{H}{D}\right) = 1.48\right)$ , and  $H3 = \left(\left(\frac{H}{D}\right) = 2.88\right)$  from the top of the column. At each axial level, the measurements were taken at four radial locations ( $r/R = 0, \pm 0.33, \pm 0.67, \pm 0.9$ ) (Figure 7) represent the diameter under thirteen different superficial inlet gas velocities,

$$(U_g = 0.3, 0.4, 0.54, 0.7, 0.8, 1, 1.08, 1.2, 1.35, 1.5, 1.6, 2.1 \text{ and } 2.4 \text{ m/s}).$$

Covering both laminar and turbulent flow conditions ( $Re = 993.78, 1325.04, 1788.80, 2318.82, 2650.08, 3312.60, 3577.61, 3975.12, 4472.001, 4968.9, 5300.16, 6956.46, \& 7950.24$ ). The superficial inlet gas velocities were defined by controlling the volumetric flow rate of the gas. After the superficial inlet gas velocity, the gas was allowed to flow for 2 to 4 minutes before collecting the data to ensure the stability of the gas flow and obtain proper results. Each experiment was replicated three times and the average of the results collected was taken as the final output. The repeatability error is 0.013. The position of the HWA was changed manually from one location to the other by removing all of the pebble in the column and repacking the column randomly with pebbles with a care is given to repeat the same method of packing, with the HWA in its probe-protector case being placed at the location where the new measurements are to be taken. The whole system was turned off between every experiment, for 5 to 10 minutes after any adjustment to the superficial inlet gas velocity or the position of the HWA, then the same steps were followed to take the new measurements.



## 5. RESULTS AND DISCUSSION

### 5.1. RADIAL PROFILES OF THE GAS VELOCITY

The local gas velocity measurements were taken at four different radial positions ( $r/R=0, \pm 0.33, \pm 0.67, \pm 0.9$ ) and at three different axial levels along the height of the test column (top, middle and bottom). These HWA measurements were taken at different superficial inlet gas velocities ( $U_g=0.3, 0.4, 0.54, 0.7, 0.8, 1, 1.08, 1.2, 1.35, 1.5, 1.6, 2.1$  and  $2.4$  m/s), corresponding to Reynold's numbers for laminar and turbulent flow ( $Re = 993.78, 1325.04, 1788.80, 2318.82, 2650.08, 3312.60, 3577.61, 3975.12, 4472.001, 4968.9, 5300.16, 6956.46, \text{ and } 7950.24$ ), in order to understand the variation of the local gas velocity inside the PBR at both laminar and turbulent flow conditions. The results, which are based on the repetition of every experiment three times were obtained with a repeatability error of 0.013 and a repeatability standard deviation of 0.0002.

Figure 8 displays the radial profiles of the gas velocity at the top, middle and bottom of the test column under various superficial inlet velocities ( $0.3$  m/s to  $2.4$  m/s), corresponding to Reynolds numbers from  $993.78$  to  $7950.24$ . It is apparent that the actual velocity of the gas increases when increasing Reynolds number, which is expected. The local gas velocities are also considerably higher at the near wall region ( $r/R = 0.9$ ), compared to the central region of the reactor ( $r/R = 0 \sim 0.67$ ), regardless of Reynolds number and the axial level in the column. The same trend was observed for the variation of the convective heat transfer coefficient between the pebbles and the gas, as reported by Abdulmohsin and Al-Dahhan, 2015, which showed higher heat transfer coefficients in the near wall region, compared to the center of the bed. Hence, we speculate that the relationship between the local actual gas velocity at different radial locations and the

corresponding local heat transfer coefficients can be quantified if the measurements of the local gas velocity and the convective heat transfer coefficients were taken at the same at different locations in the bed. The gas velocity in the central region shows a relatively uniform distribution, as the variation of the actual gas velocities between  $r/R = 0$  and  $r/R = 0.67$  is very insignificant, not exceeding 3.24% at the top of the column, 1.74% at the middle and 2% at the bottom, for all Reynolds numbers. This uniformity of the distribution of the gas velocity in the central region ( $r/R = 0 \sim 0.67$ ) is due the lower void compared to the wall region that causes higher pressure drop and energy dissipation to enforce the flow to be uniformly distributed. This remains relatively the same despite the repacking of the column every time the location of the HWA is changed (Al Falahi et al., 2018; Al Falahi and Al-Dahhan, 2016). On the other hand, Figure 9 which elucidates the difference in the variation of the local gas velocities between the center ( $r/R = 0$ ) and the near-wall region of the column ( $r/R = 0.9$ ) at different Reynolds numbers, shows clearly that regardless of the superficial inlet gas velocity (Reynolds number), the local velocity of the gas flow in the region near the wall ( $r/R = 0.9$ ) is much higher than the gas velocity in the center of the column ( $r/R = 0$ ). This is due to the higher void fractions near the wall of the column which are more pronounced for the beds of low aspect ratios (bed diameter to pebble diameter), due to the wall-pebble interactions which leave considerably bigger void gaps than the pebble-pebble contact in the center of the column. In this case the gas tends to flow toward the path of least resistance and hence larger volumetric flow of the gas flows in the wall region. Despite the structure of the test area being maintained the same between the center and the near-wall region of the column, the porosity of the packing above the HWA is the defining factor in the variation of the local gas velocity inside the bed. Furthermore, this

difference in gas velocity between the center and the wall regions of the column is more pronounced at high Reynolds numbers, as the relative difference percentage in the gas velocity between the center ( $r/R = 0$ ) and the near-wall region ( $r/R = 0.9$ ) increases from 9.22% at laminar flow conditions ( $Re=993.78$ ) to 17.27% at turbulent flow conditions ( $Re=7950.24$ ) at the top level of the column, and from 9.42% at laminar flow conditions ( $Re=993.78$ ) to 14.41% at turbulent flow conditions ( $Re=7950.24$ ) at the middle level, while at the bottom of the column, the relative difference percentage increases from 9.4% to 15.94%, when passing from  $Re=993.78$  to  $Re=7950.24$ . This increase in the relative difference percentage between the center ( $r/R = 0$ ) and the near-wall region ( $r/R = 0.9$ ) when increasing Reynolds number, and hence increasing the superficial inlet gas velocity can be also attributed to the lower resistance to the flow of the gas in the near-wall region due to the higher void fractions in this area of the bed which causes lower pressure drop means lower resistance to the gas to flow, compared to the center of the bed, where the dense packing causes more resistance to the flow of the gas, and hence higher pressure drop, especially at high Reynolds numbers. The effect of wall on the gas velocity, compared to the gas velocity in the center of the column in this study is highlighted due to the large size of the pebbles (5 cm), which is close to the actual size of the pebbles in a pebble bed reactor (6 cm), despite the low aspect ratio of 6, as the real aspect ratio of the PBR cannot currently be implemented in laboratory investigations. However, such a condition of low aspect ratio is valuable as it provides information and data for the region near the walls which is always of high void fraction even for the bed of higher aspect ratio (bed diameter to pebble diameter). Thus, the obtained data are valuable as benchmark data to validate CFD models and simulation particularly for the wall region.

Figure 10 shows the radial profiles of the local gas velocity at the top, middle and bottom of the column at four Reynolds numbers ( $Re=1325.04, 3312.6, 4472.12$ , and  $7950.24$ ). It can be seen that the local gas velocities at the top level of the column are the highest, compared to the local gas velocities in the middle and bottom level of the column. This is due to the back-effect of the probe-protector case, as more volumetric flow of the gas goes toward the location of the probe-protector case, as the short height of the bed above the probe-protector case is not enough to allow the flow of the gas to equilibrate. On the other hand, at the middle and bottom of the bed, the heights of the bed are larger above the level of the probe-protector case, which would be enough for the flow of the gas to equilibrate. Hence, the flow going through the probe-protector case in this fully developed region is representative of the flow going through the bed above it. In this case, the back-effect of the probe-protector case on the flow distribution of the gas is reduced at the middle and bottom level of the bed. However, more volumetric flow of the gas goes toward the wall which shows higher local gas velocity at the wall, hence confirming the explanation of the back effect of the case. This is because such trend of higher local gas velocity at the wall has been maintained at the middle and bottom levels of the bed, where the wall region always has higher void along the bed height, and thus, less resistance to the flow of the gas along this region.

The trend of the variation of the forced convection heat transfer coefficients in the same experimental setup is anticipated to be like the trend of local actual gas velocities across the radius of the column as it will be shown in the following manuscript. This was confirmed by the work of Al Falahi et al., 2018; Al Falahi and Al-Dahhan, 2016 and Abdulmohsin and Al-Dahhan, 2015, where the convective heat transfer in a PBR is

significantly affected by the local gas velocities, which vary with the void fractions inside the bed.

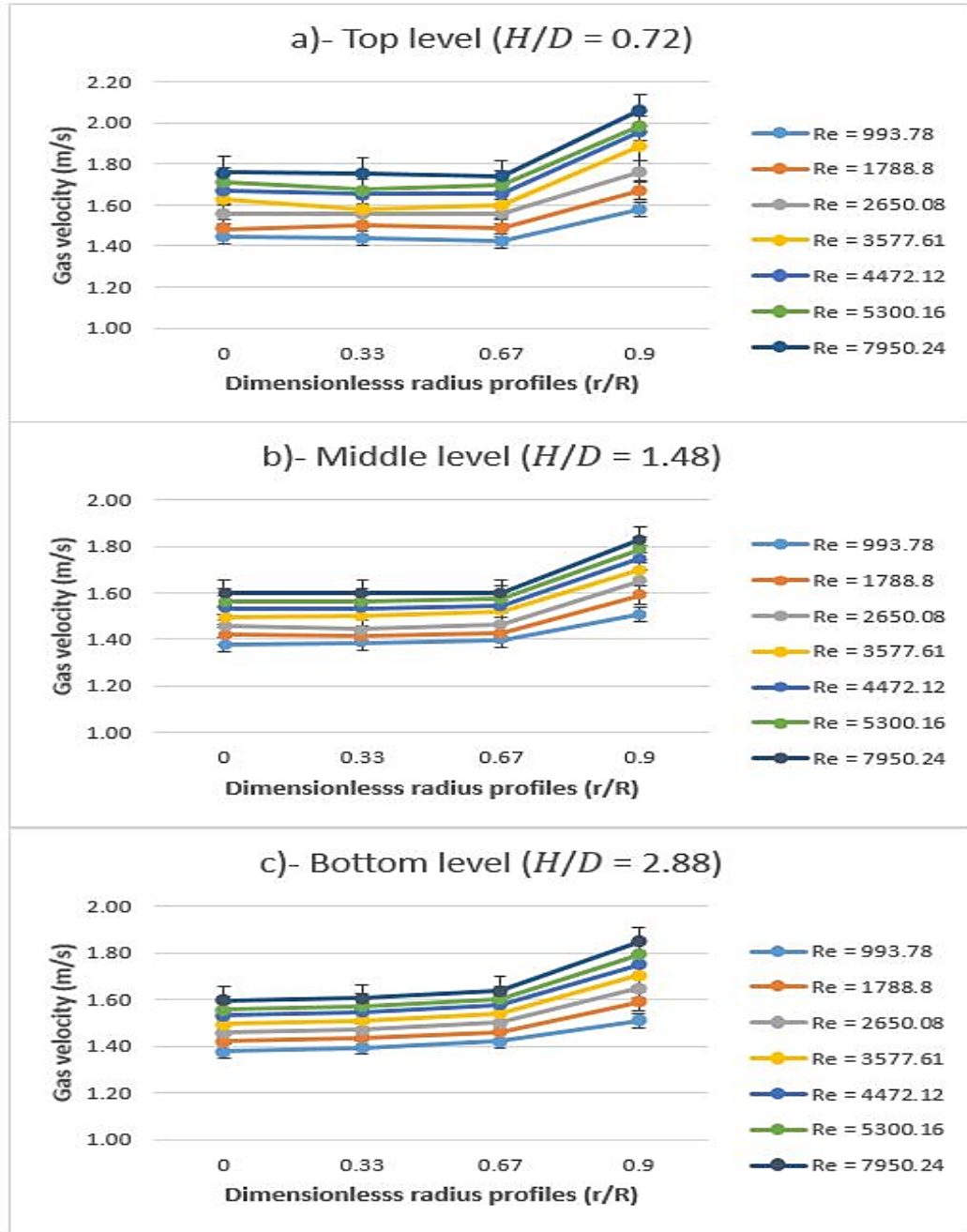


Figure 8. Local radial velocity profiles at different Reynolds number (993.78 to 7950.24) at three axial locations in the column: a)- Top level ( $H/D = 0.72$ ), b)- Middle level ( $H/D = 1.48$ ), and c)- Bottom level ( $H/D = 2.88$ ).

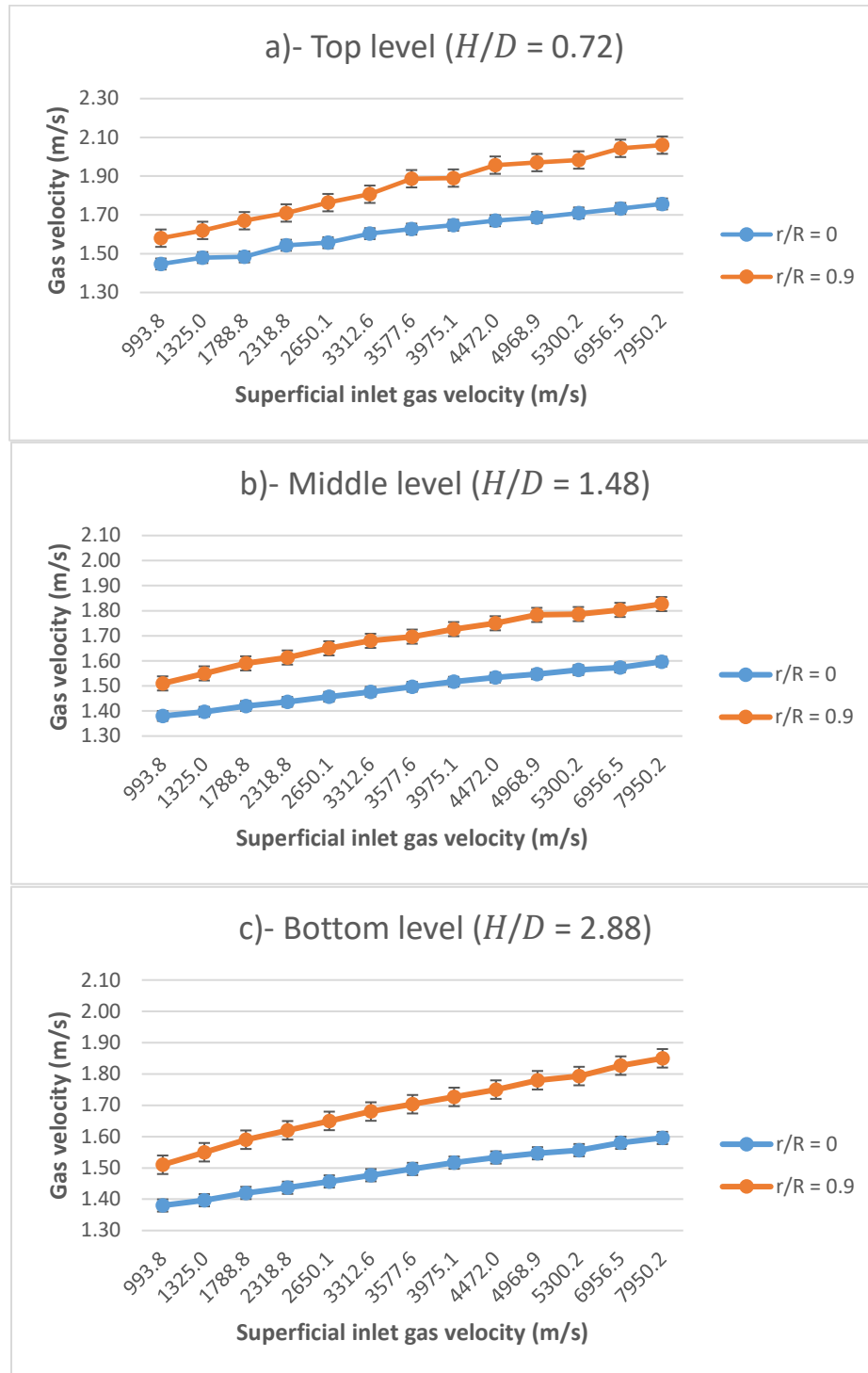


Figure 9. The variation of the local gas velocity based on Reynolds number in the center of the test column ( $r/R = 0$ ) and the in the near-wall region ( $r/R = 0.9$ ) at three axial locations: a)- Top level ( $H/D = 0.72$ ), b)- Middle level ( $H/D = 1.48$ ), and c)- Bottom level ( $H/D = 2.88$ ).

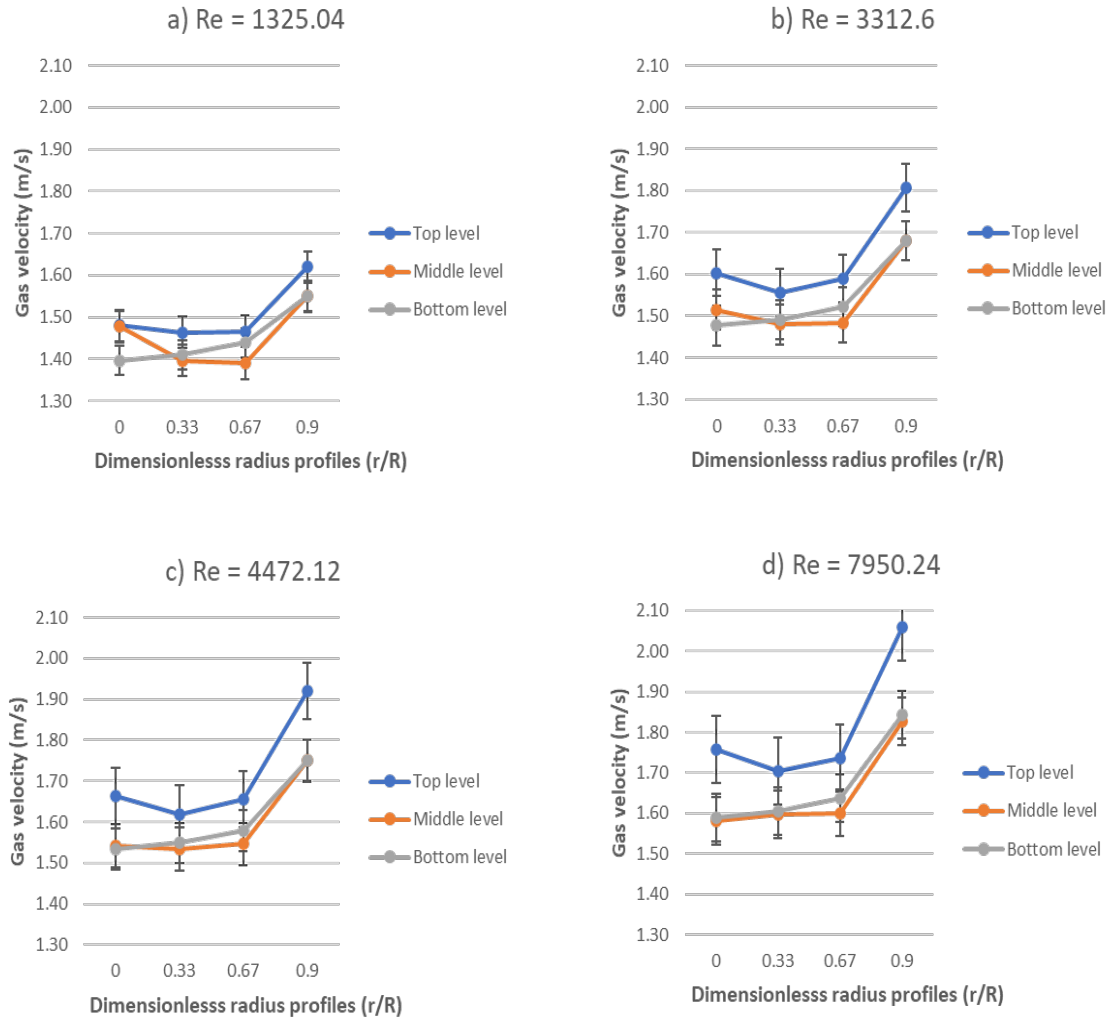


Figure 10. Radial profiles of the local gas velocity at the top ( $H/D = 0.72$ ), middle ( $H/D = 1.48$ ) and bottom ( $H/D = 2.88$ ) of the column under four superficial inlet gas velocities: a)-  $Re = 1325.04$ , b)-  $Re = 3312.6$ , c)-  $Re = 4472.12$ , and d)-  $Re = 7950.24$ .

## 5.2. CORRELATION DEVELOPMENT FOR THE LOCAL GAS VELOCITY USING POLYNOMIAL REGRESSION

To quantify the local gas velocity variation along the height and radius of the fully developed region of the PBR under different superficial inlet gas velocities, it is necessary to estimate the effect of each of these factors and the interactions between them. As shown in the above section, the local gas velocity not only depends on these input features, but

also depends on the interactions between them, as changing the superficial inlet gas velocity from a velocity that corresponds to laminar flow to a velocity that corresponds to turbulent flow changes the difference of the actual local gas velocity between the center and the wall of the column. This kind of complex interactions can be quantified using polynomial regression, where the linear effects, non-linear effects and interactions effects are quantified, and a correlation is developed for the prediction of the actual local gas velocity based on these effects in the middle and bottom of the bed (Montgomery et al., 2013). Polynomial regression is widely used in chemical engineering and process engineering applications and is especially useful when the objective is to understand the complex relationship between the input features and the response (Al-Safran, 2009; Fan et al., 2020; Hemmati et al., 2021; Saraswathi K. et al., 2021).

In this study, a second order polynomial correlation was developed for the prediction of the local gas velocity in the fully developed region (middle and lower regions) of the pebble bed based on the dimensionless input features, which are mentioned in Table 2, and within their experimental range. The experimental data consisted of 154 data points and the model development, validation and analysis were carried out using the JMP Pro 16 software (SAS, 2021). The general equation of a second order polynomial model can be presented as follows (Eq8):

$$\hat{y} = \beta_0 + \sum_{j=1}^k \beta_j \cdot X_j + \sum_{j=1}^k \beta_{jj} \cdot X_j^2 + \sum_{i < j} \sum \beta_{ij} \cdot X_i \cdot X_j \quad (8)$$

where  $\hat{y}$  is the predicted response,  $\beta_0$  is the intercept,  $\beta_j$  are the estimates of the main effects  $X_j$ ,  $\beta_{jj}$  are the estimates of the quadratic effects  $X_j^2$ ,  $\beta_{ij}$  are the estimates of the two-factor interactions  $X_i \cdot X_j$



Table 2. Input features and their range of variation.

Input feature	Range of variation
Radial location in the column ( $r/R$ )	0 – 0.9
Axial level in the bed ( $H/D$ )	1.48 – 2.88
Reynold's number ( $Re$ )	993.78 – 7950.24

For the estimation of the optimal correlation coefficients, an optimization algorithm called the normal equation (least square regression) was used. This equation can be expressed as follows (Montgomery et al., 2013):

$$X'.X.\beta = X'.y \quad (9)$$

where  $X$  is the matrix of the features of the model,  $X'$  is the transpose of  $X$ ,  $y$  is the response vector and  $\beta$  is the vector of the coefficients.

Based on the optimal coefficients obtained using this equation, the following correlation for the prediction of the local gas velocity within the design and operation conditions of our experimental setup was developed:

$$\begin{aligned}
 & \text{Local Gas velocity } U_g \text{ (m/s)} \\
 &= 1.3079 + 0.0076 \left( \frac{H}{D} \right) - 0.2996 \left( \frac{r}{R} \right) + 6.7 \times 10^{-5} Re \\
 &+ 0.4937 \left( \frac{r}{R} \right)^2 - 4.4 \times 10^{-9} Re^2 + 1.4 \times 10^{-5} \left( \frac{r}{R} \right) . Re
 \end{aligned} \quad (10)$$

### 5.2.1. Validation of the Second Order Polynomial Regression Correlation. In

order to be able to use the correlation for the prediction of the local gas velocity within the experimental range of the study, it would have to be statistically proven as valid. This validation is done using four statistical tests, which are the analysis of variance (ANOVA)

(Christensen, 2018), the lack of fit analysis (Neill and Johnson, 1984), the analysis of the coefficients of determination (Ostertagová, 2012), and the analysis of the residuals (Kim, 2019). The results of these tests are discussed in Table 3.

Table 3. The results of the validation tests of the polynomial model.

Validation Test	Statistic calculated	Result	Conclusion
Analysis of Variance (ANOVA)	F (Fischer's test between the model and the residuals)	$F = 259.41$ $p_{value} < 0.0001$	Presence of a significant linear relationship between the features and the response.
Lack of Fit	F (Fischer's test between the experimental error and the residual error.	$F = 5.26$ $p_{value} = 0.097$	Absence of a lack of fit.
Coefficient of determination	$R^2$	93.96%	The correlation explains 93.96% of the variation of the response.
Adjusted coefficient of determination	$R_{adj}^2$	93.6%	The number of the terms in the correlation was well-chosen.

For the analysis of residuals, the residuals, which are the portion of the responses that are not explained by the terms in the model, are tested against their normal quantile to verify if they follow a near-normal distribution.

Figure 11 shows that the residuals are well aligned with their normal quantiles, hence indicating a near-normal distribution of the residuals.

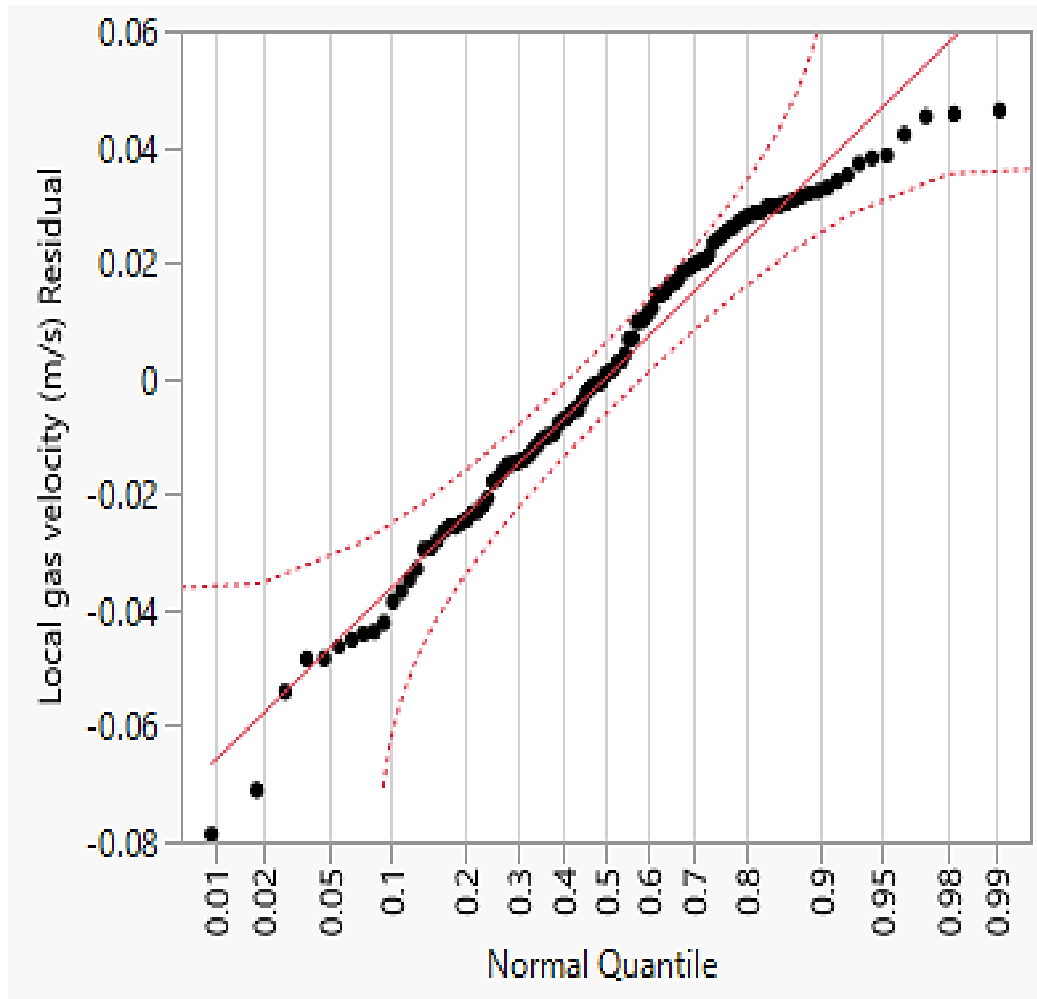


Figure 11. Residuals by normal quantile plot.

Figure 12 displays the goodness of fit between the measured local gas velocities and the predicted local gas velocities using the validated polynomial regression correlation. From Figure 11, it is obvious that the predictions of the correlation are in a very good agreement with the measured local gas velocities, as the differences between the measured and predicted gas velocities are all well within the  $\pm 10$ . The accuracy of the correlation can further be investigated by calculating the average absolute relative error (*AARE*) using the following equation (Eq11) (Ostertagová, 2012):

$$AARE = \frac{1}{N} \sum_{i=1}^{i=N} \frac{Ug_{predicted,i} - Ug_{experimental,i}}{Ug_{experimental,i}} \quad (11)$$

The *AARE* between the measured local gas velocities and the local gas velocities that were predicted by the polynomial correlation was equal to 1.47%, indicating a very high prediction accuracy of the correlation, which is due to the ability of the polynomial regression models to quantify the important interactions between the input features, which is very useful considering the complexity of the system studied.

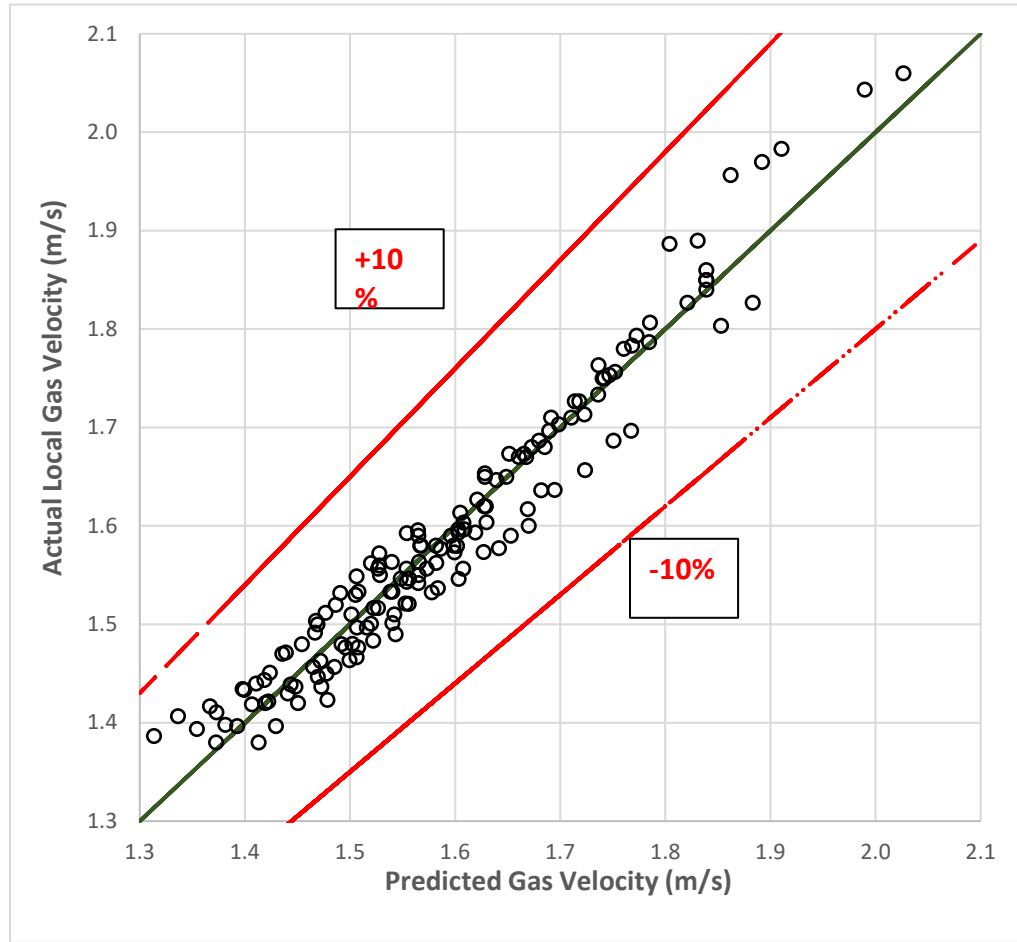


Figure 12. Goodness of fit plot.

**5.2.2. Test of Significance of the Input Features in the Correlation.** The significance test was conducted using Student's t-test, which ranks the terms of the correlation by the importance of their influence on the variation of the local gas velocity at the fully developed region of the bed (Neideen and Brasel, 2007). Student's t-test consists of a comparison between the  $t_{ratio}$  of each input feature with the  $t_{statistic}$  that is calculated based on the number of experiments and the degrees of freedom (Neideen and Brasel, 2007). A  $p_{value}$  less than **0.05** means that the term has a significant influence on the response with a confidence probability of **95%**. Due to the very low  $p_{values}$  when the terms have a very significant effect on the response, the **LogWorth** is calculated for each term as  $-\log_{10}(p_{value})$ , allowing better comparison of the significant of the terms in the correlation. The results obtained in Table 4 indicate that the flow conditions ( $Re$ ) have the most significant influence on the variation of the local gas velocity in the fully developed region of the pebble bed, as the gas velocity increases when increasing the superficial inlet gas velocity. However, this increase is not strictly linear due to the significant quadratic term  $Re^2$ , as well as the significant interactions between  $Re$  and the radial location  $\left(\frac{r}{R}\right)$  in the experimental column. As explained above and as found in Table 4, the radial location  $\left(\frac{r}{R}\right)$  considerably contributes to the variation of the response both linearly and non-linearly. On the other hand, the influence of the of the axial position  $\left(\frac{H}{D}\right)$  on the local gas velocity is insignificant in the fully developed region where the flow of the gas is equilibrated. The complex nature of the effect of the input features is better elucidated in the contour plots in Figure 13.

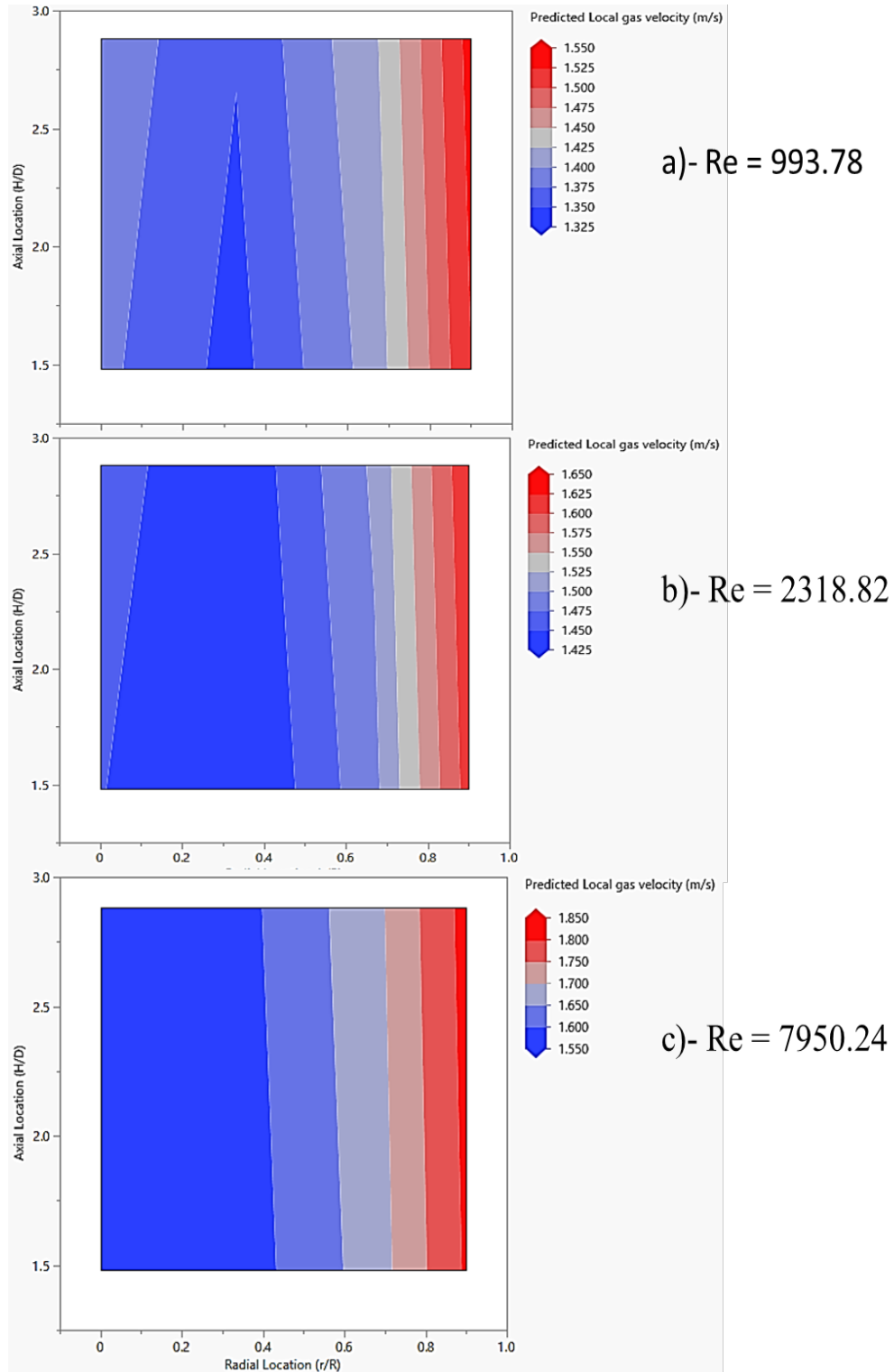








Figure 13. Contour plots showing the variation of the local gas velocity as a function of the radial and axial position in the experimental column at a)- Re = 993.78, b)- Re = 2318.82, and c)- Re = 7950.24.

Table 4. The results of student's t-test.

Source	Estimate	$p_{value}$	LogWorth	Graphical Comparison of LogWorth
$Re$	$6.7 \times 10^{-5}$	0.0000	46.536	
$\frac{r}{R}$	-0.2996	0.0000	45.643	
$\left(\frac{r}{R}\right)^2$	0.4937	0.0000	27.739	
$Re^2$	$-4.4 \times 10^{-9}$	0.0000	9.392	
$\left(\frac{r}{R}\right) \cdot Re$	$1.4 \times 10^{-5}$	0.00091	3.042	
$\frac{H}{D}$	0.0076	0.0545	1.263	

## 6. CONCLUSION

The local gas velocity inside the pebble bed reactor's core is one of the main factors that result in the non-uniformity of the local convection heat transfer in the PBR (Alshammari et al., 2023). Therefore, in this study, for the first time ever, the local gas velocities were measured in various radial locations and axial levels in an experimental pebble bed with a pebble diameter of 5 cm and an aspect ratio of 6. The advanced hot wire anemometry technique was equipped with a novel probe-protector case, which was developed inhouse at the Multiphase Flows and Reactors Engineering and Education Laboratory (mFReel) and used to conduct the experiments at various location and superficial inlet gas velocities, corresponding to both laminar and turbulent flow conditions ( $993.78 \leq Re \leq 7950.24$ ). The gas velocities were found to vary significantly, based on the radial and axial positions in the column with higher local velocities near the wall. The variation of the local gas velocity across the radius of the column can be linked to the

inhomogeneous void fractions in the pebble bed, which is higher near the wall, due to the effect of the wall-pebble contact. The variation of the gas velocity along the height of the bed was attributed to the non-uniformity of the void fractions, owing to the random packing of the pebbles.

This new approach for measuring the local gas velocity using the probe-protector case could be useful at larger bed height above the measurement locations to allow for the flow of the gas to equilibrate. However, the needed height for the flow to equilibrate varies with the aspect ratio of the bed. This can be determined by measuring the void structure at the level of the case and above it. Furthermore, a second order polynomial regression correlation was developed in order to link the experimental conditions with the variation of the local gas velocity in the fully developed region of the bed (the middle and bottom of the pebble bed) by a mathematical equation and to quantify the complex effects of the input features studied in this work and the interactions between them. These results clearly indicate the existence of a correlation between the local gas velocities and the forced convection heat transfer coefficients, which vary in similar fashion along the radius and height of the pebble bed as reported in the literature (Abdulmohsin and Al-Dahhan, 2015; Alshammari et al., 2023). The accurate local gas velocity measurements acquired in this work can be used to support and to validate the CFD simulations for the same design and operation conditions, coupled with heat transfer calculations, which will allow the validated CFD model to subsequently be used for the prediction of the convective heat transfer inside an actual PBR to be validated with the reported data in literature and with our data, which is to be published in subsequent manuscript.



## NOMENCLATURE

Symbol	Description	Unit
PBR	Pebble Bed Reactor.	(-)
HTGR	High Temperature Gas-Cooled Reactor.	(-)
HTGR-PB	High Temperature Gas-Cooled Reactor – Pebble Bed.	(-)
TRISO	Tristructural-isotropic fuel particle.	(-)
LOFA	Loss Of Flow Accident.	(-)
CFD	Computational Fluid Dynamics	(-)
DEM	Discrete Element Method	(-)
mFReel	Multiphase Flows and Reactors Engineering and Education Laboratory	(-)
HWA	Hot-Wire Anemometer	(-)
PIV	Particle Image Velocimetry	(-)
$W$	Joule heating to the wire	$J$
$h_w$	Convective heat transfer from the hot-wire to the flowing air	$w/m^2 K$
$A$	Heat surface area	$m$
$T_w$	Temperature of the wire	$K$
$T_f$	Temperature of the fluid	$K$
$I$	Current passing through the wire	$A$
$R_w$	The resistance of the wire	$\Omega$
$Re$	Reynolds number	(-)
$\varepsilon$	Average void of the bed.	(-)

$U_g$	Superficial inlet gas velocity	$m/s$
$\frac{H}{L}$	Axial position inside the column.	(-)
$\frac{r}{R}$	Radial position inside the experimental column.	(-)
$R^2$	Coefficient of determination	%
$AARE$	Average Absolute Relative Error.	%

## REFERENCES

1. Abdulmohsin, R.S., Al-Dahhan, M.H., 2017. Pressure drop and fluid flow characteristics in a packed pebble bed reactor. Nucl. Technol. 198, 17–25. <https://doi.org/10.1080/00295450.2017.1292818>
2. Abdulmohsin, R.S., Al-Dahhan, M.H., 2015. Characteristics of convective heat transport in a packed pebble-bed reactor. Nucl. Eng. Des. 284, 143–152. <https://doi.org/10.1016/j.nucengdes.2014.11.041>
3. Al-Juwaya, T., Ali, N., Al-Dahhan, M., 2019. Investigation of hydrodynamics of binary solids mixture spouted beds using radioactive particle tracking (RPT) technique. Chem. Eng. Res. Des. 148, 21–44. <https://doi.org/10.1016/j.cherd.2019.05.051>
4. Al-Juwaya, T., Ali, N., Al-Dahhan, M., 2017. Investigation of cross-sectional gas-solid distributions in spouted beds using advanced non-invasive gamma-ray computed tomography (CT). Exp. Therm. Fluid Sci. 86, 37–53. <https://doi.org/10.1016/j.expthermflusci.2017.03.029>
5. Al-Safran, E., 2009. Prediction of slug liquid holdup in horizontal pipes. J. Energy Resour. Technol. Trans. ASME 131, 0230011–0230018. <https://doi.org/10.1115/1.3120305>
6. Al Falahi, F., Al-Dahhan, M., 2016. Experimental investigation of the pebble bed structure by using gamma ray tomography. Nucl. Eng. Des. 310, 231–246. <https://doi.org/10.1016/j.nucengdes.2016.10.009>

7. Al Falahi, F., Mueller, G., Al-Dahhan, M., 2018. Pebble bed nuclear reactor structure study: A comparison of the experimental and calculated void fraction distribution. *Prog. Nucl. Energy* 106, 153–161.  
<https://doi.org/10.1016/j.pnucene.2018.03.006>
8. Alshammari, M., Alalou, A., Qi, B., Al-Dahhan, M.H., 2023. Investigation of Convective Heat Transfer in a Cold Flow Pebble Bed Nuclear Reactor [Unpublished Manuscript]. Dep. Chem. Biochem. Eng. Missouri Univ. Sci. Technol.
9. Alshammari, M., Bugis, A., Al-Dahhan, M., 2020. Designing an Experimental Tool to Protect The HWA inside The PBR core., in: *Experimental Thermal Hydraulics-III*. pp. 95–98.
10. Amini, N., Hassan, Y.A., 2014. Experimental study of bypass flow in near wall gaps of a pebble bed reactor using hot wire anemometry technique. *Ann. Nucl. Energy* 65, 60–71. <https://doi.org/10.1016/j.anucene.2013.09.046>
11. Atmakidis, T., Kenig, E.Y., 2009. CFD-based analysis of the wall effect on the pressure drop in packed beds with moderate tube/particle diameter ratios in the laminar flow regime. *Chem. Eng. J.* 155, 404–410.  
<https://doi.org/10.1016/j.cej.2009.07.057>
12. Calis, H.P.A., Nijenhuis, J., Paikert, B.C., Dautzenberg, F.M., Van Den Bleek, C.M., 2001. CFD modeling and experimental validation of pressure drop and flow profile in a novel structured catalytic reactor packing. *Chem. Eng. Sci.* 56, 1713–1720. [https://doi.org/10.1016/S0009-2509\(00\)00400-0](https://doi.org/10.1016/S0009-2509(00)00400-0)
13. Chen, L., Lee, W., Lee, J., 2017. Analysis of the thermal field and heat transfer characteristics of pebble beds packed in a face-centered cubic structure. *Appl. Therm. Eng.* 121, 473–483. <https://doi.org/10.1016/j.applthermaleng.2017.04.113>
14. Chen, L., Zhao, J., Yuan, Y., Lee, J., 2022. Numerical Study on the Thermal Field and Heat Transfer Characteristics of a Hexagonal-Close-Packed Pebble Bed. *Computation* 10. <https://doi.org/10.3390/computation10010001>
15. Christensen, R., 2018. Analysis of Variance, Design, and Regression. *Anal. Variance, Des. Regres.* <https://doi.org/10.1201/9781315370095>
16. Das, S., Deen, N.G., Kuipers, J.A.M., 2017. A DNS study of flow and heat transfer through slender fixed-bed reactors randomly packed with spherical particles. *Chem. Eng. Sci.* 160, 1–19. <https://doi.org/10.1016/j.ces.2016.11.008>

17. Fan, Y., Al-Safran, E., Pereyra, E., Sarica, C., 2020. Modeling liquid holdup in pseudo-slugs. *Int. Pet. Technol. Conf. 2020, IPTC 2020*. <https://doi.org/10.2523/19769-abstract>
18. Gui, N., Yang, X., Tu, J., Jiang, S., 2014. Effect of bed configuration on pebble flow uniformity and stagnation in the pebble bed reactor. *Nucl. Eng. Des.* 270, 295–301. <https://doi.org/10.1016/j.nucengdes.2013.12.055>
19. Hassan, Y., 2019. High-fidelity experimental measurements for modeling and simulation of nuclear engineering applications. *Nucl. Eng. Des.* 354, 110181. <https://doi.org/10.1016/j.nucengdes.2019.110181>
20. Hassan, Y.A., 2008. Large eddy simulation in pebble bed gas cooled core reactors. *Nucl. Eng. Des.* 238, 530–537. <https://doi.org/10.1016/j.nucengdes.2007.02.041>
21. Hassan, Y.A., Dominguez-Ontiveros, E.E., 2008. Flow visualization in a pebble bed reactor experiment using PIV and refractive index matching techniques. *Nucl. Eng. Des.* 238, 3080–3085. <https://doi.org/10.1016/j.nucengdes.2008.01.027>
22. Hassan, Y.A., Kang, C., 2012. Pressure drop in a pebble bed reactor under high reynolds number. *Nucl. Technol.* 180, 159–173. <https://doi.org/10.13182/NT12-A14631>
23. Hemmati, A., Ghaemi, A., Asadollahzadeh, M., 2021. RSM and ANN modeling of hold up, slip, and characteristic velocities in standard systems using pulsed disc-and-doughnut contactor column. *Sep. Sci. Technol.* 56, 2734–2749. <https://doi.org/10.1080/01496395.2020.1842890>
24. Jiang, S., Tu, J., Yang, X., Gui, N., 2021. Multiphase Flow and Heat Transfer in Pebble Bed Reactor Core, *Multiphase Flow and Heat Transfer in Pebble Bed Reactor Core*. <https://doi.org/10.1007/978-981-15-9565-3>
25. Jiang, S., Tu, J., Yang, X., Gui, N., 2019. A review of pebble flow study for pebble bed high temperature gas-cooled reactor. *Exp. Comput. Multiph. Flow* 1, 159–176. <https://doi.org/10.1007/s42757-019-0006-1>
26. Khane, V., Taha, M.M., Al-Dahhan, M.H., 2016. Experimental investigation of the overall residence time of pebbles in a pebble bed reactor (PBR) using radioactive pebble. *Prog. Nucl. Energy* 93, 267–276. <https://doi.org/10.1016/j.pnucene.2016.09.001>
27. Khane, V., Taha, M.M., Mueller, G.E., Al-Dahhan, M.H., 2017. Discrete element method-based investigations of granular flow in a pebble bed reactor. *Nucl. Technol.* 199, 47–66. <https://doi.org/10.1080/00295450.2017.1324729>

28. Khane, V.B., 2014. Experimental and Computational Investigation of Flow of Pebbles in a Pebble Bed Nuclear Reactor. Missouri University of Science and Technology.
29. Kim, H.-Y., 2019. Statistical notes for clinical researchers: simple linear regression 3 – residual analysis. *Restor. Dent. Endod.* 44, 1–8.  
<https://doi.org/10.5395/rde.2019.44.e11>
30. Koster, A., Matzner, H.D., Nicholsi, D.R., 2003. PBMR design for the future. *Nucl. Eng. Des.* 222, 231–245. [https://doi.org/10.1016/S0029-5493\(03\)00029-3](https://doi.org/10.1016/S0029-5493(03)00029-3)
31. Lee, J.J., Park, G.C., Kim, K.Y., Lee, W.J., 2007. Numerical treatment of pebble contact in the flow and heat transfer analysis of a pebble bed reactor core. *Nucl. Eng. Des.* 237, 2183–2196. <https://doi.org/10.1016/j.nucengdes.2007.03.046>
32. Lee, J.Y., Lee, S.Y., 2009. Flow visualization in the scaled up pebble bed of high temperature gas-cooled reactor using particle image velocimetry method. *J. Eng. Gas Turbines Power* 131, 1–4. <https://doi.org/10.1115/1.3098417>
33. Li, Y., Xu, Y., Jiang, S., 2009. DEM simulations and experiments of pebble flow with monosized spheres. *Powder Technol.* 193, 312–318.  
<https://doi.org/10.1016/j.powtec.2009.03.009>
34. Liu, L., Deng, J., Zhang, D., Gu, H., 2021. Review of the experimental research on the thermal-hydraulic characteristics in the pebble bed nuclear reactor core and fusion breeder blankets. *Int. J. Energy Res.* 45, 11352–11383.  
<https://doi.org/10.1002/er.5378>
35. Liu, L., Zhang, D., Li, L., Yang, Y., Wang, C., Qiu, S., Su, G.H., 2018. Experimental investigation of flow and convective heat transfer on a high-Prandtl-number fluid through the nuclear reactor pebble bed core. *Appl. Therm. Eng.* 145, 48–57. <https://doi.org/10.1016/j.applthermaleng.2018.09.017>
36. Meng, X., Sun, Z., Xu, G., 2012. Single-phase convection heat transfer characteristics of pebble-bed channels with internal heat generation. *Nucl. Eng. Des.* 252, 121–127. <https://doi.org/10.1016/j.nucengdes.2012.05.041>
37. Meyer, M.K., Fielding, R., Gan, J., 2007. Fuel development for gas-cooled fast reactors. *J. Nucl. Mater.* 371, 281–287.  
<https://doi.org/10.1016/j.jnucmat.2007.05.013>
38. Montgomery, D.C., Peck, E.A., Vining, G.G., 2013. Introduction to Linear Regression Analysis. John Wiley & Sons, Inc.

39. Mueller, G.E., 2012. A simple method for determining sphere packed bed radial porosity. Powder Technol. 229, 90–96. <https://doi.org/10.1016/j.powtec.2012.06.013>
40. Mueller, G.E., 2010. Radial porosity in packed beds of spheres. Powder Technol. 203, 626–633. <https://doi.org/10.1016/j.powtec.2010.07.007>
41. Mueller, G.E., 1992. Radial void fraction distributions in randomly packed fixed beds of uniformly sized spheres in cylindrical containers. Powder Technol. 72, 269–275. [https://doi.org/10.1016/0032-5910\(92\)80045-X](https://doi.org/10.1016/0032-5910(92)80045-X)
42. Nabielek, H., Kühnlein, W., Schenk, W., Heit, W., Christ, A., Ragoss, H., 1990. Development of advanced HTR fuel elements. Nucl. Eng. Des. 121, 199–210. [https://doi.org/10.1016/0029-5493\(90\)90105-7](https://doi.org/10.1016/0029-5493(90)90105-7)
43. Neideen, T., Brasel, K., 2007. Understanding Statistical Tests. J. Surg. Educ. 64, 93–96. <https://doi.org/10.1016/j.jsurg.2007.02.001>
44. Neill, J.W., Johnson, D.E., 1984. Testing For Lack Of Fit In Regression - A Review. Commun. Stat. - Theory Methods 13, 485–511. <https://doi.org/10.1080/03610928408828696>
45. Ostertagová, E., 2012. Modelling using polynomial regression. Procedia Eng. 48, 500–506. <https://doi.org/10.1016/j.proeng.2012.09.545>
46. Pioro, I.L., 2016. Handbook of Generation IV Nuclear Reactors, Handbook of Generation IV Nuclear Reactors. <https://doi.org/10.1016/C2014-0-01699-1>
47. Reger, D., Merzari, E., Balestra, P., Schunert, S., Hassan, Y.A., 2021. Comparison of pebble bed velocity profiles between high-fidelity and intermediate-fidelity codes. Int. Conf. Nucl. Eng. Proceedings, ICONE 4, 1–10. <https://doi.org/10.1115/ICONE28-65759>
48. Saraswathi K., S., Bhosale, H., Ovhal, P., Parlikkad Rajan, N., Valadi, J.K., 2021. Random Forest and Autoencoder Data-Driven Models for Prediction of Dispersed-Phase Holdup and Drop Size in Rotating Disc Contactors. Ind. Eng. Chem. Res. 60, 425–435. <https://doi.org/10.1021/acs.iecr.0c04149>
49. SAS, I. inc, 2021. JMP.
50. Schena, E., Massaroni, C., Saccomandi, P., Cecchini, S., 2015. Flow measurement in mechanical ventilation: A review. Med. Eng. Phys. 37, 257–264. <https://doi.org/10.1016/j.medengphy.2015.01.010>

51. Schröder, E., Class, A., Krebs, L., 2006. Measurements of heat transfer between particles and gas in packed beds at low to medium Reynolds numbers. *Exp. Therm. Fluid Sci.* 30, 545–558. <https://doi.org/10.1016/j.expthermflusci.2005.11.002>
52. Taha, M.M., Said, I.A., Usman, S., Al-Dahhan, M.H., 2019. Temperature and velocity instrumentation and measurements within a separate-effects facility representing modular reactor core. *Int. J. Therm. Sci.* 136, 148–158. <https://doi.org/10.1016/j.ijthermalsci.2018.10.024>
53. Taha, M.M., Said, I.A., Usman, S., Al-Dahhan, M.H., 2018. Natural convection inside heated channel of a facility representing prismatic modular reactor core. *AIChE J.* 64, 3467–3478. <https://doi.org/10.1002/aic.16185>
54. Wu, H., Gui, N., Yang, X., Tu, J., Jiang, S., 2017. Numerical simulation of heat transfer in packed pebble beds: CFD-DEM coupled with particle thermal radiation. *Int. J. Heat Mass Transf.* 110, 393–405. <https://doi.org/10.1016/j.ijheatmasstransfer.2017.03.035>
55. Wu, Z., Lin, D., Zhong, D., 2002. The design features of the HTR-10. *Nucl. Eng. Des.* 218, 25–32. [https://doi.org/10.1016/S0029-5493\(02\)00182-6](https://doi.org/10.1016/S0029-5493(02)00182-6)
56. Yang, X., Gui, N., Tu, J., Jiang, S., 2014. 3D DEM simulation and analysis of void fraction distribution in a pebble bed high temperature reactor. *Nucl. Eng. Des.* 270, 404–411. <https://doi.org/10.1016/j.nucengdes.2014.02.010>
57. Yildiz, M.A., Botha, G., Yuan, H., Merzari, E., Kurwitz, R.C., Hassan, Y.A., 2020. Direct Numerical Simulation of the Flow through a Randomly Packed Pebble Bed. *J. Fluids Eng. Trans. ASME* 142, 1–14. <https://doi.org/10.1115/1.4045439>
58. Zhang, Z., Dong, Y., Li, F., Zhang, Z., Wang, H., Huang, X., Li, H., Liu, B., Wu, X., Wang, H., Diao, X., Zhang, H., Wang, J., 2016. The Shandong Shidao Bay 200 MWe High-Temperature Gas-Cooled Reactor Pebble-Bed Module (HTR-PM) Demonstration Power Plant: An Engineering and Technological Innovation. *Engineering* 2, 112–118. <https://doi.org/10.1016/J.ENG.2016.01.020>
59. Zou, L., Hu, G., O’Grady, D., Hu, R., 2022. Explicit modeling of pebble temperature in the porous-media model for pebble-bed reactors. *Prog. Nucl. Energy* 146, 104175. <https://doi.org/10.1016/j.pnucene.2022.104175>

## II. INVESTIGATION OF CONVECTIVE HEAT TRANSFER IN A COLD FLOW PEBBLE BED NUCLEAR REACTOR

Muhna Alshammari [1,3], Ahmed Alalou [2,5], Binbin Qi [2], Muthanna H Al-Dahhan [1,2,4]\*

<sup>[1]</sup> Nuclear Engineering and Radiation Science Department, Missouri University of Science and Technology, Rolla, MO 65409, USA.

<sup>[2]</sup> Linda and Bipin Doshi Chemical and Biochemical Engineering Department, Missouri University of Science and Technology, Rolla, MO 65409, USA.

<sup>[3]</sup> National Center for Nuclear Technology, King Abdulaziz City for Science and Technology, Riyadh, Kingdom of Saudi Arabia.

<sup>[4]</sup> TechCell, Mohammed VI Polytechnic University, Lot 660, Hay Moulay Rachid 43150, Ben Guerir, Morocco.

<sup>[5]</sup> Applied Organic Chemistry Labs, Faculty of Sciences and Technologies, Sidi Mohammed Ben Abdellah University, B.P. 2202 Fez, Morocco.

### ABSTRACT

The aim of this study was to investigate the local heat transfer coefficients between the pebbles and the coolant gas in a PBR using a sophisticated and advanced measurement technique that consists of a heated pebble probe, a micro-foil heat flux sensor flushed mounted on the surface of the heated pebble probe, and a thermocouple in the center of bed void in front the sensor. In this work, the local heat transfer coefficients were measured along various axial levels, and radial and angular locations at different superficial inlet gas velocities that cover both laminar and turbulent flow conditions. The local heat transfer coefficients were found to be higher near the wall due to higher volumetric flow at the wall where larger bed void exists compared to the center region of the bed where the flow of gas in packed bed follows the least resistance path. High deviations were obtained between



the experimental overall heat transfer in the bed and the predictions of four correlations reported in the literature. Furthermore, these correlations cannot predict the local heat transfer coefficients inside the PBR. This necessitates the development of new correlations for the prediction of the local heat transfer coefficients using the obtained data of this work. A pseudo-3D correlation was developed and found to provide accurate predictions, with an averaged absolute relative error (*AARE*) of 3.33% at high Reynolds numbers of our operation and design conditions.

## 1. INTRODUCTION

The very high-temperature nuclear reactors (VHTRs) or high-temperature gas-cooled nuclear reactors (HTGRs) have been designated by the energy policy act of 2005 to represent the Next Generation Nuclear Plants (NGNP), also termed as Generation IV (Gen-IV) nuclear plants, which are characterized with sustainability, high efficiency, proliferation-resistance, safety, and reliability (Koster et al., 2003; Yamoah et al., 2012).

Pebble Bed Reactors (PBRs) are one type of the proposed HTGRs, which are being studied and developed in a race between different countries that have launched major programs to commercialize these reactors (Jiang et al., 2021). In PBRs, thousands of TRISO nuclear fuel particles are placed in 6 cm diameter composite graphite pebbles. Each TRISO particle consists of a fuel kernel (i.e., uranium  $^{235}\text{U}$  or mixed fissile materials) enveloped by four layers of carbon and ceramic for containment of the fission product (Abdulmohsin and Al-Dahhan, 2015; Almusafir et al., 2023). The pebbles move downward where graphite pebbles move in the central zone while the pebbles of TRISO nuclear fuel particles move in the annulus zone (Al-Juwaya et al.,

2019, 2017; Almusafir et al., 2023). At the outlet of the reactor's core, one pebble is taken at a time and is checked for burnup. The pebble is returned to the core if it is still active and is removed if it is completely burned up and a new pebble is inserted.

The PBRs are built and developed to be cooled by Helium gas coolants and moderated by graphite pebbles, and reflector blocks that are characterized by high thermal conduction and are used to control the heat released either during normal operations or during the loss of flow accidents (LOFA) for the protection of the core from reaching the melting point (Kadak, 2005). During normal operations, the coolant flows at a range of high Reynolds numbers ( $Re$ ) and passes downward through the voids between the hot fuel and graphite pebbles to remove the heat released due to the fission reaction. The coolant Helium gas temperature may reach elevated temperatures (i.e., up to over  $1000^{\circ}\text{C}$ ) before leaving the reactor (Yamoah et al., 2012). In the case of a LOFA, this forced cooling system is lost and natural circulation of the coolant Helium gas is stimulated because of the temperature differences in the reactor. Licensing all nuclear reactors, including the PBR, necessitates fulfilling high safety standards and high operation efficiency. In PBRs, heat transfer from the pebbles to the flowing coolant helium gas is one of the most important operating, design, and safety parameters (Kadak, 2005).

It is noteworthy that, the heat transfer occurs inside the PBR in different mechanisms (Figure 1) such as (Abdulmohsin, 2013; Abdulmohsin et al., 2011; Abdulmohsin and Al-Dahhan, 2017, 2010):

- Conduction heat transfer (i.e., pebble to pebble, pebble to the wall, etc.)
- Convection heat transfer (i.e., pebble to flow coolant gas)

- Radiation heat transfer (i.e., pebble to pebble, pebble to wall or core reflector, and core barrel to the wall)

The complex nature of heat transfer in PBR necessitates various types of studies to characterize heat transfer and predict the distribution of temperatures that are needed for designing, operating, safety analysis and scaling up PBRs. Although all of these mechanisms can occur simultaneously, forced convection is the governing mechanism during the normal operation of the PBRs (Achenbach, 1995). Therefore, many theoretical, empirical, and experimental studies have been conducted to characterize convective heat transfer in PBRs. *Rimkevicius et al., 2006* and *Rimkevicius and Uspuras, 2008* investigated heat transfer in two different configurations of air-cooled pebble beds at different Reynolds numbers (i.e.,  $500 < Re < 35000$ ). The heat transfer coefficient was estimated by using thermocouples to measure the temperatures of an electrically heated copper sphere and adjacent air gas while the heat flux was determined by the measurements of the input electrical energy. *Liu et al., 2020, 2018* characterized convective heat transfer in Fluoride-salt and water-cooled PBR test facility. In both studies, carbon steel pebbles with different diameters (i.e., 0.008 and 0.01 m) were heated by an electromagnetic induction heating coil surrounding the test column. Thermocouples were utilized for the measurement of the temperatures of the heated pebbles and the adjacent coolant fluid (i.e., water). The heat transfer coefficients were estimated by using temperature measurements along with the input power value induced by the heating system. The same concept was adopted by *Nazari et al., 2017* to investigate the effect of steel pebbles diameter (i.e., 0.0055, 0.0065, and 0.0075 m), coolant gas (i.e., air) velocity (i.e.,  $4500 < Re < 10,000$ ), and internal heat generation (i.e., 54 W to 82 W) on the forced convection heat transfer under turbulent flow

regime conditions. Heat transfer by conduction and radiation was disregarded in these studies. However, the pebbles used were made of metals with high thermal conductivities enough to influence the temperatures of the surrounding pebbles. Therefore, *Schröder et al., 2006* used a wire mesh to surround the heated pebble to minimize interactions between the heated pebble and its surroundings. Additionally, the high conductivity of the pebbles used may lead to uncertainties in the constant surface temperature assumption adopted to estimate the heat flux by the direct energy input method (Abdulmohsin and Al-Dahhan, 2015). The bed structure and porosity are reported to significantly influence the local heat transfer coefficients in a PBR, due to the variation of the actual local velocity of the fluid depending on the void fractions inside the bed (Auwerda et al., 2011). *Al Falahi et al., 2018* and *Al Falahi and Al-Dahhan, 2016* showed that for a bed structure with an aspect ratio ( $D/d_p$ ) of 6, the distribution was non-uniform with larger void fractions near the wall of the column due the contact between the wall and the pebbles. Similar results were reported in a Discrete Element Method (DEM) simulation by *Khane et al., 2017*. The effect of the local gas velocity in pebble bed is only reported in the work of *Alshammari et al., 2023b*, where the local gas velocities were measured for the first time using a Hot Wire Anemometer at different location in a pebble bed with a bed diameter to pebble diameter ratio of 6. The results showed clearly that the local gas velocities are higher at the wall region compared to the center of the bed, regardless of the axial location in the bed. In order to confirm the relationship between the local gas velocity in the pebble bed and the local heat transfer coefficients, measurements of the local heat transfer coefficients at the same locations in the same bed should be taken, which is the objective of this work.

To overcome the shortcomings related to the measurement of the convective heat transfer coefficients, in our Multiphase Flows and Reactors Engineering and Education Laboratory (mFReel), *Abdalmohsin and Al-Dahhan, 2015* developed and implemented a noninvasive new heat probe in the form of a pebble and reported reliable measurements of convective heat transfer coefficients in a PBR operating at different gas (i.e., air) velocities (i.e., 0.02 to 2 m/s) and at a different local central line positions inside the packed bed core. Details of the principles of the newly developed heat transfer probe are discussed in the following sections. Indeed, other measurement techniques were used in previous studies to characterize heat transfer in PBRs such as the mass transfer analogy or the regenerative heating technique. However, our newly developed heat transfer probe is characterized by its simplicity, reliability and accuracy. Various parameters impact the heat transfer convection in a pebble bed reactor. Nevertheless, the best way to characterize the heat transfer behavior is using dimensionless groups such as the Reynold number ( $Re$ ), Nusselt number ( $Nu$ ), and Prandtl number ( $Pr$ ). The relationship between these dimensionless groups can be described using the following expression (Eq.1)

$$Nu = f(\varepsilon, Re, Pr) \quad (1)$$

where  $\varepsilon$  is the bed porosity.

Each dimensionless group  $Nu$ ,  $Re$ , and  $Pr$  can be calculated by the following equations:

$$Nu = \frac{h d_p}{k} \quad (2)$$

where  $h$  is the heat transfer coefficient ( $kW / m^2 . K$ ),  $d_p$  is the diameter of the pebble (m) and  $k$  is the thermal conductivity of flowing gas ( $kW / m . K$ ).

$$Re = \frac{\rho U_g d_p}{\mu} \quad (3)$$

where  $\rho$  is the density of the fluid ( $\text{kg/m}^3$ ),  $U_g$  is the superficial gas velocity ( $\text{m/s}$ ) and  $\mu$  is the dynamic viscosity of fluid ( $\text{kg / m.s}$ ).

$$Pr = \frac{\mu C_p}{k} \quad (4)$$

where  $C_p$  is the heat capacity in  $\text{J/kg.k}$ .

*Abdalmohsin and Al-Dahhan, 2015* has previously developed and used our non-invasive measurement technique to measure the forced convective heat transfer coefficient in a pebble-bed reactor of a diameter of 0.3 m and aspect ratio ( $D/dp$ ) of 6. In this study, the heat transfer coefficient was measure at three axial locations (top, middle and bottom of the column) and four radial (diameter) positions ( $r/R = 0.0, \pm 0.33, \pm 0.67$ , and  $\pm 0.9$ ) at inlet superficial gas velocities that ranged from 0.02  $\text{m/s}$  to 2  $\text{m/s}$ , covering both laminar and turbulent flow of the gas in the column. The heat transfer coefficient showed great dependence on the superficial inlet gas velocity and on the radial position as well. However, these measurements were taken over one angular location at each radius, without consideration of other angular locations where the heat transfer coefficients might be different since the distribution of the void fractions in the bed is non-uniform, particularly in the wall region (*Abdalmohsin and Al-Dahhan, 2015*). *Abdalmohsin and Al-Dahhan, 2015* and *Abdalmohsin, 2013* evaluated various empirical heat transfer coefficients reported in the literature and they found that the *KTA, 1983* correlation predicts their results better than the others at high superficial inlet gas velocity (Achenbach, 1995; Gnielinski, 1978; Wakao and S, 1982). However, it is important to note that the equation used for averaging the local heat transfer in the work of *Abdalmohsin and Al-Dahhan, 2015* was

wrong, as reported in *Abdulgohsin and Al-Dahhan, 2016*, and hence, the results of the comparison between the averaged heat transfer coefficient and the correlations cannot be considered as reliable.

Therefore, the objectives of the current study are to complement the work of *Abdulgohsin and Al-Dahhan, 2015* by manufacturing our new heat transfer probe, and to provide reliable heat transfer coefficients measurements at various angular and radial locations along the bed height to advance the knowledge on the local distribution of the heat transfer coefficients and how it is affected by the void structure in a pebble bed with a low column diameter to pebble diameter ratio ( $D/d_p$ ) of 6. Low ( $D/d_p$ ) was used to represent the wall region in the PBRs and the region of non-uniform void distribution for which the data will be useful as benchmark data to validate CFD simulations with heat transfer calculations that can estimate the heat transfer coefficients and for the evaluation and development of heat transfer coefficients correlations.

To achieve this objective, the convective heat transfer coefficients were measured at three axial levels in the column, where at each axial level, the measurements were taken at seven radial (diameter) positions ( $r/R = 0.0, \pm 0.33, \pm 0.67, \text{ and } \pm 0.9$ ) along four angular planes (X, Y, Z, and L). The superficial inlet gas velocity was also varied from 0.3 to 2 m/s in order to cover both laminar and turbulent flow of the gas in the column. The overall convective heat transfer coefficient, calculated based on the local heat transfer data, was compared with the predictions of three correlations which were developed by *Gnielinski, 1978; Wakao and S, 1982; KTA, 1983* and *Achenbach, 1995*. Additionally, we developed a pseudo-3D model for the prediction of the local heat convective heat transfer coefficients within our experimental domain.

The experimental local heat transfer data obtained in this work is vital for validating computational fluid dynamics (CFD) simulation and heat transfer calculation that can estimate the heat transfer coefficients in the measured locations, and for the future new numerical correlations particularly for the regions near the walls.

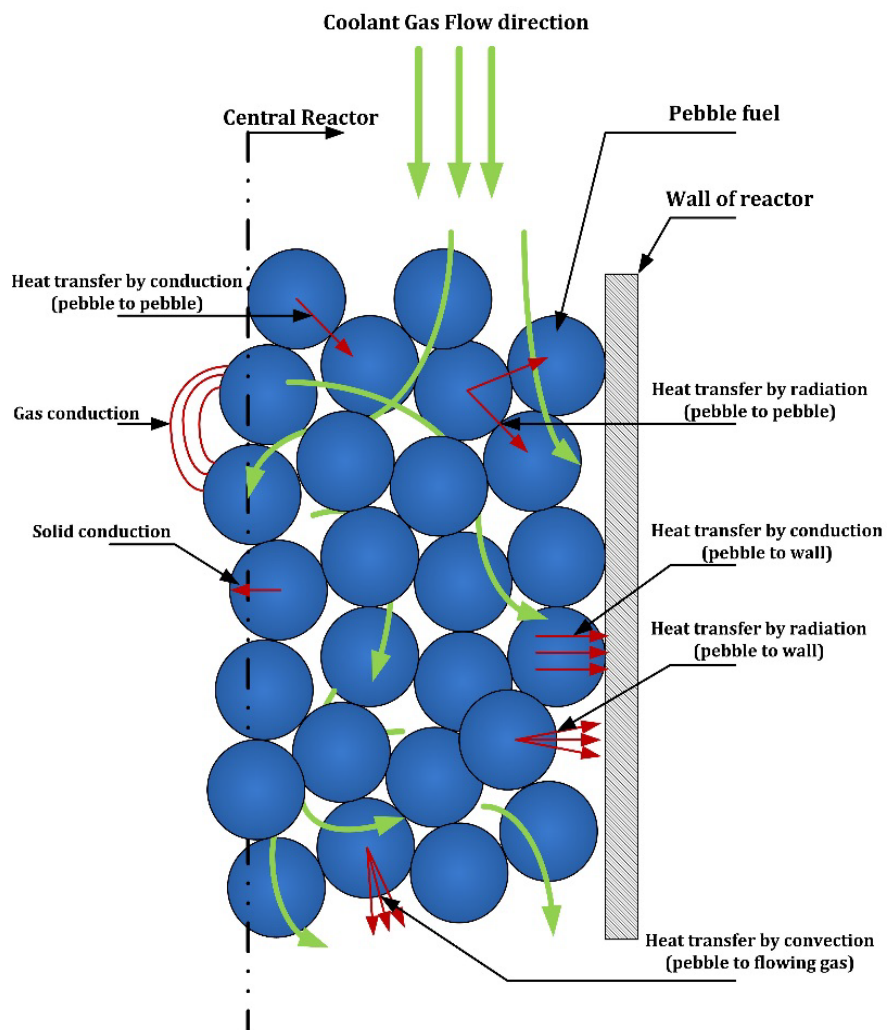


Figure 1. Illustration of the heat transfer mechanisms inside the pebble bed reactor.



## 2. EXPERIMENTAL WORK

### 2.1. EXPERIMENTAL SETUP

The cold flow pebble bed reactor setup used in the current study was designed and built in our laboratory as shown in Figure 2(a). In real PBRs, pebbles slowly move downward by gravity inside the reactor core and leave the core from the bottom to be examined through the burnup level measurement to determine whether they are to be recycled or replaced, while Helium gas as a coolant flows downward at very high flow rate (Abdulmohsin and Al-Dahhan, 2015; Koster et al., 2003). Therefore, due to the high differences between gas velocities and pebbles' movement speed inside the bed, in the current study, and to simplify the experiments, the pebbles were maintained stagnant as a fixed bed in the column (Abdulmohsin and Al-Dahhan, 2015; Nazari et al., 2017). This cold flow pebble bed consists of a plexiglass column with a height and a diameter of 0.9 m and 0.3 m, respectively. A conical-shaped plenum with 30 cm in diameter and a height of 10 cm was mounted on top of the column as shown in Figure 2(b), while a plastic cone with a diameter of 30 cm and a height of 8 cm was placed at the bottom of the column. This cone contains an opening with a diameter of 5 cm in the center to vent gas. A distributor plate containing 140 holes, each 0.03 cm in diameter, (shown in Figure 2 (c)) was placed between the upper plenum and the column to uniformly distribute the inlet gas into the column, which is randomly packed with glass pebbles that are 5 cm in diameter, and hence the column diameter to pebbles diameter ratio is 6. This size of the glass pebbles was easy to obtain and close to the size of real pebbles of 6 cm in diameter. The bed porosity ( $\varepsilon_b$ ) was estimated by the direct balance method and found to be 0.397. This

method consists of calculating the volume occupied by the pebbles as well as the volume of the empty column. The number of the pebbles in the column is known as well as the diameter of each pebble, which is equal to 5 cm, with the assumption that the glass pebbles are perfect spheres. This volume occupied by the pebbles is then subtracted from the total volume of the empty column, which is calculated using the column dimensions, in order to obtain the volume of the void. This volume is then divided by the total volume of the column to attain the fraction of the column that is occupied by the void (i.e. average bed porosity). During experimentation, dry and oil-free compressed air was introduced from the top of the column, from where it flows downwards through the void in the bed, and finally exits through the bottom outlet half-cone with a  $60^\circ$  angle. The gas flow rate was measured and controlled by two parallel rotameters (Omega HFL6715A-0045-14) as shown in Figure 2(a).

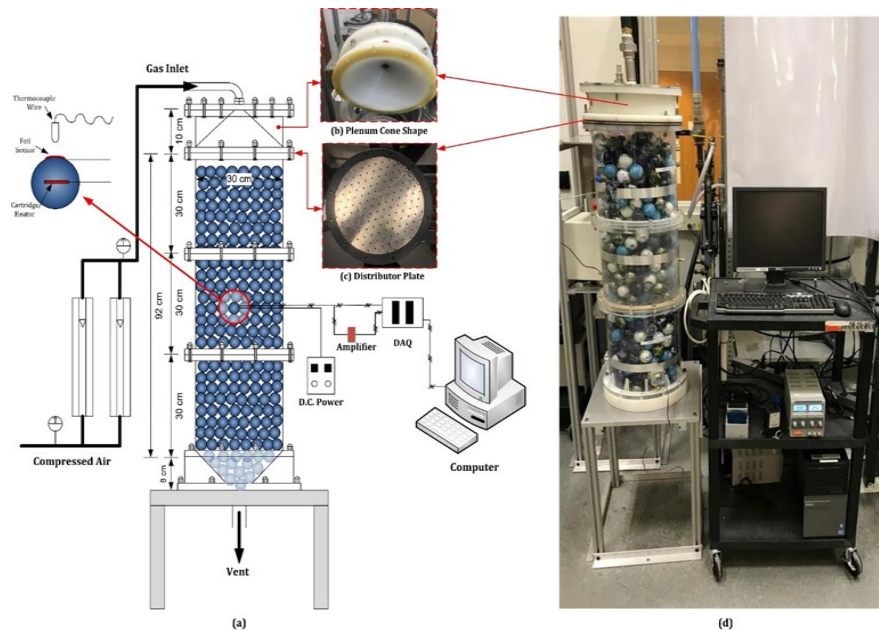


Figure 2. (a) Schematic diagram of the cold flow pebble bed experimental setup, (b) plenum cone shape, (c) distributor plate, and (d) setup picture.

## 2.2. HEAT TRANSFER COEFFICIENT MEASUREMENT TECHNIQUE

The heat transfer coefficient was quantified using a sophisticated non-invasive spherical heat transfer probe, as shown in Figure 3. This probe was manufactured in-house at our Multiphase Flows and Reactors Engineering and Education Laboratory (mFReel) (Abdulmohsin and Al-Dahhan, 2015). The principle of the technique was adapted and modified based on the work of *Li and Prakash, 1997* and *Wu et al., 2007*.

The operating principle of this technique is based on measuring heat flux by a sensor, surface temperature of the sensor and the bulk temperature in front of the sensor to directly estimate the time series of heat transfer coefficients between differently heated or heated/unheated pebbles. For this purpose, *Abdulmohsin and Al-Dahhan, 2015* manufactured a spherical-shaped probe that is made of copper, has the same diameter as the glass pebbles (i.e., 5 cm) and can be placed at different locations in the packing as a part of the packing structure (Figure 3 (a)). This pebble was heated by embedding an electrical cartridge heater (Chromalox, model number CIR-1012), illustrated in Figure 3(b), inside the copper sphere to heat up its surface. The heating intensity of this heater was controlled by a D.C power supply with a range of 20 – 40 V. A fast response heat transfer micro-foil sensor (Mdf Corporation No. 20453-1), with dimensions of (11 mm × 11 mm × 0.08 mm), was flush mounted on the outer surface of the copper sphere to obtain instantaneous measurements of the local heat flux ( $q_i$ ) from a hot surface sensor to the adjacent surroundings and surface temperature of the copper sphere ( $T_{si}$ ) as shown in Figure 3(a) (Abdulmohsin and Al-Dahhan, 2015). An amplifier was placed between the heat flux sensor and the data acquisition (DAQ) system which was used to convert and amplify the microvolts signal indicating the heat flux. These foil sensors were implemented

successfully in both single-phase systems (Abdulmohsin and Al-Dahhan, 2015; Taha et al., 2019) and multiphase systems (Kagumba et al., 2019; Wu et al., 2007). Additionally, a thermocouple (T-type K) was placed in the void directly in front of the sphere probe and its micro-foil sensor to measure the temperature of the surrounding medium, called bulk temperature ( $T_{bi}$ ). In contrast to the flux foil sensors, thermocouples are directly connected to the DAQ. Due to the low thermal conductivity of the glass balls, it is reasonable to neglect the heat loss from the contact between the spherical heat transfer probe and the glass balls.

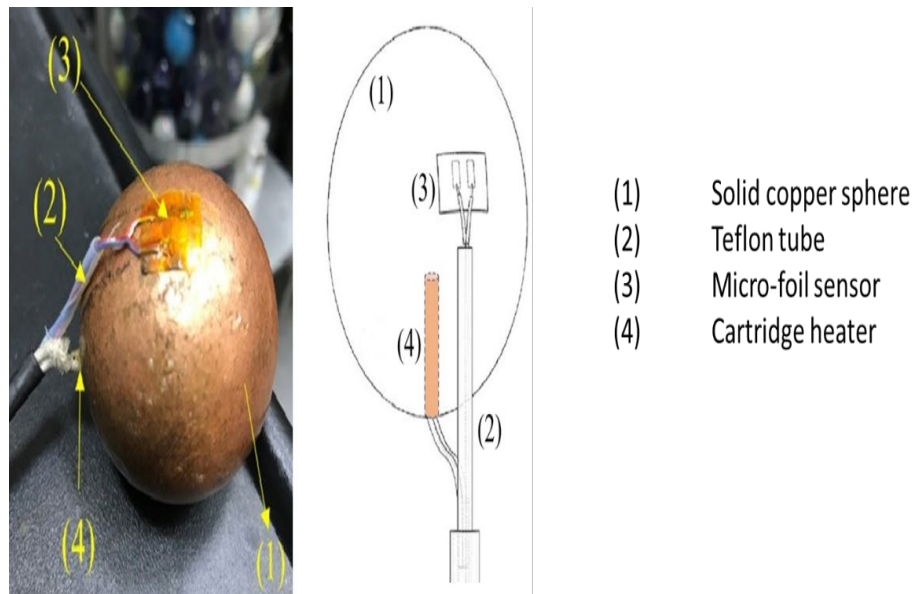


Figure 3. Picture of the heat transfer pebble probe technique and schematic of the pebble probe.

### 2.3. EXPERIMENTAL CONDITIONS

Heat transfer coefficients between the electrically heated copper sphere and the flowing gas were measured at different superficial gas velocities and different locations of

the heat transfer problem inside the packing as mentioned above. The superficial inlet gas velocities used in this study are  $U_g = 0.3, 0.6, 1.2, 1.6$  and  $2 \text{ m/s}$ , ) covering both laminar and turbulent flow conditions ( $Re = 993.78, 1987.56, 3975.12, 5300.16$ , and  $6625.20$ ).

Three axial levels, which were measured as the distance from the top of the distributor, were used to measure the cross sectional distribution of the heat transfer coefficient;

$$(H1 = 21.6 \text{ cm}, \left(\frac{H}{D}\right) = 0.72, H2 = 44.5 \text{ cm}, \left(\frac{H}{D}\right) = 1.48, H3 = 86.4 \text{ cm}, \left(\frac{H}{D}\right) = 2.88).$$

As shown in Figure 4(a). Furthermore, at each axial level, The copper pebble probe was moved and placed at different angular locations in each plane of the cross-section (i.e., X, Y, Z, and L), the heat transfer was characterized at seven radial locations to measure four diameters profiles of heat transfer coefficients at each axial level ( $r/R = 0.0, \pm 0.33, \pm 0.67$ , and  $\pm 0.9$ ) that were positioned as shown in Figure 4(b). To change the location of the pebble, the column was emptied of the pebbles and then repacked with the pebbles again, with the copper pebble probe being placed at the location where the measurement is supposed to be taken, as shown in Figure 4.

The test section of the column was repacked carefully in the same structure throughout the experiments to prevent any contact between the surface of the sensor and the surface of the surrounding pebbles. In the other parts of the column, the pebbles were repacked randomly, and the heat transfer coefficient was measured at all the superficial inlet gas velocities studied, before moving the copper pebble probe to the next location in the same way, by unpacking and repacking the pebbles in the column.

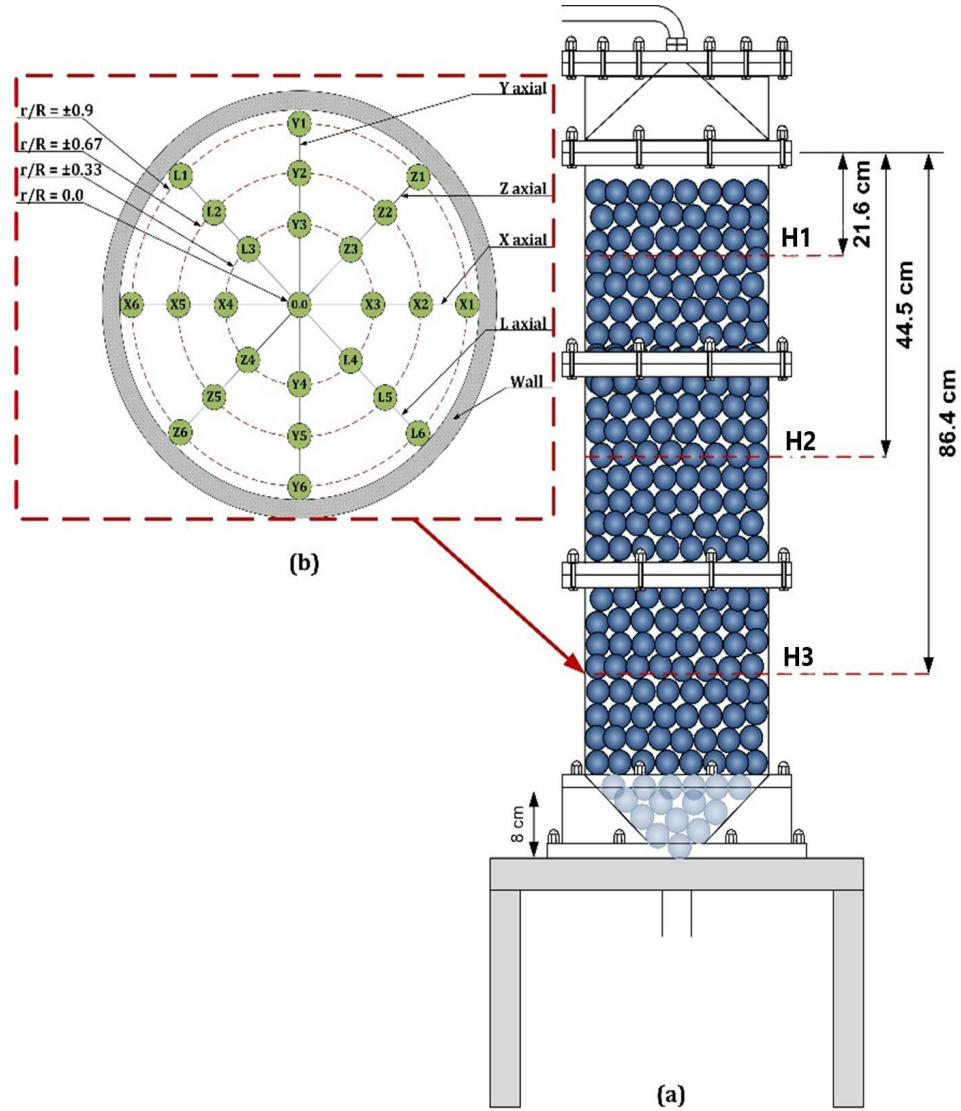


Figure 4. (a) Schematic showing the three axial levels H1  $\left(\left(\frac{H}{D}\right) = 0.72\right)$ , H2  $\left(\left(\frac{H}{D}\right) = 1.48\right)$ , and H3  $\left(\left(\frac{H}{D}\right) = 2.88\right)$ , (b) Schematic of measurement locations at different radial and angular positions for each axial level.

### 3. DATA COLLECTION AND ANALYSIS

Preliminary experiments were conducted to determine the time needed to reach thermal stability. This time is defined as the time after which the differences between the

temperatures of the bulk and the surface of the copper pebble probe were almost maintained constant, as shown by the plateau in

Figure 5. The system should be running for at least 30 min before collecting data to ensure reaching steady-state conditions. Hence, all the measurements in this study were obtained after 35 minutes of the experiment's start.

In this study, the amplified heat flux signals and the thermocouple signals were collected at a sampling frequency of 50 Hz. The sampling time of collecting data was tested by plotting the instantaneous heat transfer coefficients as a function of sampling time as shown in Figure 6. Therefore, Figure 6 reveals that no significant variation in the heat transfer coefficients occurs after surpassing a sampling time of 200s. Hence, all measurements were conducted after 35 min from the initial operation and 240s of sampling time. Instantaneous heat transfer coefficients ( $h_i$ ) were obtained by using the following equation 5 (Abdulmohsin and Al-Dahhan, 2015):

$$h_i = \frac{q_i}{T_{si} - T_{bi}} \quad (5)$$

where  $q_i$  is the instantaneous heat flux measured by the sensor,  $T_{si}$  is the instantaneous temperature of the sensor probe surface, and  $T_{bi}$  is the instantaneous bulk temperature of the fluid media.

Since the measurement technique was operated at a frequency of 50 Hz and a sampling time of 240 s. The time-averaged heat transfer coefficients ( $h$ ) were estimated at each location by averaging the instantaneous heat transfer data collected as follows:

$$h = \frac{1}{N} \sum_{i=1}^N h_i = \frac{1}{N} \sum_{i=1}^N \frac{q_i}{T_{si} - T_{bi}} \quad (6)$$

where  $N$  is the total number of experimental samples ( $N = 12000$ ) for 240 seconds.

As mentioned earlier, the measurements were taken at different axial levels  $H1$ ,  $H2$ , and  $H3$  as shown in Figure 2(a). At each axial level, measurements were obtained at four different radial positions ( $r/R = 0.0, \pm 0.33, \pm 0.67$ , and  $\pm 0.9$ ) for different angular planes (X, Y, Z, and L). Accordingly, the averaged heat transfer coefficients ( $h_{avg}$ ) at each radial position were obtained by azimuthally averaging the time-averaged heat transfer coefficient as shown below (7):

$$h_{avg}|_{r/R} = \frac{1}{n} \sum_{i=1}^n h(\theta) \quad (7)$$

where  $n$  is the number of locations or data points obtained at each radial position for each angular plane (i.e.,  $n = 4$ ).

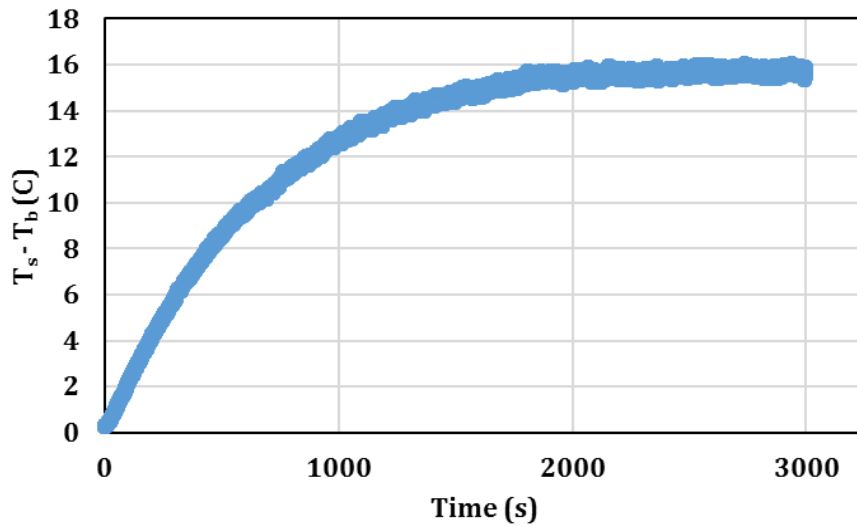


Figure 5. Time series of the difference between the temperatures of the bulk and the surface of the copper pebble probe.



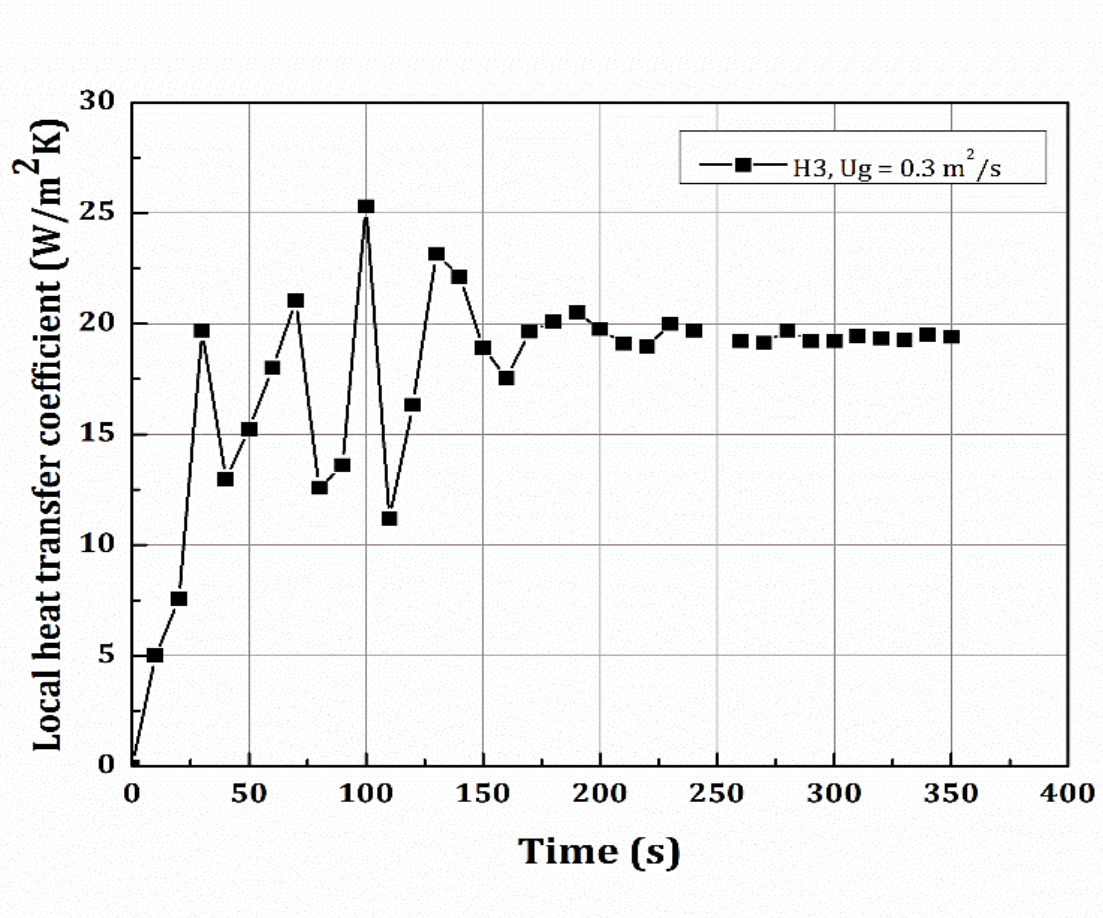


Figure 6. The stability of the heat transfer coefficients as function of the sampling time.

#### 4. RESULT AND DISCUSSION

As mentioned earlier the local heat transfer coefficient measurements were taken at three axial locations, which are located at different distances from the top distributor, specifically:

$$(H1 = 21.6 \text{ cm}, \left(\frac{H}{D}\right) = 0.72, H2 = 44.5 \text{ cm}, \left(\frac{H}{D}\right) = 1.48, H3 = 86.4 \text{ cm}, \left(\frac{H}{D}\right) = 2.88).$$

At each axial position, the pebble probe was placed at four different angular places (i.e.,  $X, Y, Z$ , &  $L$ ) and seven radial locations ( $r/R = 0, \pm 0.33, \pm 0.67, \text{ and } \pm 0.9$ ) for each diameter line ( $X, Y, Z$ , &  $L$ ).

Figure 7,8,and 9 show the local convective heat transfer coefficients in the column at three different superficial inlet gas velocities ( $0.3 \text{ m/s}$ ,  $1.2 \text{ m/s}$  &  $2 \text{ m/s}$ ) at the top, middle and bottom of the column, respectively. The experiments were repeated three times at each location, with a repeatability error of  $\pm 0.5 \text{ W/m}^2\text{K}$  and a repeatability standard deviation of 0.56. From these figures, it is apparent that the local heat transfer coefficients obtained at the same radial position vary with the angular location ( $X, Y, Z$ , and  $L$ ), where the structure of the test bed is being maintained the same for all the measurements where the structure of the test bed is being maintained the same for all the measurements. The variation at the same radial positions is further elucidated in the diameter profiles of the local heat transfer coefficients (Figure 10, 11, and 12). It can be seen that the differences in the heat transfer coefficients at the same radial positions are more pronounced at a low and moderate superficial inlet gas velocities ( $0.3 \text{ m/s}$  and  $1.2 \text{ m/s}$ ). This is especially the case at the top level  $\left(\left(\frac{H}{D}\right) = 0.72\right)$  of the column, where the highest percentage difference between two local heat transfer values at the same radius from the center was as high as 20.4% between the angular planes  $Z$  and  $L$ , in the region near the wall of the column ( $r/R = \pm 0.9$ ), at a superficial inlet gas velocity of  $0.3 \text{ m/s}$ .

In the same radial location and under the same superficial inlet velocity, the highest percentage differences in the local heat transfer coefficients at the middle of the bed  $\left(\left(\frac{H}{D}\right) = 1.48\right)$  was found to be 7.31% between the angular locations  $Y$  and  $L$ , while at bottom of the bed  $\left(\left(\frac{H}{D}\right) = 2.88\right)$ , the highest percentage difference was found to be 12.03% between the angular locations  $X$  and  $L$ . These variations in the local heat transfer coefficients at the four different angular planes ( $X, Y, Z$ , and  $L$ ) for the same azimuth are

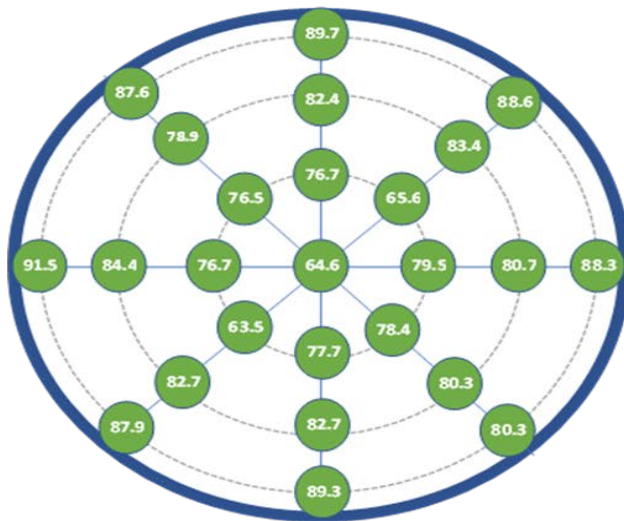
not confined to the near-wall region of the column, but are also observed in the annular regions near the center of the column as the heat transfer coefficient difference between the angular location  $Z$  and  $L$ , at a dimensionless radial profile of 0.33 was as high as 18.94% at the top axial level  $\left(\left(\frac{H}{D}\right) = 0.72\right)$  of the column for a moderate superficial inlet gas velocity of 1.2 m/s. For the same superficial inlet gas velocity (1.2 m/s), the highest percentage differences in the middle  $\left(\left(\frac{H}{D}\right) = 1.48\right)$  and bottom  $\left(\left(\frac{H}{D}\right) = 2.88\right)$  of the bed between the angular locations are 3.83% and 4.19%, respectively.

These differences at the same azimuth could have resulted from the differences in the local gas velocities, depending on the angular location, and these local velocity differences emanate from the inhomogeneous arrangement of the pebbles that results in a random distribution of the void fractions, along the angular locations (Hassan and Dominguez-Ontiveros, 2008; Khane et al., 2017; Khane, 2014).

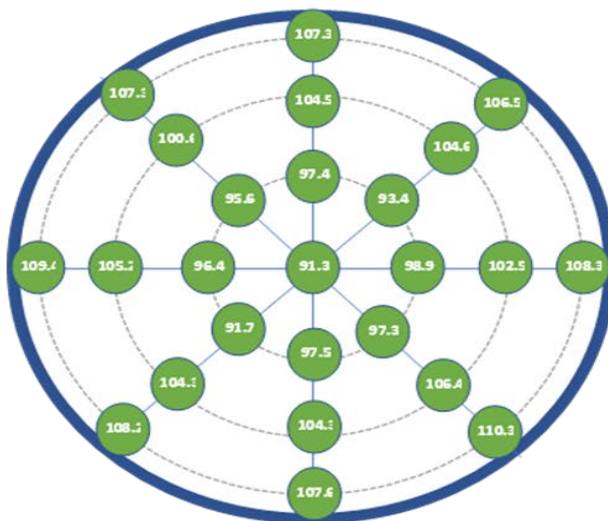
The variation of the heat transfer coefficients obtained at the same radial position when changing the angular location is more pronounced at the top level of the bed. This could be due to more non-uniformity of the local velocity that could be to the low height of the bed from the inlet of the gas flow, which does not allow for the bed to equilibrate. When the gas flows from top level to the middle and bottom levels, the packing will help in enhancing the uniformity of the distribution of the flow, because the height of the bed above these axial locations allows for the flow of the gas to equilibrate (Alshammari et al., 2023b). Hence decreasing the effect of the variation of the local gas velocities at the different angular locations on the local convective heat transfer coefficients.



a)-  $U_g = 0.3 \text{ m/s}$



b)-  $U_g = 1.2 \text{ m/s}$



c)-  $U_g = 2 \text{ m/s}$

Figure 7. Local heat transfer coefficients at the top axial level of the bed ( $H/D = 0.72$ ) at three different superficial inlet gas velocities: a)-  $U_g = 0.3 \text{ m/s}$ , b)-  $U_g = 1.2 \text{ m/s}$ , c)-  $U_g = 2 \text{ m/s}$ .

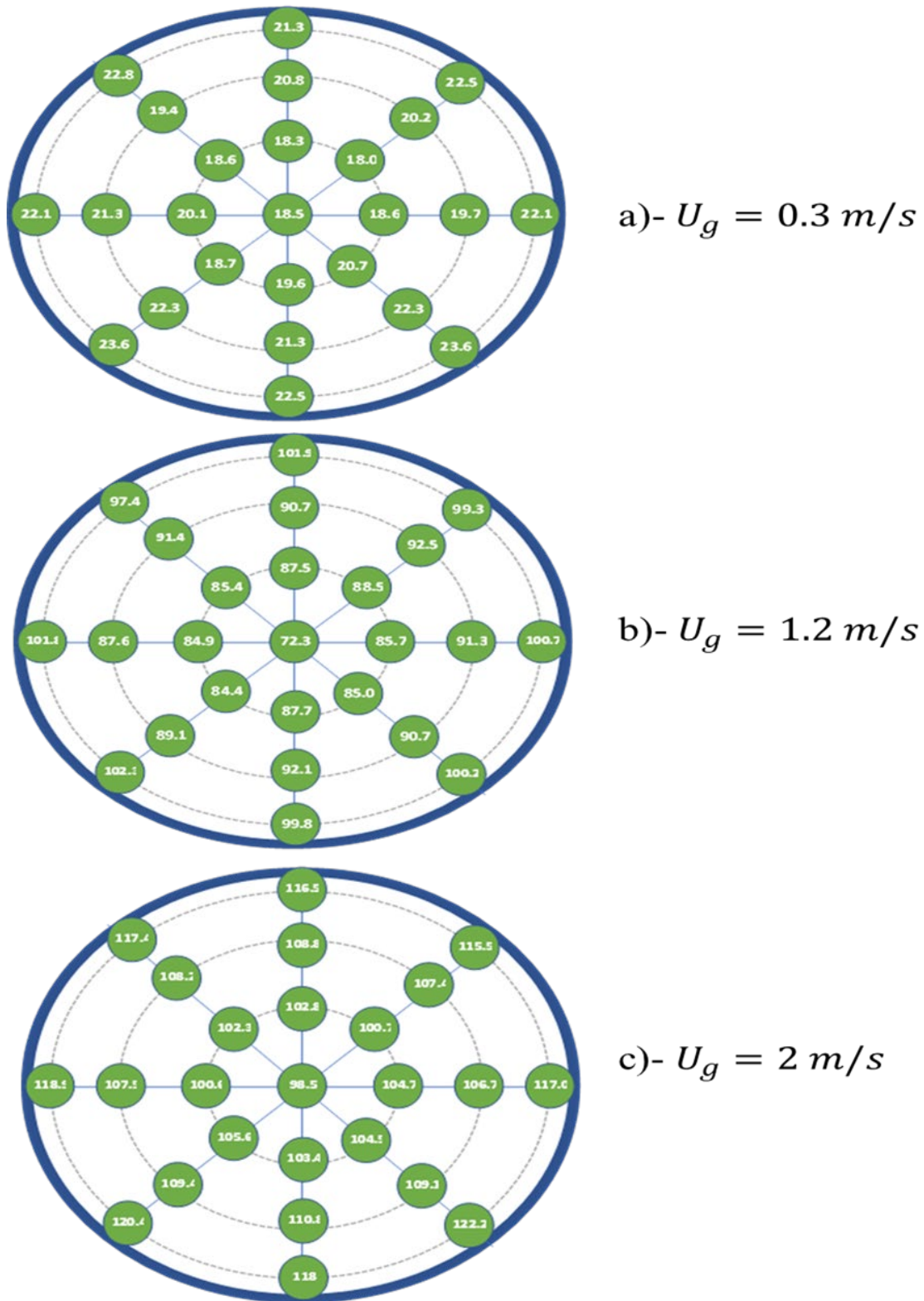


Figure 8. Local heat transfer coefficients in the middle axial level of the bed ( $H/D = 1.48$ ) at three different superficial inlet gas velocities: a)-  $U_g = 0.3 \text{ m/s}$ , b)-  $U_g = 1.2 \text{ m/s}$ , c)-  $U_g = 2 \text{ m/s}$ .

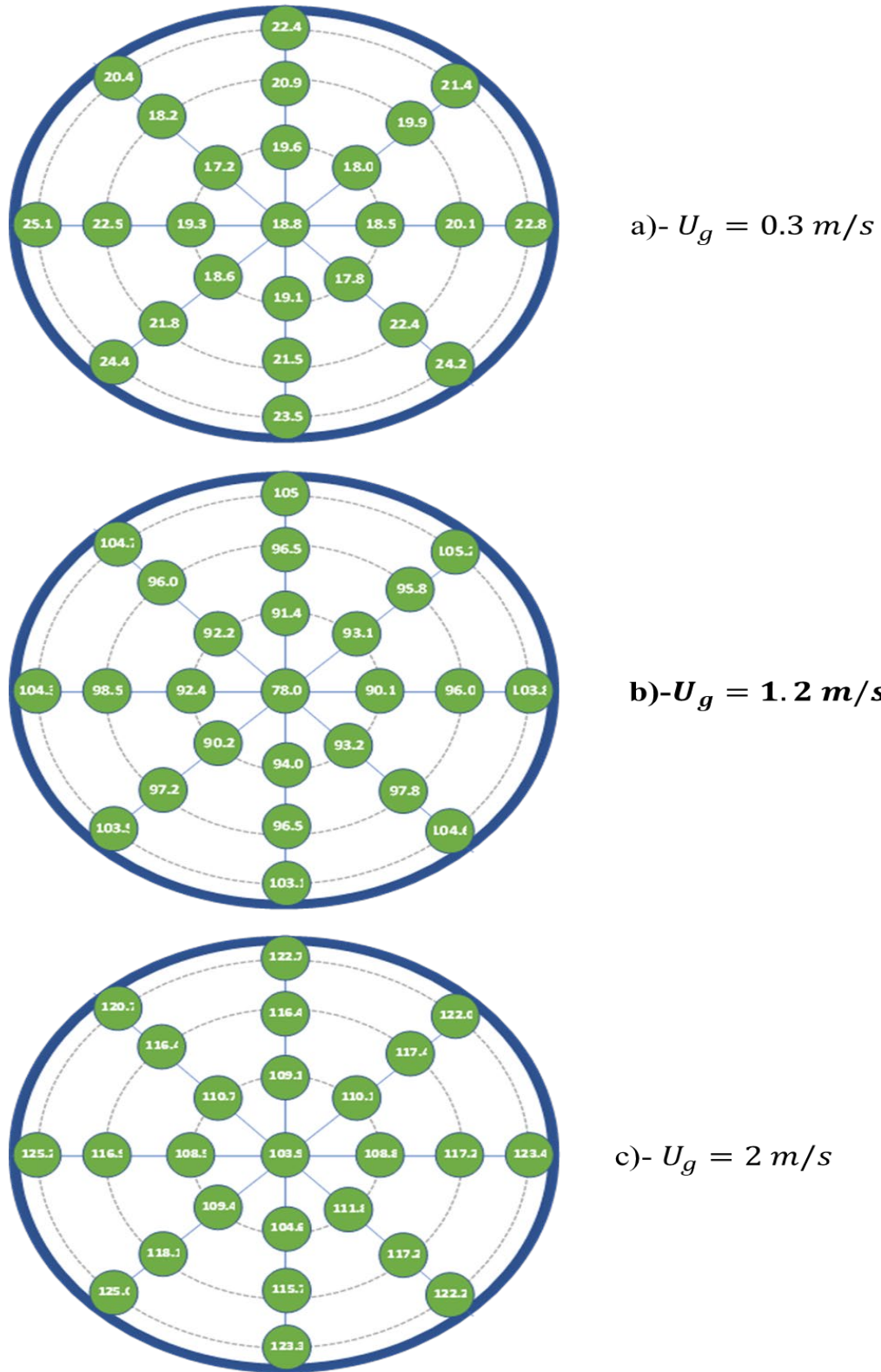


Figure 9. Local heat transfer coefficients at the bottom axial level of the bed ( $H/D = 2.88$ ) at three different superficial inlet gas velocities: a)-  $U_g = 0.3 \text{ m/s}$ , b)-  $U_g = 1.2 \text{ m/s}$ , c)-  $U_g = 2 \text{ m/s}$ .



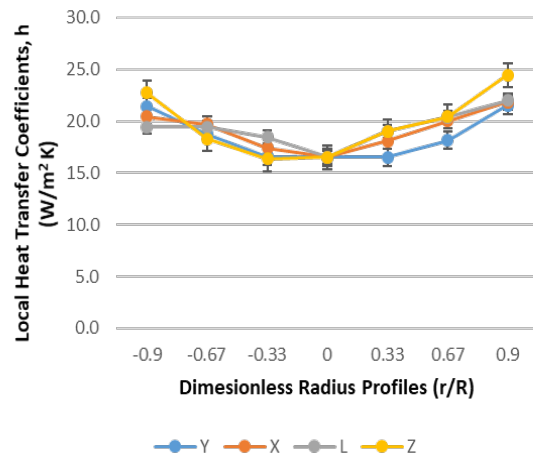
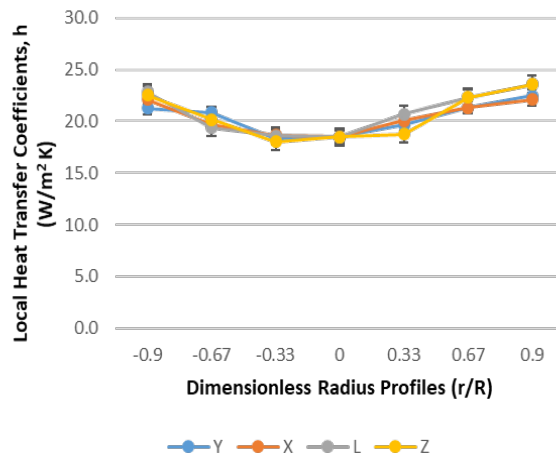
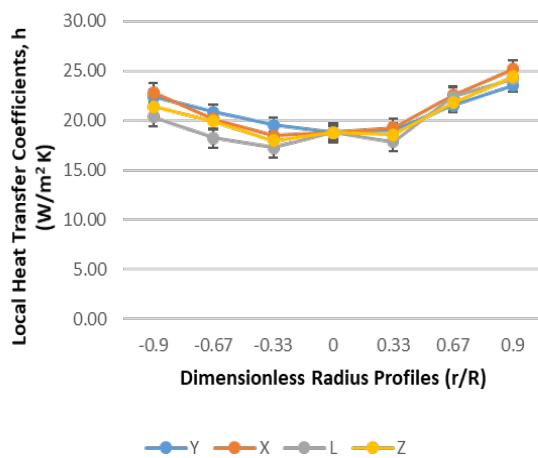
a)- Top Level ( $H/D = 0.72$ )b)- Middle Level ( $H/D = 1.48$ )c)- Bottom Level ( $H/D = 2.88$ )

Figure 10. Diameter profiles of the local heat transfer at a superficial inlet gas velocity of 0.3 m/s at three different axial levels: a)- Top level ( $H/D = 0.72$ ), b)- Middle level ( $H/D = 1.48$ ), and c)- Bottom level ( $H/D = 2.88$ ).

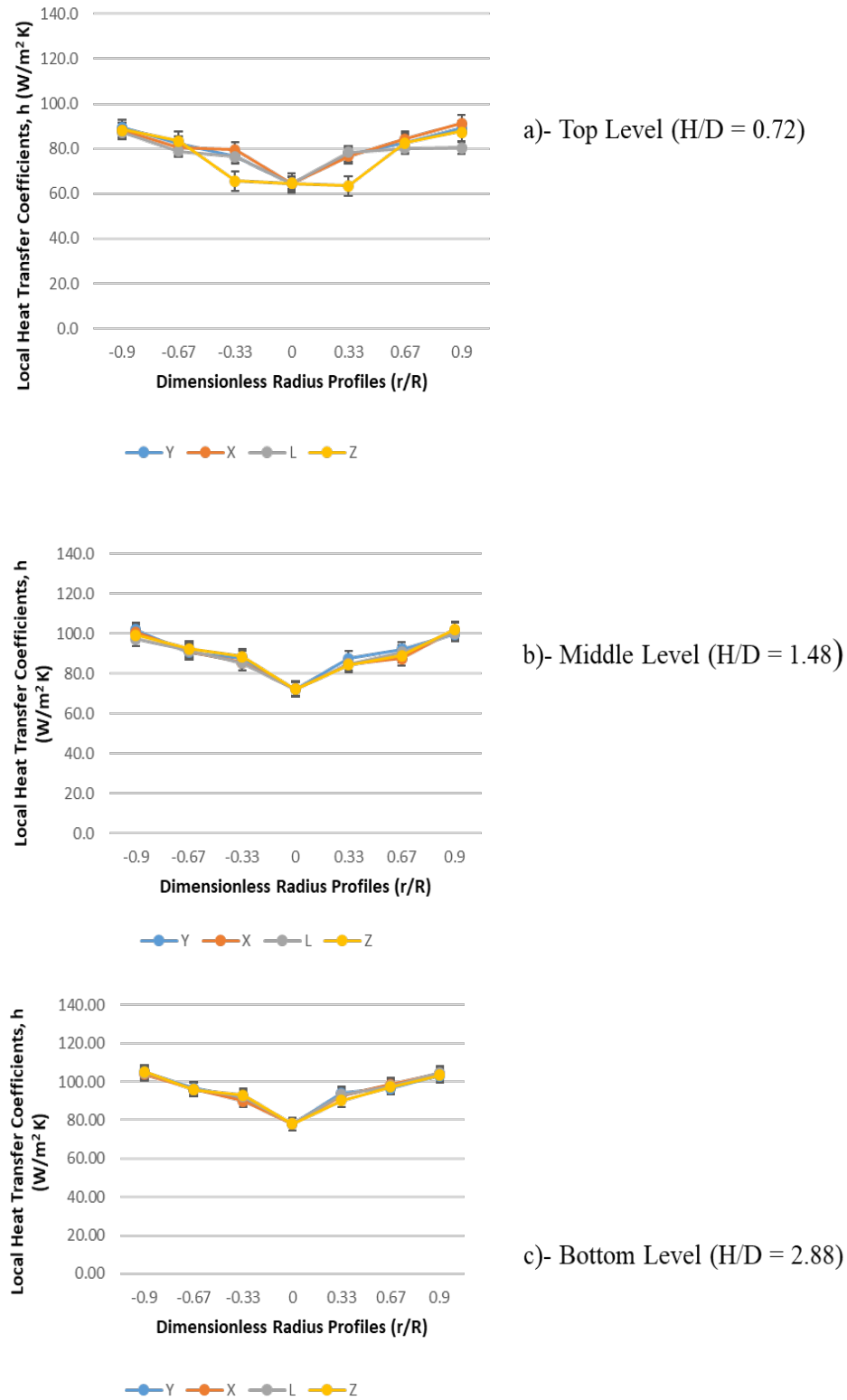


Figure 11. Diameter profiles of the local heat transfer at a superficial inlet gas velocity of 1.2 m/s at three different axial levels: a)- Top level ( $H/D = 0.72$ ), b)- Middle level ( $H/D = 1.48$ ), and c)- Bottom level ( $H/D = 2.88$ ).



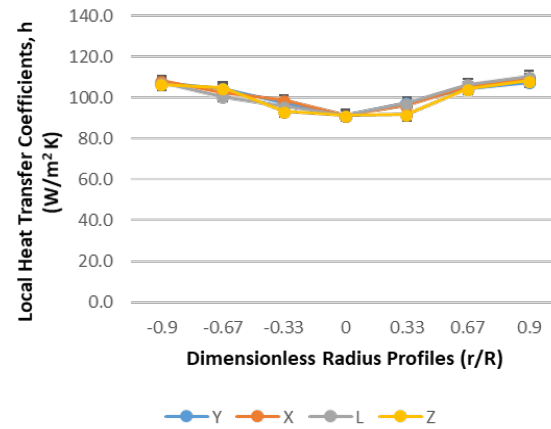
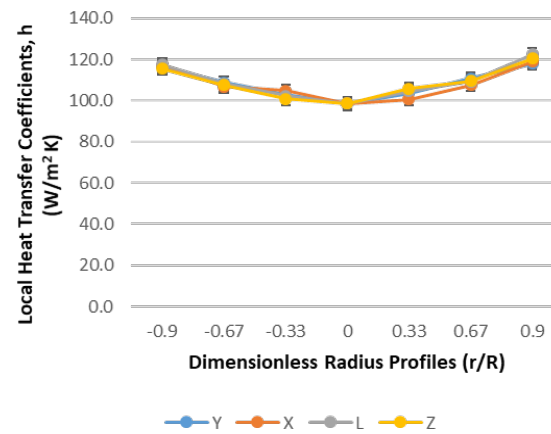
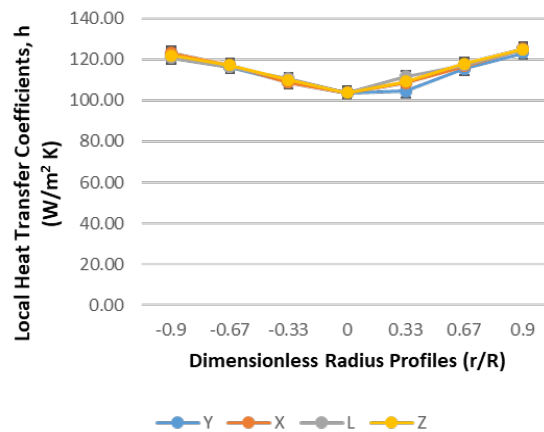
a)- Top Level ( $H/D = 0.72$ )b)- Middle Level ( $H/D = 1.48$ )c)- Bottom Level ( $H/D = 2.88$ )

Figure 12. Diameter profiles of the local heat transfer at a superficial inlet gas velocity of 2 m/s at three different axial levels: a)- Top level ( $H/D = 0.72$ ), b)- Middle level ( $H/D = 1.48$ ), and c)- Bottom level ( $H/D = 2.88$ ).

Figure 13 displays the angularly averaged heat transfer coefficients for each radial location of the four diameter lines (X,Y,Z, and L) using various superficial inlet gas velocities at the three-bed heights (top, middle and bottom level) (Figure 4). It was observed that the convective heat transfer coefficients are higher in the locations that are near the wall of the column at all the three axial levels of the packed bed regardless of the superficial inlet gas velocity (Figure 13), as was noted from the local heat transfer diameter profiles (Figure 10, 11 and 12). At a low superficial inlet gas velocity of 0.3 m/s, corresponding to laminar flow conditions, the azimuthally averaged convective heat transfer coefficients at the near-wall regions ( $r/R = \pm 0.9$ ) are 31.63%, 22.07% and 22.55% higher than the heat transfer coefficients at the center of the bed ( $r/R = 0$ ) at the top, middle and bottom axial locations of the bed, respectively. The difference in the heat transfer coefficients between the center of the bed and wall region are most pronounced at a superficial inlet velocity of 1.2 m/s, where the azimuthally averaged heat transfer coefficients at the wall region ( $r/R = \pm 0.9$ ) are 36.07%, 38.9% and 33.73% higher than the heat transfer coefficients at the center of the bed ( $r/R = 0$ ) at the top, middle and bottom axial locations of the bed, respectively.

At the superficial inlet gas velocity of 0.3 m/s, the flow is more uniform across the cross-section of the column because the momentum imparted on the solids by the flowing gas through its movement within the non-uniform void is low and hence the variation of the local gas velocities from the center of the column to the near-wall region of the column is not large. This is the case for the middle and bottom axial levels of the bed, where the flow of the gas has had enough height to equilibrate, while at the top of the bed, the flow is non-uniform since there is not enough height for the flow to equilibrate and this effect

of the bed height above the measurement location is most pronounced at low superficial inlet gas velocities.

On the other hand, the lowest values of the heat transfer coefficients were found at the center of the column where the pebbles are tightly packed and hence provide larger resistance to the flow of the gas. This increase in the heat transfer coefficients when moving from the center of the column to the region near the wall can be attributed to the differences in the local gas velocities due to the void structure of the bed, where the higher void fractions near the wall cause less resistance to the gas to flow through. This causes the non-uniform distribution of the gas flow and local actual velocity inside the bed. This is more pronounced when the ratio of the bed diameter to the particle diameter is low as in the case of this experimental set-up where the bed diameter to the pebble diameter is  $30\text{cm}/5\text{cm} = 6$  (Al Falahi et al., 2018; Al Falahi and Al-Dahhan, 2016). Hence, larger local velocities of the gas are found in the regions near the wall where more gas to flow through this region due to larger void fraction and hence less resistance to the flow. This was shown in the work of *Alshammari et al., 2023b* who measured the local gas velocities in the same bed, with the same dimensions, aspect ratio and under various superficial inlet gas velocities using the Hot Wire Anemometry technique.

The larger local gas velocities in the regions near the wall allow for higher transfer rate of heat between the pebbles and the flowing air (Alshammari et al., 2023b). The differences in the heat transfer coefficients between the center of the bed and the near wall regions are more pronounced at high superficial gas velocities, which correspond to high Reynolds numbers (high local gas velocities) in these locations. The increase of the superficial inlet gas velocity, and thus, the increase of local Reynolds numbers (local

velocities) increases the heat transfer coefficient, regardless of the location inside the bed. However, when increasing the superficial inlet gas velocity from  $1.2 \text{ m/s}$  to  $2 \text{ m/s}$ , the differences in the azimuthally averaged heat transfer coefficients between the center and the wall of the column decrease from 36.07%, 38.9% and 33.73% to 18.39%, 20.07% and 18.84% at the top, middle and bottom axial locations in the bed, respectively. This could be an indication that the effect of the superficial inlet gas velocity on the difference in the local gas velocities between the center of the bed and the wall region is not as significant beyond a certain superficial inlet gas velocity, which in our case is  $1.2 \text{ m/s}$ , and hence the effect of the void fractions in the bed would also be less significant at very high superficial inlet gas velocities. It would be interesting to investigate the variation of the heat transfer coefficients at a superficial inlet gas velocity higher than  $2 \text{ m/s}$ , hence, when further increasing the turbulence of the gas flow in the bed. One may also ask about why the experiments are not conducted at a larger ratio of bed to particle diameters, as in the use of a larger column diameter when 5 or 6 *cm* pebbles are used. Besides what has been stated above in the introduction, it is because this would require a high capacity of compressed air flow and a column that has a diameter that is larger than a meter, which is not currently available.

Instead, the available setup that we have at the Multiphase Flows and Reactors Engineering & Education Laboratory (mFReel) has been used in this work with the objective of demonstrating how the local distribution of the convective heat transfer coefficients varies with the locations inside the reactor when the void structure varies due to the low ratios of the bed to particle diameters where the local flow velocities vary accordingly and this would represent the void in the wall region for larger diameter beds.

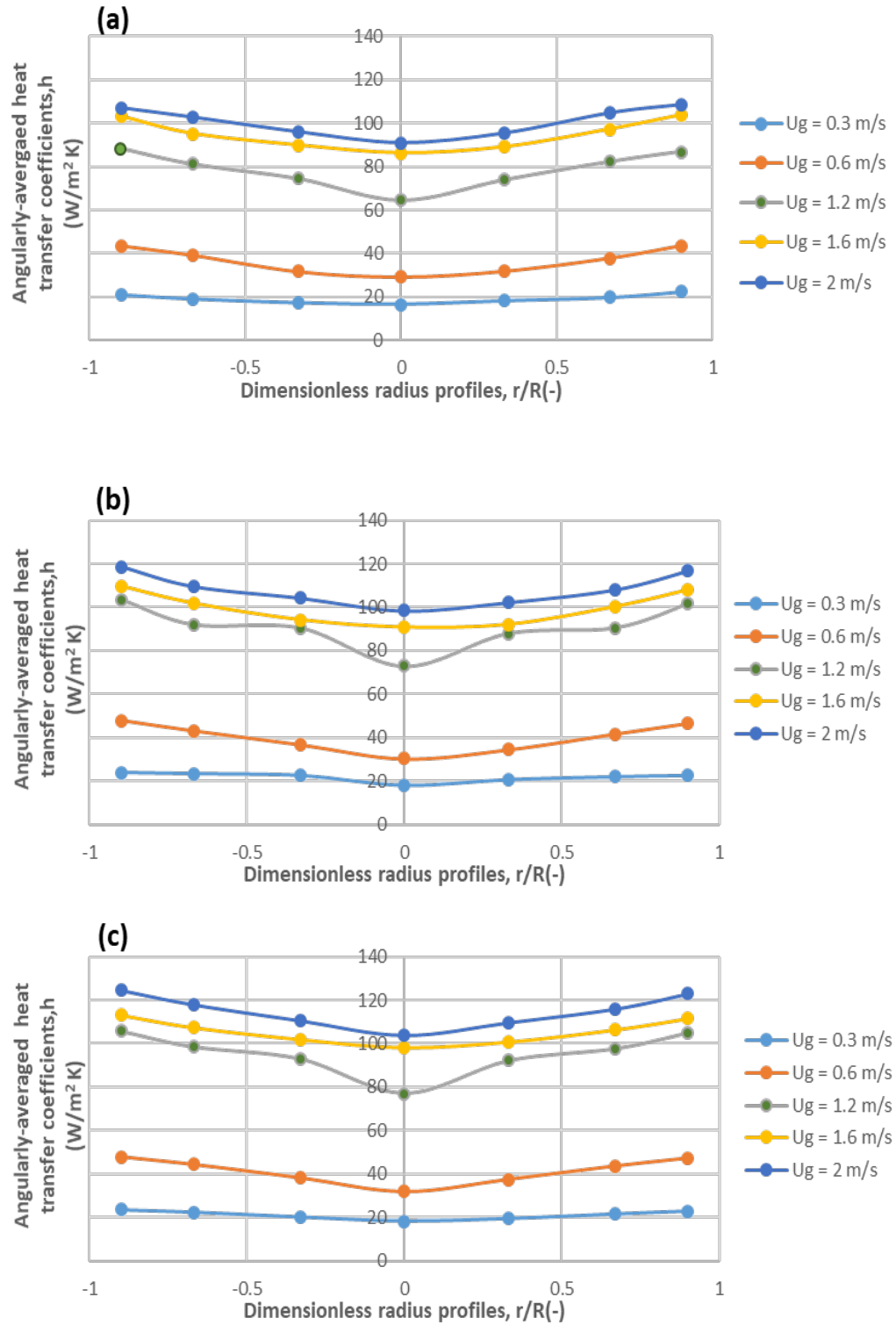


Figure 13. Diameter profiles of angularly averaged heat transfer coefficients for each radial location of Y, X, Z, and L diameter lines using various superficial inlet gas velocities from  $U_g = 0.3 \text{ m/s}$  to  $U_g = 2.0 \text{ m/s}$  at three axial positions: a)- Top level ( $H/D = 0.72$ ), b)- Middle level ( $H/D = 1.48$ ), and c)- Bottom level ( $H/D = 2.88$ ).

The values of the heat transfer coefficient also vary from top to bottom of the column.

At low gas velocity, as shown in Figure 13(a), for the three axial levels  $H1$ ,  $H2$ , and  $H3$  the angularly averaged heat transfer coefficients variations are not large, particularly at the middle and bottom (between  $18$  and  $24 \text{ W/m}^2\text{K}$ ), while the variation is larger for the top level (between  $16$  and  $25 \text{ W/m}^2\text{K}$ ). This could be attributed to the short height of the bed at this region, which does not allow the flow of the gas equilibrate, causing less uniformity of the flow distribution, as explained above for the variation of the local heat transfer coefficients at the different angular locations ( $X$ ,  $Y$ ,  $Z$ , and  $L$ ). The variation of the values of the heat transfer coefficients follows the same trend when moving from the center to the wall of the column owing to same reasons that are explained above. On the other hand, at a high superficial inlet velocity of the coolant gas Figure 13(b), the heat transfer coefficient increases to the range of  $90$  to  $125 \text{ W/m}^2\text{K}$ , with the bottom level having the highest heat transfer coefficients at all radial positions, followed by the middle level and then the top level of the column. This is due to the higher local velocities at the bottom level, owing to the bed porosity structure at this axial position.

However, *Al Falahi and Al-Dahhan, 2016* found that the cross-sectional average porosity of the bed fluctuates along the bed height and there could be other axial positions in the bottom where the porosity is lower than the middle and top axial levels. Hence, it is not a general conclusion that the heat transfer coefficient is higher at the bottom, but rather specific to our exact axial position of  $86.4 \text{ cm}$  from the distributor and to our operating and design conditions of this work.

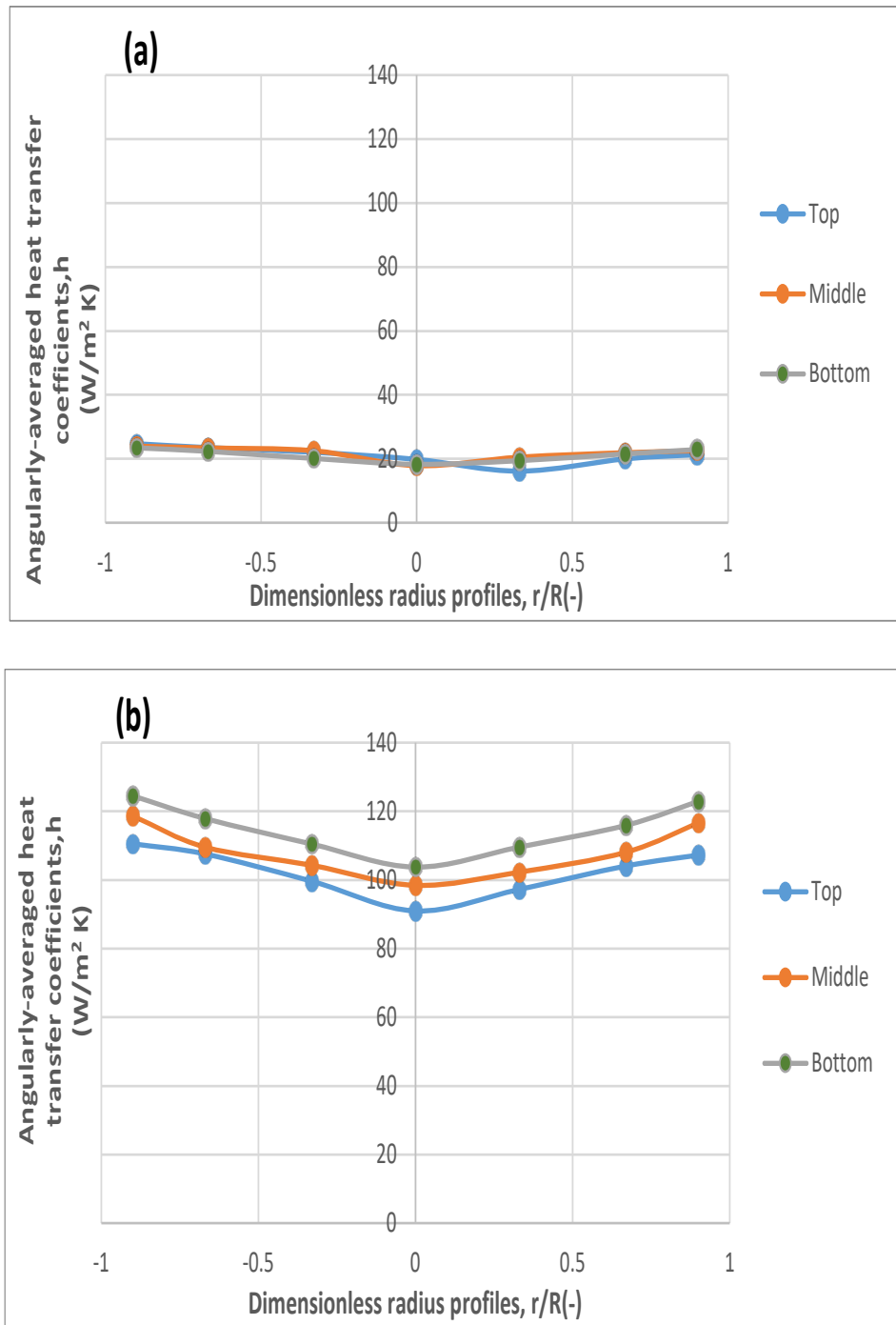


Figure 14. Diameter profiles of angularly averaged heat transfer coefficients for the three axial levels (Top ( $H/D = 0.72$ ), Middle ( $H/D = 1.48$ ), & Bottom ( $H/D = 2.88$ )) at the lowest and highest superficial inlet gas velocity: (a)  $U_g = 0.3 \text{ m/s}$ . (b)  $U_g = 2.0 \text{ m/s}$ .

## 5. COMPARISON WITH CORRELATIONS REPORTED IN THE LITERATURE

The local convective heat transfer coefficients were averaged angularly by averaging the local heat transfer values for the locations (i.e., X, Y, Z, and L) for each radial position. These angularly averaged heat transfer coefficients were then radially and axially averaged in order to obtain the overall heat transfer in the column at each superficial inlet gas velocity (0.3, 0.6, 1.2, 1.6 and 2 m/s).

As mentioned earlier, there are many parameters that can impact the heat transfer convection in a pebble bed reactor and that is why it is better to characterize the heat transfer in a PBR using the dimensionless parameters which are described in equations Eq. 2,3 and 4). Many correlations predicting the heat transfer inside a pebble bed reactor using these parameters exist in the literature (Abdulmohsin, 2013). Three correlations were selected for the comparison with the experimental results of this study, which are *Gnielinski, 1978; Wakao and S, 1982; KTA, 1983; and Achenbach, 1995*. These correlation were also used for comparison with experimental data by *Abdulmohsin and Al-Dahhan, 2015*, however, due to a mistake the averaging equation used in their work, the comparison is not reliable as the average heat transfer coefficients were calculated incorrectly. These correlations were chosen since their range of application is convenient for the experimental data obtained in this study.

*Gnielinski, 1978* developed a semi-empirical correlation for the prediction of the convective heat transfer coefficients from arbitrary particles using the equations for a flat plate, where laminar and turbulent heat transfer rates are combined. The range of applicability is claimed to be for  $0.24 \leq \varepsilon \leq 0.935$ ,  $0.71 \leq Pr \leq 10^4$  and  $Re/\varepsilon \leq 7.7 \times 10^5$ .



The correlation of *Gnielinski, 1978* is expressed as:

$$Nu = f_{\varepsilon} Nu_{sp}$$

where,

$$f_{\varepsilon} = 1 + 1.5(1 - \varepsilon) \quad (8)$$

And

$$Nu_{sp} = 2 + \sqrt{\left(0.664 \left(\frac{Re}{\varepsilon}\right)^{1/2} Pr^{1/3}\right)^2 + \left(\frac{0.037(Re/\varepsilon)^{0.8} Pr}{1 + 2.443 \left(\frac{Re}{\varepsilon}\right)^{-0.1} (Pr^{2/3} - 1)}\right)^2} \quad (9)$$

*Wakao and S, 1982* developed the following semi-empirical correlation for the estimation of the pebble-fluid convective heat transfer in a packed bed:

$$Nu = 2 + 1.1 Pr^{1/3} Re^{0.6} \quad (10)$$

where  $Nu$  is Nusselt's number,  $Re$  is Reynold's number and  $Pr$  is Prandtl number. These dimensionless numbers can be expressed by the equations (Eq 2,3, and 4) mentioned above, respectively.

The German Nuclear Safety Standards Commision (KTA) proposed the following equation *KTA, 1983* for the estimation of the heat transfer between spherical fuel elements and the flowing fluid in the core of High-Temperature Gas-cooled Reactors (HTGRs):

$$Nu = 1.27 \left(\frac{Pr^{1/3}}{\varepsilon^{1.18}}\right) Re^{0.36} + 0.033 \left(\frac{Pr^{1/2}}{\varepsilon^{1.07}}\right) Re^{0.86} \quad (11)$$

where  $\varepsilon$  is the average bed porosity.

This correlation has been tested using experimental data and its range of application was found to be usable for a Reynold's number between 100 and 100000 ( $10^2 \leq Re \leq 10^5$ ).

Achenbach, 1995 proposed another empirical correlation that can be used for the estimation of the overall forced convective heat transfer in a packed bed at  $Re/\epsilon \leq 7.7 \times 10^5$ . The equation can be expressed as follows:

$$Nu = [(1.18Re^{0.58})^4 + (0.23(Re_h)^{0.75})^4]^{1/4} \quad (12)$$

where  $Re_h$  is the effective Reynolds Number and can be written as:

$$Re_h = \frac{\rho \cdot V \cdot d_h}{\mu} = \frac{1}{(1 - \epsilon)} Re \quad (13)$$

where  $V$  is the average interstitial velocity ( $U_g/\epsilon$ ),  $d_h$  is the hydraulic diameter ( $d \times \frac{\epsilon}{1-\epsilon}$ ).

The experimental data in this investigation was compared to these selected correlations as elucidated in Figure 15, which plots the Nusselt number ( $Nu$ ) as a function of the effective Reynolds number ( $Re_h$ ).

The relative variation between the experimental and the predicted results is expressed as the average absolute relative error ( $AARE$ ) and can be calculated using the following expression (Ostertagová, 2012):

$$AARE = \frac{1}{N} \sum_{i=1}^{i=N} \frac{Nu_{predicted,i} - Nu_{experimental,i}}{Nu_{experimental,i}} \quad (14)$$

The *AARE* was calculated to quantify the difference between the Nusselt's numbers that were obtained based on the experimental overall heat transfer coefficients and the Nusselt's numbers estimated by the three correlations

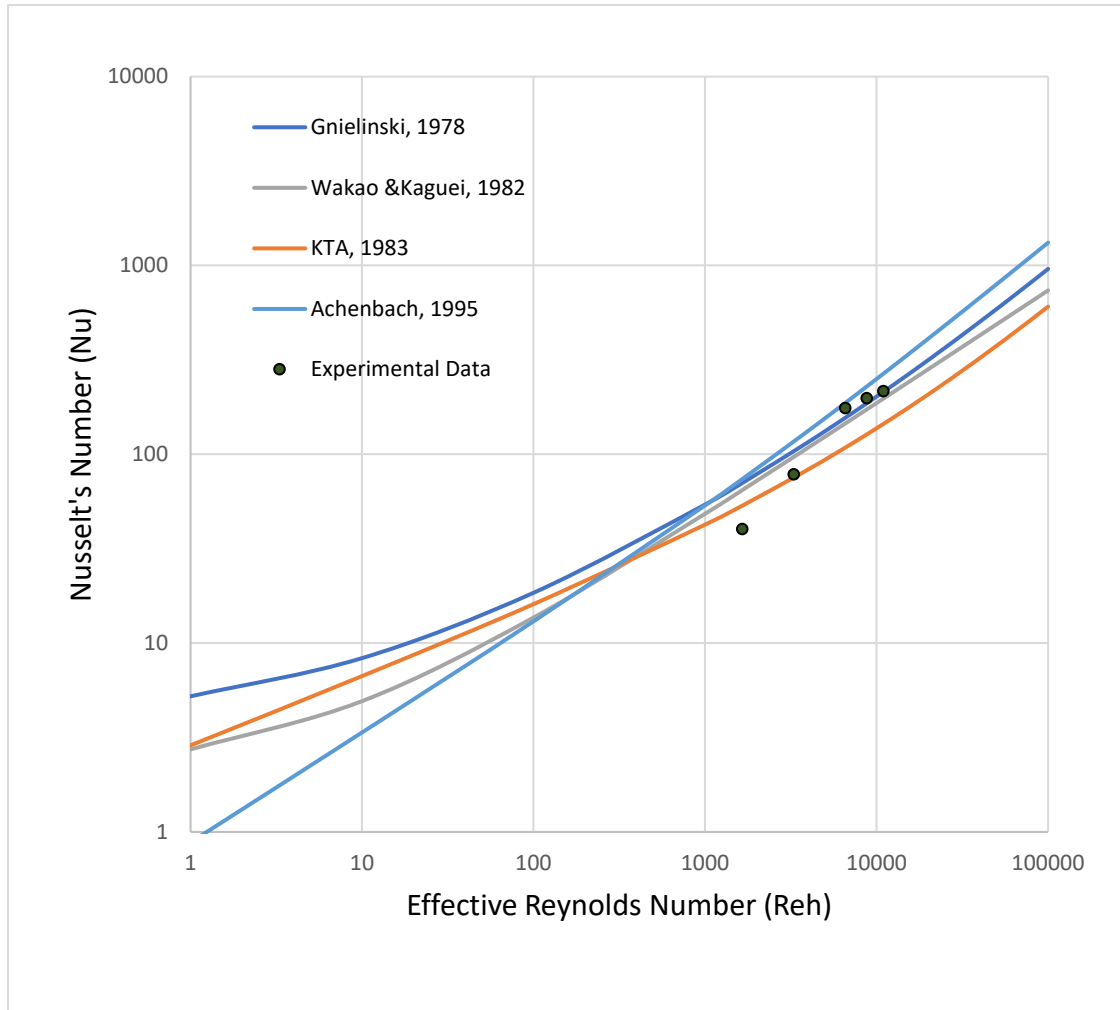


Figure 15. Comparison of the empirical correlations with the measured overall convective heat-transfer at the superficial inlet gas velocities studied (0.3 m/s to 2 m/s).

From Figure 15, we can see that the experimental data correlates well with the predictions based on the correlations proposed by *Gnielinski, 1978* and *Wakao and S, 1982*

at turbulent flow conditions that correspond to high effective Rerynold's numbers ( $Re_h \geq 3000$ ), where the *AARE* values are 5.90% and 12.77%, for the *Gnielinski, 1978* and *Wakao and S, 1982* correlations, respectively. However, at low effective Rerynold's numbers ( $Re_h < 3000$ ), where the flow of the gas is laminar, these two correlations overestimate the Nusselt's number, with an *AARE* of 54.13% and 42.28% at low  $Re_h$  for the *Gnielinski, 1978* and *Wakao and S, 1982* correlations, respectively. However, the *Wakao and S, 1982* correlation provided slightly better overall estimates to our experimental data, with an overall *AARE* of 24.58%, compared to an overall *AARE* of 25.20% for the *Gnielinski, 1978* correlation. In contrast, the *KTA, 1983* correlation predictions are better in laminar flow conditons ( $Re_h < 3000$ ) with an *AARE* of 18.65% than at turbulent flow conditions ( $Re_h \geq 3000$ ), where the *AARE* of 35.58% is the highest when compared with the other correlations at high  $Re_h$ . The correlation of *Achenbach, 1995* provides the least accurate overall estimates with an overall *AARE* of 35.88%.

Based on the above, it seems that the deviation between the experimental data and the predicted data varies depending on the flow regime in the column, with the predictions of the *KTA, 1983* correlation being the best at laminar flow, while the predictions of the *Gnielinski, 1978* correlation are the closest to the experimental data at turbulent flow conditions. However, the overall *AARE* values are still high, indicating that there is not enough similarity between the experimental values the predictions and hence, these correlations cannot be used to predict the convective heat transfer coefficients for our experimental setup and operation conditions particularly for local values.

The high deviation between the correlations and the experimental data, especially at laminar flow conditions, where the superficial inlet gas velocity is low, is due to the

difference in the operation conditions that were taken in consideration for the development and testing of the correlations. These operation and design conditions for the investigation of the forced convective heat transfer include the aspect ratio, the void fraction in the bed and the local flow conditions (i.e. local fluid velocities in the void). The high uncertainties of the measurements techniques could also be the reason behind the high deviation between the measured heat transfer coefficients and the predictions of the correlations. Also, in our work, we measured the local heat transfer coefficient and averaged for the three axial locations where the final averaged value was considered as the overall heat transfer coefficient. Hence, the acquisition of accurate heat transfer data like the experimental data obtained in this work is necessary for developing new comprehensive empirical correlations for the prediction of the local heat transfer coefficient in a pebble bed reactor rather than the overall heat transfer coefficient. Therefore, we developed a new pseudo-3D model for the prediction of the local heat transfer coefficients for our operation and design conditions at various superficial inlet gas velocities that cover both laminar and turbulent flow.

## **6. NEW CORRELATION DEVELOPMENT**

In order to develop an elaborate understanding of the mechanisms by which the heat transfer coefficient varies as well as the effect of the flow regime of the coolant gas on the heat transfer coefficients inside the pebble bed reactors, the ability to predict the heat transfer coefficients at local points inside the reactor's core is imperative. However, as discussed above, the correlations found in the literature are not able to predict the heat transfer coefficients accurately. Hence, we developed a new pseudo-3D correlation for the

prediction of the local heat transfer coefficients, expressed in Nusselt's number for our operation and design conditions. The general equation for such correlation is expressed in eq15:

$$Nu = f(Re, \frac{r}{R}, \frac{z}{D}, Pr, \varepsilon) \quad (15)$$

After the statistical fitting using the experimental data, the model found is expressed by (Eq 16):

$$Nu = 5.25 \times (3.91 \ln(Re) - 25.9) \times \left(0.38 \frac{r}{R} + 1.9\right) \times \left(-0.11 \frac{H}{D} + 2.46\right) - 64.91 \left(\frac{Pr}{\varepsilon}\right)^{0.05} \quad (16)$$

The goodness of fit plot for the comparison between the experimental data and the predicted data, which was obtained using the new correlation (Eq. 4) can be found in Figure 16. It is apparent from the figure that the correlation fits the experimental data relatively well as most of the experimental data is within the  $\pm 15\%$  error lines. The overall *AARE* (Average Absolute Relative Error) was found to be equal to 12.96%. However, as can be seen from Figure 16, the correlation's predictions are not accurate at low superficial inlet gas velocities, which correspond to laminar flow conditions ( $U_g = 0.3 - 0.6 \text{ m/s}$ ), with an *AARE* of 27.4%. On the other hand, at turbulent flow conditions ( $U_g = 1.2 - 2 \text{ m/s}$ ), the correlation provides accurate predictions with an *AARE* of 3.33%. This is important information, because real pebble reactors are operated at high superficial inlet gas velocities.

However, despite the high accuracy of this pseudo-3D model to predict the convective heat transfer coefficients at different radial and axial positions, it is only valid with the range of our experimental setup and operation conditions, with a low aspect ratio

of 6. It was not trained or fitted to predict the local heat transfer in inside the bed of a high aspect ratio reactor, as is the case in pebble bed reactors and hence it may only be used with caution for inside the bed where the void is close to be uniform. However, it can be used to estimate the local heat transfer in the wall region within the gas flow conditions of the correlation ( $993.78 \leq Re \leq 6625.20$ ).

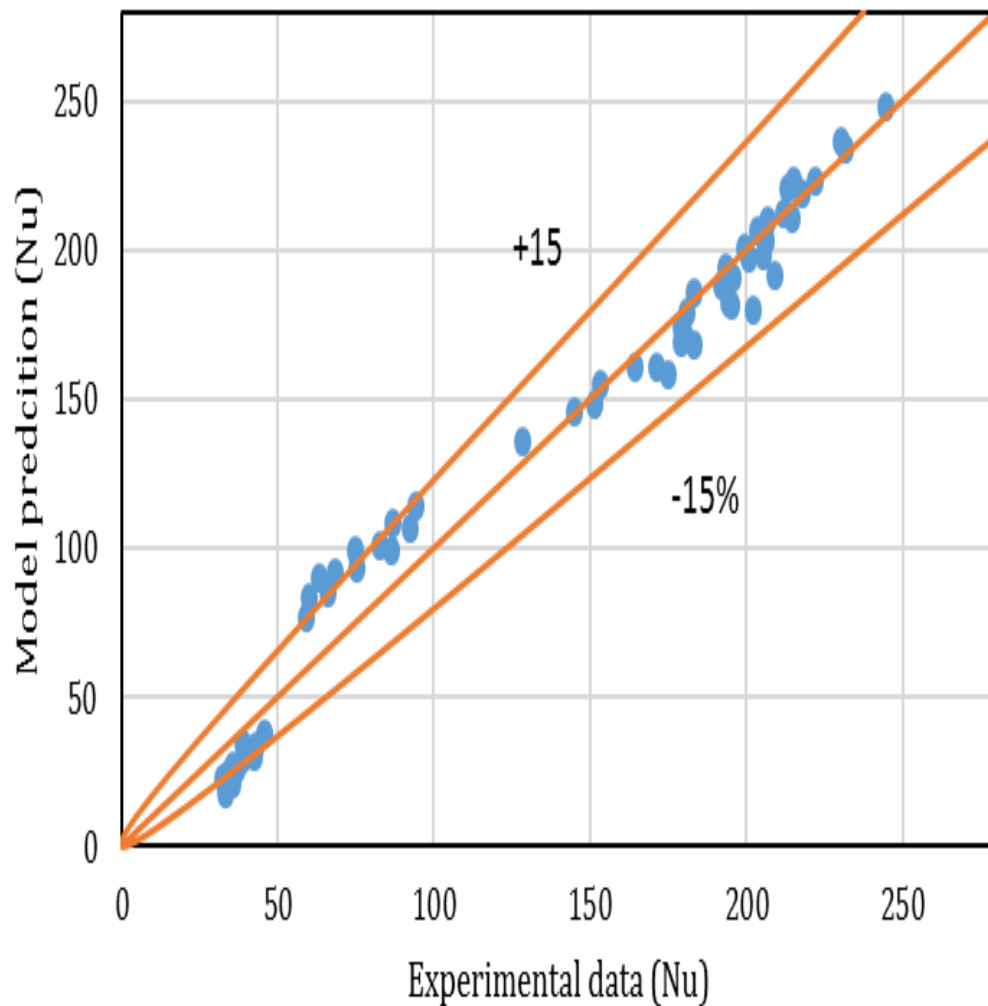


Figure 16. Goodness-of-fit plot of the Pseudo-3D model prediction against experimental data.

## 7. CONCLUDING REMARKS

The heat transfer coefficients were obtained at various axial levels, radial positions, angular locations and under different superficial inlet gas velocities, in order to account for both laminar and turbulent flow inside the bed, which is characterized by a low aspect ratio of 6. The heat transfer measurements were taken using an advanced technique consisting of a heated pebble probe, a micro-foil heat flux sensor and a thermocouple that provide highly accurate and reliable results.

The heat transfer coefficients were found to vary depending on the location in the column. Higher heat transfer values were found near the wall of the column, in comparison to the center of the column. This was attributed to the differences in the local gas velocities that emanate from the differences in the local void fractions inside the column, which are higher near the wall due to the wall effect and lower in the center where the pebbles are tightly packed (Alshammari et al., 2023b). Taking the measurements along four angular locations for each radial position elucidated the differences in the heat transfer coefficients, even at the same azimuth, due to the random structure of the bed.

The influence of the superficial inlet velocity of the coolant gas was studied and it was found that the local heat transfer coefficients between the pebbles and the coolant gas increase with the increase of the turbulence of the flow of the gas, regardless of the position inside of the column.

The overall heat transfer coefficient was calculated based on the experimental local heat transfer data and was then compared with *Gnielinski, 1978, Wakao and S, 1982, KTA, 1983* and *Achenbach, 1995* correlations. The high deviation between the experimental results and the predictions of the correlations indicates that newer correlations that are



validated by highly accurate experimental heat transfer data such as the data presented in this work are needed.

A pseudo-3D correlation was developed for the prediction of the local heat transfer coefficients and it was proved to have a high accuracy at high superficial inlet velocities of the coolant gas, which is the case for the pebble bed reactors. However, the model would not be applicable for the prediction of the local heat transfer inside the central region bed of a real pebble bed reactor, because it was trained using the data from this work which was conducted in a much smaller column, with a low aspect ratio of 6 that could represent the regions near the walls of real pebble bed reactors.

The results of this work show that future studies should focus on the investigation of the local heat transfer coefficients under turbulent flow regime only as the superficial inlet gas velocities used in a real PBR are high. Also, the convective heat transfer coefficients were obtained at only one location in the center of the void, while the convective heat transfer coefficients can be different depending on the orientation of the heat transfer probe and the thermocouple, which is investigated in another one of our works and which will be published soon (Alshammari et al., 2023a). Due to the disparity in the estimation of the correlations at laminar flow compared to turbulent flow conditions, it would also be interesting if separate correlation could be developed for each of the two flow conditions.

Due to the high influence of the local actual velocities of the coolant gas on the heat transfer coefficients, it is necessary to study the local flow conditions, especially in packed beds with 5 cm pebbles and a higher aspect ratio of the bed diameter to pebble diameter that would better represent an actual PBR. CFD simulation studies with integrated heat

transfer calculations to estimate heat transfer coefficients are also essential for developing a better understanding of the mechanisms of the convective heat transfer in a PBR. The accurate local heat transfer data obtained in this work can serve as benchmark data for the validation of the CFD simulations with heat transfer calculations by comparing its estimations with the measured ones.

### NOMENCLATURE

Symbol	Discretion	Unit
$D$	Inside column diameter	$m$
$d_h$	Effective pebble diameter,	$m$
$d_p$	Pebble diameter, m	$m$
$g$	gravitational force	$m/s^2$
$n$	total number of experimental data points	(-)
$N$	the data point number	(-)
$\mu$	dynamic viscosity of the fluid	$Kg.m/s$
$\rho$	density of fluid	$kg/m^3$
$V_g$	gas velocity	$m/s$
$Z$	axial distance along the bed	$m$
$\varepsilon$	Average void of the bed	(-)
$Nu$	Nusselt number	(-)
$Nu_s$	Nusselt number of a single sphere	(-)
$Nu_{lam}$	Nusselt number of a single sphere for laminar flow	(-)

$Nu_{turb}$	Nusselt number of a single sphere for turbulent flow	(-)
$Pr$	Prandtl number	(-)
$Re$	Reynolds number	(-)
$Re_h$	Effective Reynolds number	(-)
DAQ	Data acquisition system	
HTR	high temperature reactor	
HTGR	high temperature gas-cooled reactor	
KTA	German nuclear safety standard commission (Kern-technischer Ausschuss <a href="http://www.kta-gs.de/">http://www.kta-gs.de/</a> )	
PBR	pebble bed reactor	

## REFERENCES

1. Abdulmohsin, R., 2013. Gas dynamics and heat transfer in a packed pebble-bed reactor for the 4th generation nuclear energy. Missouri University of Science and Technology.
2. Abdulmohsin, R.S., Abid, B.A., Al-Dahhan, M.H., 2011. Heat transfer study in a pilot-plant scale bubble column. Chem. Eng. Res. Des. 89, 78–84. <https://doi.org/10.1016/j.cherd.2010.04.019>
3. Abdulmohsin, R.S., Al-Dahhan, M.H., 2017. Pressure drop and fluid flow characteristics in a packed pebble bed reactor. Nucl. Technol. 198, 17–25. <https://doi.org/10.1080/00295450.2017.1292818>
4. Abdulmohsin, R.S., Al-Dahhan, M.H., 2016. Erratum: Corrigendum to “Characteristics of convective heat transport in a packed pebble-bed reactor” (Nuclear Engineering and Design (2015) 284 (143–152) (S0029549314006700) (10.1016/j.nucengdes.2014.11.041)). Nucl. Eng. Des. 305, 723. <https://doi.org/10.1016/j.nucengdes.2016.05.001>
5. Abdulmohsin, R.S., Al-Dahhan, M.H., 2015. Characteristics of convective heat transport in a packed pebble-bed reactor. Nucl. Eng. Des. 284, 143–152. <https://doi.org/10.1016/j.nucengdes.2014.11.041>

6. Abdulmohsin, R.S., Al-Dahhan, M.H., 2010. Impact of internals on the heat transfer rate and coefficient in a bubble column. *AIChE Annu. Meet. Conf. Proc.*
7. Achenbach, E., 1995. Heat and flow characteristics of packed beds. *Exp. Therm. Fluid Sci.* 10, 17–27. [https://doi.org/10.1016/0894-1777\(94\)00077-L](https://doi.org/10.1016/0894-1777(94)00077-L)
8. Al-Juwaya, T., Ali, N., Al-Dahhan, M., 2019. Investigation of hydrodynamics of binary solids mixture spouted beds using radioactive particle tracking (RPT) technique. *Chem. Eng. Res. Des.* 148, 21–44. <https://doi.org/10.1016/j.cherd.2019.05.051>
9. Al-Juwaya, T., Ali, N., Al-Dahhan, M., 2017. Investigation of cross-sectional gas-solid distributions in spouted beds using advanced non-invasive gamma-ray computed tomography (CT). *Exp. Therm. Fluid Sci.* 86, 37–53. <https://doi.org/10.1016/j.expthermflusci.2017.03.029>
10. Al Falahi, F., Al-Dahhan, M., 2016. Experimental investigation of the pebble bed structure by using gamma ray tomography. *Nucl. Eng. Des.* 310, 231–246. <https://doi.org/10.1016/j.nucengdes.2016.10.009>
11. Al Falahi, F., Mueller, G., Al-Dahhan, M., 2018. Pebble bed nuclear reactor structure study: A comparison of the experimental and calculated void fraction distribution. *Prog. Nucl. Energy* 106, 153–161. <https://doi.org/10.1016/j.pnucene.2018.03.006>
12. Almusafir, R.S., Jasim, A.A., Al-Dahhan, M.H., 2023. Review of the Fluid Dynamics and Heat Transport Phenomena in Packed Pebble Bed Nuclear Reactors. *Nucl. Sci. Eng.* 0, 1–37. <https://doi.org/10.1080/00295639.2022.2146993>
13. Alshammari, M., Alalou, A., Al-Dahhan, M.H., 2023a. Experimental investigation of the convective heat transfer coefficient at different angular orientations inside the void in a cold flow Pebble Bed Reactor using a non-invasive heat transfer pebble probe [Unpublished Manuscript]. *Dep. Chem. Biochem. Eng. Missouri Univ. Sci. Technol.*
14. Alshammari, M., Alalou, A., Alhameedi, H.A., Al-Dahhan, M.H., 2023b. Experimental investigation of the variation of the local gas velocities in a cold flow Pebble Bed Reactor (PBR) using a hot wire anemometry technique [Unpublished Manuscript]. *Dep. Chem. Biochem. Eng. Missouri Univ. Sci. Technol.*
15. Auwerda, G.J., Zhang, Y., Lathouwers, D., Kloosterman, J., 2011. Effect of Non-uniform Porosity Distribution on Thermohydraulics in a Pebble Bed Reactor, in: *Proceedings of NURETH-14*.
16. Gnielinski, V., 1978. Formula for Calculating the Heat and Mass Transfer In Through Flow of a Fixed Bed at Medium and Large Peclet. *Process-Technology* 12, 363–366.

17. Hassan, Y.A., Dominguez-Ontiveros, E.E., 2008. Flow visualization in a pebble bed reactor experiment using PIV and refractive index matching techniques. *Nucl. Eng. Des.* 238, 3080–3085. <https://doi.org/10.1016/j.nucengdes.2008.01.027>
18. Jiang, S., Tu, J., Yang, X., Gui, N., 2021. Multiphase Flow and Heat Transfer in Pebble Bed Reactor Core, *Multiphase Flow and Heat Transfer in Pebble Bed Reactor Core*. <https://doi.org/10.1007/978-981-15-9565-3>
19. Kadak, A.C., 2005. A future for nuclear energy: Pebble bed reactors. *Int. J. Crit. Infrastructures* 1, 330–345. <https://doi.org/10.1504/IJCIS.2005.006679>
20. Kagumba, M., Al-Naseri, H., Al-Dahhan, M.H., 2019. A new contact time model for the mechanistic assessment of local heat transfer coefficients in bubble column using both the four-optical fiber probe and the fast heat transfer probe-simultaneously, *Chemical Engineering Journal*. Elsevier B.V. <https://doi.org/10.1016/j.cej.2018.12.046>
21. Khane, V., Taha, M.M., Mueller, G.E., Al-Dahhan, M.H., 2017. Discrete element method-based investigations of granular flow in a pebble bed reactor. *Nucl. Technol.* 199, 47–66. <https://doi.org/10.1080/00295450.2017.1324729>
22. Khane, V.B., 2014. Experimental and Computational Investigation of Flow of Pebbles in a Pebble Bed Nuclear Reactor. Missouri University of Science and Technology.
23. Koster, A., Matzner, H.D., Nicholisi, D.R., 2003. PBMR design for the future. *Nucl. Eng. Des.* 222, 231–245. [https://doi.org/10.1016/S0029-5493\(03\)00029-3](https://doi.org/10.1016/S0029-5493(03)00029-3)
24. KTA, 1983. Reactor Core Design of High-Temperature Gas-Cooled Reactors Part 2 : Heat Transfer in Spherical Fuel Elements. *Saf. Stand. Nucl. Saf. Stand. Com.* 3102.2, 1–5.
25. Li, H., Prakash, A., 1997. Heat Transfer and Hydrodynamics in a Three-Phase Slurry Bubble Column. *Ind. Eng. Chem. Res.* 36, 4688–4694. <https://doi.org/10.1021/ie9701635>
26. Liu, L., Deng, J., Zhang, D., Wang, C., Qiu, S., Su, G.H., 2020. Experimental analysis of flow and convective heat transfer in the water-cooled packed pebble bed nuclear reactor core. *Prog. Nucl. Energy* 122. <https://doi.org/10.1016/j.pnucene.2020.103298>
27. Liu, L., Zhang, D., Li, L., Yang, Y., Wang, C., Qiu, S., Su, G.H., 2018. Experimental investigation of flow and convective heat transfer on a high-Prandtl-number fluid through the nuclear reactor pebble bed core. *Appl. Therm. Eng.* 145, 48–57. <https://doi.org/10.1016/j.applthermaleng.2018.09.017>

28. Nazari, M., Jalali Vahid, D., Saray, R.K., Mahmoudi, Y., 2017. Experimental investigation of heat transfer and second law analysis in a pebble bed channel with internal heat generation. *Int. J. Heat Mass Transf.* 114, 688–702. <https://doi.org/10.1016/j.ijheatmasstransfer.2017.06.079>
29. Ostertagová, E., 2012. Modelling using polynomial regression. *Procedia Eng.* 48, 500–506. <https://doi.org/10.1016/j.proeng.2012.09.545>
30. Rimkevičius, S., Uspuras, E., 2008. Experimental investigation of pebble beds thermal hydraulic characteristics. *Nucl. Eng. Des.* 238, 940–944. <https://doi.org/10.1016/j.nucengdes.2007.08.001>
31. Rimkevicius, S., Vilemas, J., Uspuras, E., 2006. Experimental investigation of heat transfer and flow mixing in pebble beds. *Heat Transf. Eng.* 27, 9–15. <https://doi.org/10.1080/01457630600793939>
32. Schröder, E., Class, A., Krebs, L., 2006. Measurements of heat transfer between particles and gas in packed beds at low to medium Reynolds numbers. *Exp. Therm. Fluid Sci.* 30, 545–558. <https://doi.org/10.1016/j.expthermflusci.2005.11.002>
33. Taha, M.M., Said, I.A., Usman, S., Al-Dahhan, M.H., 2019. Temperature and velocity instrumentation and measurements within a separate-effects facility representing modular reactor core. *Int. J. Therm. Sci.* 136, 148–158. <https://doi.org/10.1016/j.ijthermalsci.2018.10.024>
34. Wakao, N., S, K., 1982. *Heat and Mass Transfer in Packed Beds*. Gordon and Breach Science Publishers Ltd., Paris.
35. Wu, C., Al-Dahhan, M.H., Prakash, A., 2007. Heat transfer coefficients in a high-pressure bubble column. *Chem. Eng. Sci.* 62, 140–147. <https://doi.org/10.1016/j.ces.2006.08.016>
36. Yamoah, S., Akaho, E.H.K., Ayensu, N.G.A., Asamoah, M., 2012. Analysis of fluid flow and heat transfer model for the pebble bed high temperature gas cooled reactor. *Res. J. Appl. Sci. Eng. Technol.* 4, 1659–1666.

### **III. EXPERIMENTAL INVESTIGATION OF THE CONVECTIVE HEAT TRANSFER COEFFICIENT AT DIFFERENT ANGULAR ORIENTATIONS INSIDE THE VOID IN A COLD FLOW PEBBLE BED REACTOR USING A NON-INVASIVE PEBBLE PROBE**

Muhna Alshammari, [1,3], Saud Aldawood [1,2], Ahmed Alalou [2,5], Zeyad Zeitoun [2], Muthanna H Al-Dahhan [1,2,4]\*

<sup>[1]</sup> Mining and Nuclear Engineering Department, Missouri University of Science and Technology, Rolla, MO 65409, USA.

<sup>[2]</sup> Linda and Bipin Doshi Chemical and Biochemical Engineering Department, Missouri University of Science and Technology, Rolla, MO 65409, USA.

<sup>[3]</sup> National Center for Nuclear Technology, King Abdulaziz City for Science and Technology, Riyadh, Kingdom of Saudi Arabia.

<sup>[4]</sup> TechCell, Mohammed VI Polytechnic University, Lot 660, Hay Moulay Rachid 43150, Ben Guerir, Morocco.

<sup>[5]</sup> Applied Organic Chemistry Labs, Faculty of Sciences and Technologies, Sidi Mohammed Ben Abdellah University, B.P. 2202 Fez, Morocco.

### **ABSTRACT**

The objective of this study was to investigate the effect of the location inside the reactor, the angular orientation of the probe pebble and the velocity of the coolant gas on the convective heat transfer coefficient in a pebble bed reactor. An advanced technique consisting of a probe pebble, a micro-foil sensor and a thermocouple probe was used to obtain accurate measurements of the local heat transfer coefficients. The heat transfer coefficients were higher in the near-wall region due to the higher local gas velocities near the wall owing to the higher void fraction. This effect was highlighted due to the high diameter of the pebbles (5 *cm*) used in this work. The local measurements showed that the location inside the void substantially impacts the heat transfer, with higher heat transfer

coefficients in the center and bottom of the void. Furthermore, the dimensionless Nusselt's number (Nu) was used to compare the experimental data with the empirical correlations available in the literature and a second order polynomial model with an  $R^2 = 0.9807$  and an average absolute relative error (AARE) equal to 9.08%, was developed for the prediction of the local heat transfer coefficient within the design and operation conditions of this work. The accurate local heat transfer data collected in this study are necessary for understanding the complex heat transfer mechanisms and can be used as benchmark data for the validation of computational fluid dynamics (CFD) simulations and other numerical models.

## 1. INTRODUCTION

The pebble bed reactor (PBR), which is a fourth generation (Gen IV) very high temperature gas-cooled reactor (VHTGR), is considered one of the most promising technologies for future energy generation, which can contribute to responding to the increasing global energy demand. This consideration is due to the various characteristics of these reactors, which include their high efficiency, cost-effectiveness, inherent safety, and environmental friendliness. The possibility of continuous reloading of these reactors and their broad industrial applications as a source of high-temperature energy for the generation of electricity and hydrogen production have motivated many governments and energy companies, especially in the USA and China to make important investment in research that is dedicated for optimizing the performance of PBRs in large-scale applications (Goodjohn, 1991; Koster et al., 2003).

The core of a PBR is packed with fuel pebbles that are 6 *cm* in diameter. Each pebble consists of numerous spherical fuel particles that are developed for use in gas-



cooled high temperature reactors. A fuel particle is called a tristructural-isotropic (TRISO) fuel element and consists of uranium dioxide particles that are covered by four protective layers that prevent the release of radiation due to the fission reaction (Abdulmohsin and Al-Dahhan, 2015a; Yamoah et al., 2012). These coating layers are composed of a porous carbon buffer, an inner layer of pyrolytic carbon, a silicon carbide barrier, and finally an outer layer of pyrolytic carbon. The heat that is generated by the pebbles due to the fission reaction, which may rise to as high as  $1800^{\circ}\text{C}$  is transferred to the coolant gas, which absorbs the heat and cools the fuel pebbles (Al-Juwaya et al., 2019, 2017; Meyer et al., 2007; Nabielek et al., 1990). Thus, the downward flow of the coolant gas serves as a transportation agent of the heat from the reactor's core to the industrial units, where the heat is utilized for various applications, mainly the generation of electricity. Helium is the most commonly used coolant gas in PBRs due to its chemical and radiological inertness (Wu et al., 2002). The use of the coolant gas includes the prevention of the melt down of the reactor's core by cooling the core during normal operation and the extraction of decay heat in case of loss of flow accidents (LOFA), during which the density of the decay-heated helium gas decreases and the gas flows upwards (Kadak, 2005).

Heat transfer in pebble bed reactors is a complex phenomenon and of crucial importance for nuclear reactors design, operation, and safety. This phenomenon is carried out by three mechanisms simultaneously: i) Conduction heat transfer (i.e., pebble to pebble, pebble to the wall, etc.), ii) Convection heat transfer (i.e., pebble to flowing coolant gas), iii) Radiation heat transfer (i.e., pebble to pebble, pebble to wall or core reflector, and core barrel to the wall) (Fenech, n.d.). However, forced convection heat transfer is the predominant mechanism during normal operation and LOFA conditions. Many research

projects have focused on studying the forced convective heat transfer inside the PBR's core. (Rimkevicius et al., 2006; Rimkevičius and Uspuras, 2008) investigated the forced convective heat transfer in two types of pebble beds (thin annular pebble beds and pebble beds placed between cylinders with an aspect ratio of  $D/dp = 4.29$ ). The pebbles spheres were electrically heated, and the heat flux was calculated based on the input electrical energy, while the temperature at the surface of the spheres and the temperature of the adjacent air were measured using thermocouples. The heat transfer coefficients were estimated at Reynolds numbers between 400 and 35000. (Hu et al., 2019) utilized the same approach to compare the forced convective heat transfer in a randomly packed bed with various configurations of grille-composite packed beds, using particle diameters of 6,9 mm and 12 mm and using the combination of electrical heating, heat flux sensors and thermocouples for obtaining the measurements. (Nazari et al., 2017) used electromagnetic induction heating to estimate the convective heat transfer coefficients at five locations along the length of three pebble beds that are formed of steel pebbles with pebble diameters of 5.5 mm, 6.5 mm and 7.5 mm, which correspond to low aspect ratios ( $D/dp$ ) of 4.91, 4.15, 3.6, respectively. The temperatures of the pebble spheres and the flowing dry air were measured using thermos sensors and the measurements were taken at turbulent flow conditions ( $4500 < Re < 10000$ ). Steel pebbles were also used in a study by (Liu et al., 2018) and (Liu et al., 2020) for the measurement of the heat transfer by the application of electrical heating and the measurement of the pebble sphere temperature and flowing fluid (water) temperature were taken by thermocouples. The inner diameter of the test tube was 80 mm and aspect ratios investigated were 10 and 8 for pebble diameters of 8 mm and 10 mm, respectively. In these studies, the natural convective heat transfer is

negligible due to the flow conditions of the fluid ( $Re > 300$ ), while the radiation heat transfer is also negligible due to the low temperatures studied ( $< 300\text{ }^{\circ}\text{C}$ ). However, due to the use of the steel pebbles, the accuracy of the forced convective heat transfer is slightly compromised by the conduction heat transfer between the metallic pebbles (Schröder et al., 2006). To limit the influence of the conduction heat transfer between the pebbles, (Schröder et al., 2006) used a wire mesh around the particles, which are electrically heated. Yet, the accuracy of the measurements was still compromised as the heat flux was estimated using the direct input method with the boundary conditions for constant surface temperature assumed when electrical induction or electromagnetic induction are used for heating. The estimation of the heat flux is unreliable as the boundary conditions for constant surface temperature were assumed, which should not be the case as isotherm surface temperature is not attained due to the thermal conductivity not being large enough (Kaviany, 1995).

Besides the lack of accuracy of the heat transfer measurements, the pebble diameters in these studies are also smaller than the actual size of the pebbles in a PBR, which is 6 *cm*. This size of pebbles was only used by (De Beer et al., 2018) to investigate the effective thermal conductivity due to conduction and radiation in the near-wall region in structured and randomly cubic packed beds. The forced convective heat transfer experiments using the actual size of the pebbles in the PBR was not possible until the development of a sophisticated measurements technique at the Multiphase Flows and Reactors Engineering and Education Laboratory (mFREEL) at Missouri University of Science and Technology. This technique utilizes a copper probe pebble, a micro-foil heat flux sensor, and a thermocouple probe and provides accurate measurement of the local

convective heat transfer. The development of such accurate techniques allows better understanding of the effect of the design and operation conditions of the reactor on the local heat transfer coefficients. Nevertheless, the influence of these design and operation parameters can be better described using dimensionless groups such as the Reynold number ( $Re$ ), Nusselt number ( $Nu$ ), and Prandtl number ( $Pr$ ). The relationship between these dimensionless groups can be described using the following equation:

$$Nu = f(\varepsilon, Re, Pr) \quad (1)$$

where  $\varepsilon$  is the bed porosity.

Each dimensionless group  $Nu$ ,  $Re$ , and  $Pr$  can be calculated by equations (Eq 2, Eq3, and Eq4) respectively;

$$Nu = \frac{h d_p}{k} \quad (2)$$

where  $h$  is the heat transfer coefficient ( $kW / m^2. K$ ),  $d_p$  is the diameter of the pebble (m) and  $k$  is the thermal conductivity of flowing gas ( $kW / m. K$ ).

$$Re = \rho V_g d_p \mu \quad (3)$$

where  $\rho$  is the density of the fluid ( $kg/m^3$ ),  $V_g$  is the superficial gas velocity (m/s) and  $\mu$  is the dynamic viscosity of fluid ( $kg / m.s$ ).

$$Pr = \frac{\mu C_p}{k} \quad (4)$$

where  $C_p$  is the heat capacity in  $J/kg.k$ .

(Abdulmohsin and Al-Dahhan, 2015) used this technique in order to investigate the local heat transfer between the heated pebbles and the flowing gas (air) in a pebble bed reactor with a pebble diameter of 5 cm and an aspect ratio of 6. The measurements were carried out at three axial locations (top, middle and bottom of the column) and four radial

positions ( $r / R = 0.0, \pm 0.33, \pm 0.67$ , and  $\pm 0.9$ ) and under different superficial inlet gas velocities ( $0.02 - 2 \text{ m/s}$ ) to cover both laminar and turbulent flow conditions. It was found that with this pebble size, the convective heat transfer coefficient is significantly higher in the near-wall region, compared to the center of the reactor. This was attributed to the difference in the local velocities of the gas (Auwerda et al., 2011). The differences in the local velocity between the center and near-wall region were reported to be due to the higher void fraction near the wall owing to the contact between the wall and the pebbles (Al Falahi et al., 2018; Al Falahi and Al-Dahhan, 2016). A discrete element method (DEM) simulation developed for packing randomly packed beds with pebbles of different sizes showed that the bed porosity is substantially higher near the wall of the reactor and that the wall effect is more pronounced when the diameter of the pebbles is high (Khane et al., 2017). However, in the study by (Abdulmohsin and Al-Dahhan, 2015), the heat transfer measurements were taken in only one position in the center of the void with the thermocouple placed directly in front of the center of the copper probe pebble, despite the void between the pebbles being high. The experimental measurement of the velocity fields in the void between the pebbles have shown that the local velocity of the flowing fluid varies in the void depending on the vertical position and proximity to the pebbles, hence indicating that the heat transfer in the void is also non-uniform (Dominguez-ontiveros et al., 2008; Hassan and Dominguez-Ontiveros, 2008; Lee and Lee, 2009).

Therefore, to complement the work of (Abdulmohsin and Al-Dahhan, 2015), in this study, the local convective heat transfer measurements are taken at three different positions vertical in the void with angular orientations of the probe pebble at every axial position (top, middle and bottom of the bed) and at four radial locations ( $r/R =$

0.0,  $\pm 0.33$ ,  $\pm 0.67$ , and  $\pm 0.9$ ) along one diameter line. The objective of this study is to further understand the variation of the local heat transfer inside the PBR and to quantify the effect of the operation parameters on this variation. To achieve this objective, a unique scaled-down experimental setup which was designed at the Multiphase Flows and Reactors Engineering and Education Laboratory (mFReel) at Missouri University of Science and Technology was used for experimentation. The test section of the setup consists of a column that has a diameter of 30 cm, packed with 5 cm pebbles, and hence the aspect ratio of the packed bed is 6. Despite the low aspect ratio of the bed, since the pebbles are large, we are able to mimic the void fluctuations in the near-wall region. For the measurement of the heat transfer coefficients, a sophisticated non-invasive measurement technique consisting of a heat transfer probe pebble, a foil sensor and a thermocouple probe was used in order to obtain accurate results. A second-order polynomial model is also developed for the prediction of the heat transfer coefficient based on the design and operation conditions of the PBR, within the experimental range of this work.

## 2. EXPERIMENTAL SETUP

The experimental setup was designed and manufactured at the Multiphase Flows and Reactors Engineering and Education Laboratory (mFReel) to conduct the experimental measurements of the heat transfer coefficient as shown in Figure 1 a. In a real PBR, the pebbles move slowly downwards until they reach the outlet, where the pebbles are tested for burnup and are either returned to the reactor or replaced, while the coolant gas (helium) flows downwards, transferring the heat from the heated pebbles and cooling the core of the reactor (Abdulmohsin and Al-Dahhan, 2015; Koster et al., 2003). Due to the high

differences in the velocity of the coolant gas and the velocity of the downward movement of the pebbles, the pebbles were maintained stagnant as a fixed bed in the test column (Abdulmohsin, 2013; Nazari et al., 2017). The setup consists of a Plexiglas column of  $0.3\text{ m}$  in diameter and  $0.9\text{ m}$  in height that is randomly packed with glass pebbles ( $0.05\text{ m}$  in diameter). The diameter of the pebbles is close to the size of the pebbles used in a real PBR ( $0.06\text{ m}$ ). However, the bed diameter to pebble diameter ratio ( $\frac{D}{d_p} = 6$ ) is much smaller than the ratio in a real PBR, which cannot be mimicked in a laboratory due to the unavailability of the high capacity of compressed air flow which is required when the diameter of the reactor is larger than  $1\text{ m}$ .

A perforated distributor plate with 140 holes (each hole is  $0.03\text{ cm}$  in diameter (Figure 1b) is placed above the column, to ensure the uniform distribution of air inside the column. A cone, which is upper plenum, that has a height of  $0.1\text{ m}$  and a diameter of  $0.3\text{ m}$  is connected to two air compressors to force the air to flow downward in the column (Figure 1b).

Two rotameters (Omega HFL6715A-0045-14) were used to control the air flow rate. The bottom part of the column (lower plenum) is composed of a plastic cone, with a height of  $0.08\text{ m}$  and a  $60^\circ$  angle and is equipped with a gas outlet vent in the center that has a diameter of  $0.05\text{ m}$ , used for the release of the air out of the system. It is worth mentioning that the height of the randomly packed bed is  $98\text{ cm}$  and its porosity was previously measured to be ( $\varepsilon = 0.397$ ) using the direct balance method (Eq. 5).

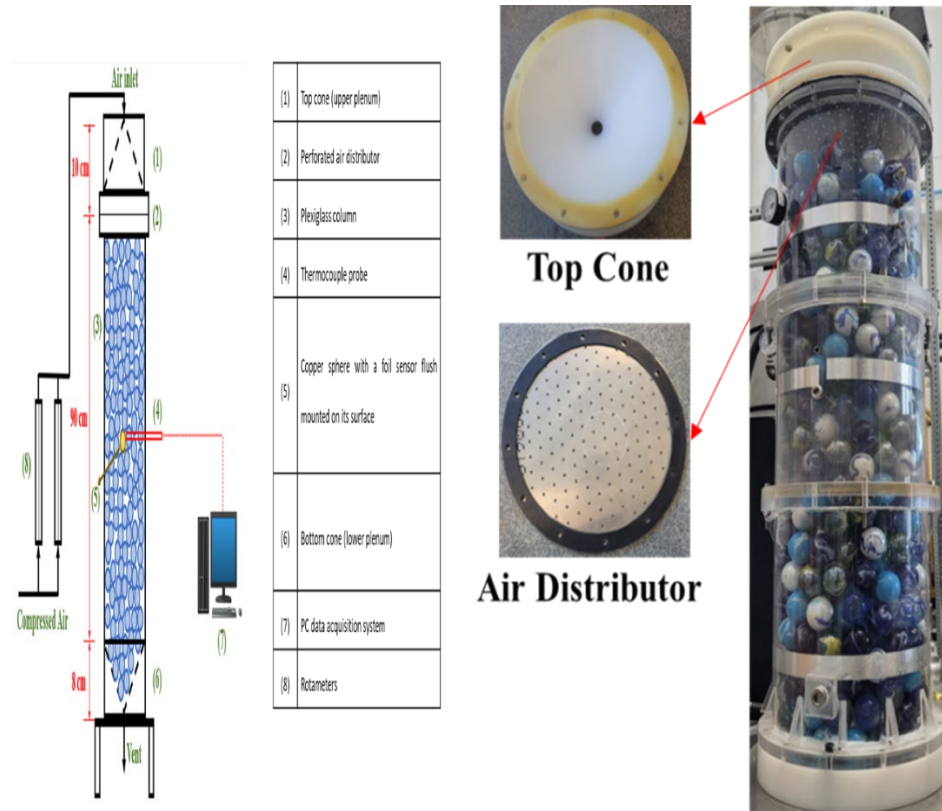


Figure 1. Experimental setup: a) Schematic diagram; b) Pictorial representation for the bed, top cone (upper plenum), and air distributor.

$$\varepsilon = \frac{V_c - V_p}{V_c} \quad (5)$$

where  $V_c$  the volume of the column calculated is based on the known length and diameter of the column and  $V_p$  is the volume occupied by the pebbles, which is calculated using the number of pebbles in the column and the known diameter of the pebbles, which are considered perfect spheres. The column with the upper and lower plenum were placed on a strong heavy table to minimize the vibrations and to keep it fixed in placed during the operation of the experiments.



### 3. MEASUREMENT TECHNIQUES

#### 3.1. NONINVASIVE HEAT TRANSFER PROBE PEBBLE WITH MICRO-FOIL SENSOR AND A THERMOCOUPLE

The heat transfer measurements were obtained using an advanced and sophisticated technique that was developed by the research team of the Multiphase Flows and Reactors Engineering and Education Laboratory (mFREEL) (Abdulmohsin, 2013). This technique was adapted and modified based on the work of (Li and Prakash, 1997; Wu et al., 2007).

This technique consists of an advanced, reliable, and fast response micro-foil sensor (Figure 2) with dimensions of  $11\text{ mm} \times 11\text{ mm} \times 0.08\text{ mm}$ , which was purchased from RDF Corporation (model no. 27036 – 1). The sensor was flush mounted on the surface of a heated solid copper pebble, as shown in Figure 3 to measure simultaneously the pebble surface temperature ( $T_{s,i}$ ) and local instantaneous heat flux ( $q_i$ ) from the hot sphere surface to the adjacent surroundings. The spherical-shaped copper pebble has a diameter of  $5\text{ cm}$ , the same as the glass pebbles used in the bed, and it can be placed at different locations in the packing as part of the bed structure. The heating of the copper sphere was carried out using a cartridge heater ( $120\text{V}, 150\text{W}$ ) that is embedded inside the copper sphere and heats its surface. The cartridge heater was purchased from Next Thermal Corporation (model no. 184595) (Figure 4) and its intensity was controlled by a D.C power supply with a range of  $20 - 40\text{ V}$ . A thermocouple probe (T-type K) with a diameter of  $1.6\text{ mm}$  is implemented in the current study to measure the flowing air temperature ( $T_{b,i}$ ) by placing it in the void, directly in front of the micro-foil sensor that is flushed on the surface of the copper sphere.

An amplifier was placed between the heat flux sensor and the data acquisition (DAQ) system which was used to convert and amplify the microvolt signals indicating the heat flux. The implementation of these foil sensors was successful in both single-phase systems (Abdulmohsin and Al-Dahhan, 2015b; Taha et al., 2018) and multiphase systems (Kagumba et al., 2019; Wu et al., 2007). In contrast to the flux foil sensors, thermocouples are directly connected to the DAQ.

The heat loss due to conduction by contact between the heated copper pebble and the glass pebbles is considered to be reasonably negligible due to the low thermal conductivity of the glass balls.



Figure 2. Micro-foil heat flux sensor.

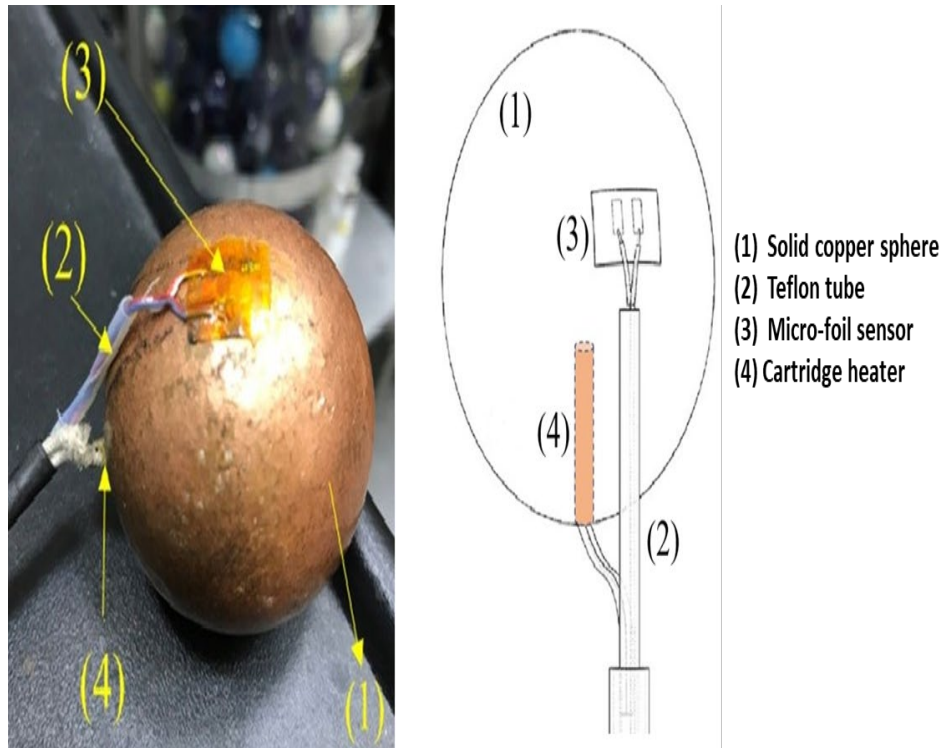


Figure 3. Solid copper sphere with a micro-foil sensor and cartridge heater.



Figure 4. Cartridge heater.

### 3.2. DATA ACQUISITION

Preliminary experiments were conducted to determine the time needed to reach thermal stability. This time is defined as the time after which the differences between the

temperatures of the bulk and the surface of the copper pebble probe were almost maintained constant, as shown by the plateau in Figure 5. The system should be running for at least 30 *min* before collecting data to ensure reaching steady-state conditions. Hence, all the measurements in this study were obtained after 35 minutes of the start of the experiment.

In this study, the amplified heat flux signals and the thermocouple signals were collected at a sampling frequency of 50 *Hz*. The sampling time of collecting data was tested by plotting the instantaneous heat transfer coefficients as a function of sampling time as shown in Figure 6. Therefore, Figure 6 reveals that the absence of any significant variation in the heat transfer coefficients that occurs after a sampling time of 200s is surpassed. Hence, all measurements were conducted after 35 *min* from the initial operation and the time-averaged measurement was taken after 240s of sampling time.

Instantaneous heat transfer coefficients ( $h_i$ ) were obtained by using the following equation (Eq.6) (Abdulmohsin, 2013):

$$h_i = \frac{q_i}{T_{si} - T_{bi}} \quad (6)$$

where  $q_i$  is the instantaneous heat flux per unit area of the sensor,  $T_{si}$  is the instantaneous temperature of the sensor probe surface, and  $T_{bi}$  is the instantaneous bulk temperature of the fluid media.

Since the measurement technique was operated at a frequency of 50 *Hz* and a sampling time of 240 *s*. The time-averaged heat transfer coefficients ( $h$ ) were estimated at each location by averaging the instantaneous heat transfer data collected as follows:

$$h = \frac{1}{N} \sum_{i=1}^N h_i = \frac{1}{N} \sum_{i=1}^N \frac{q_i}{T_{si} - T_{bi}} \quad (7)$$

where  $N$  is the total number of experimental samples ( $N = 12000$ ) for 240 seconds.

As mentioned earlier, the measurements were taken at different axial levels,  $H1$ ,  $H2$ , and  $H3$ . At each axial level, measurements were obtained at four different radial positions ( $r/R = 0.0, \pm 0.33, \pm 0.67$ , and  $\pm 0.9$ ) along one diameter line. Accordingly, the averaged heat transfer coefficients ( $h_{avg}$ ) at each radial position were obtained by azimuthally averaging the time-averaged heat transfer coefficient as shown below:

$$h_{avg}|_{r/R} = \frac{1}{n} \sum_{i=1}^n h(\theta) \quad (8)$$

where  $n$  is the number of locations or data points obtained at each radial position for each azimuth.

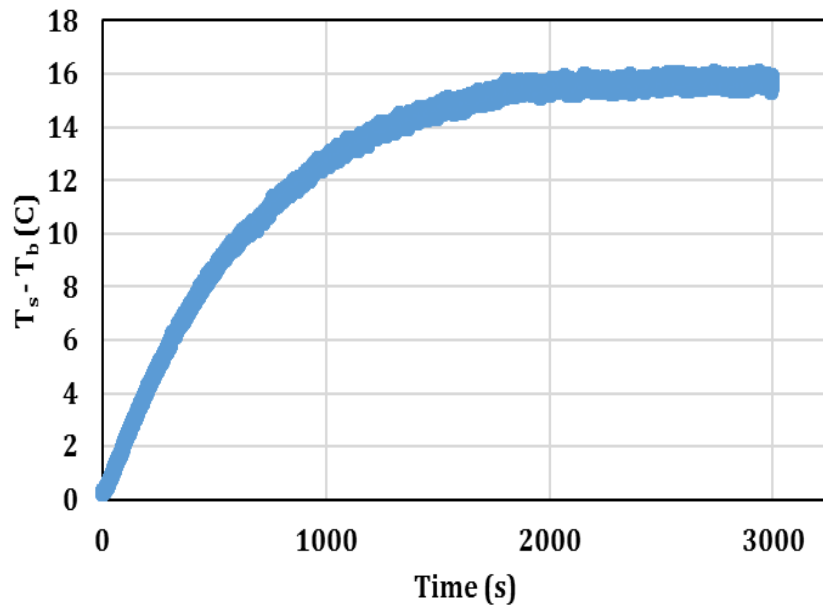


Figure 5. Steady-state time series with different temperatures between the bulk temperature and the surface temperature.

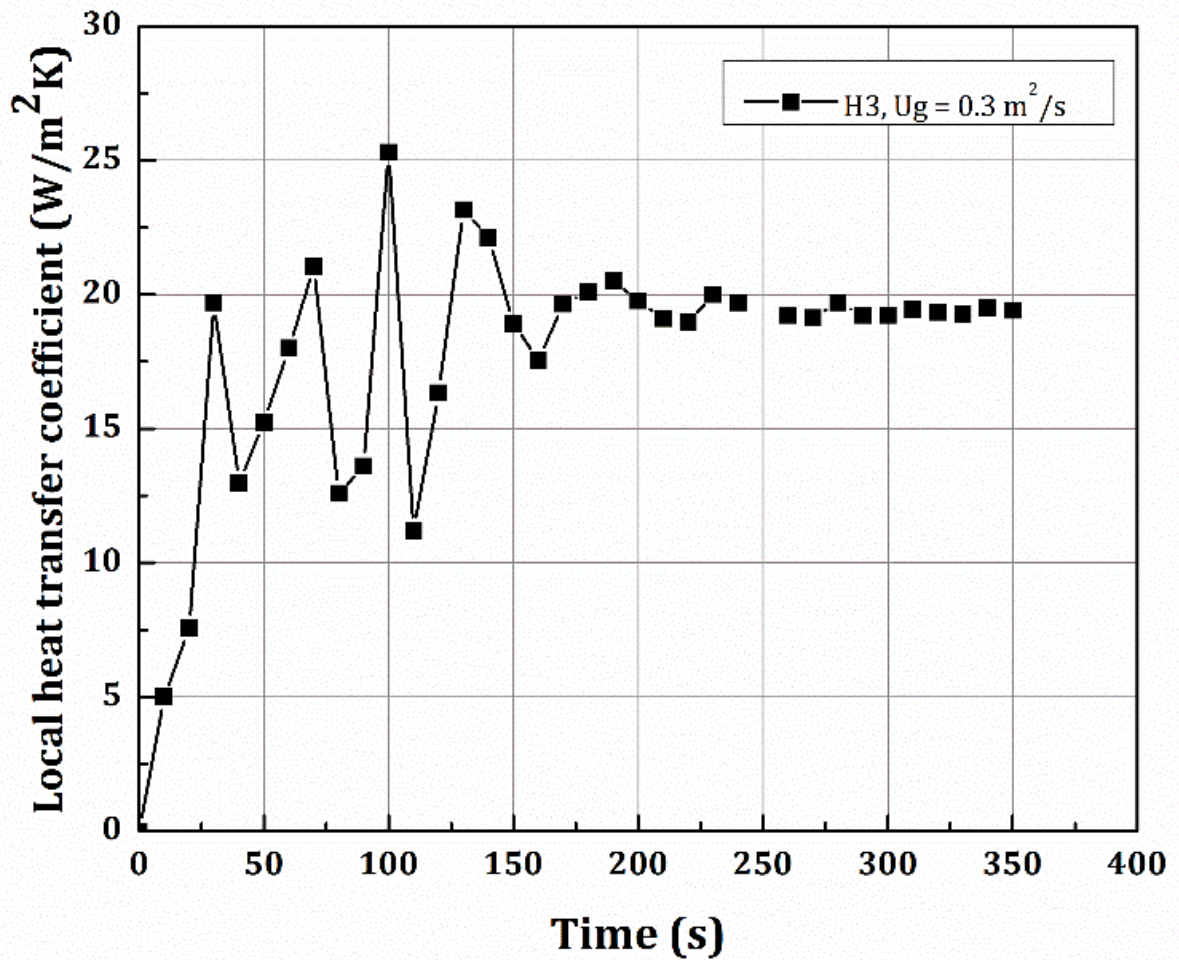


Figure 6. The stability of heat transfer coefficients as a function of the sampling time.

#### 4. EXPERIMENTAL PROCEDURES

The flowing air temperature, the sphere surface temperature and the heat flux between the sphere and flowing air were measured by the thermocouple probe and micro-foil sensor in order to estimate the local convective heat transfer at three different axial levels, which were measured as the distance from the top of the distributor ( $H1 =$

21.6 cm,  $H2 = 44.5$  cm and  $H3 = 86.4$  cm). At each axial level, the measurement were taken at four different radial positions ( $r/R = 0.0, \pm 0.33, \pm 0.67$ , and  $\pm 0.9$ ) along one diameter line, as shown in Figure 7. At each location, the measurements were taken at three vertical positions inside the void by changing the angular orientation of the heated copper pebble and hence, also changing the position of the thermocouple accordingly, as it should be directly in front of the heat flux sensor, as shown in Figure . All experiments were repeated three times to ensure the repeatability and accuracy of the results. To change the location of the probe pebble, the column was emptied of the pebbles and then repacked with the pebbles again, with the copper pebble probe being placed at the location where the measurement is supposed to be taken. The test section of the column was repacked carefully in the same structure throughout the experiments to prevent any contact between the surface of the sensor and the surface of the surrounding pebbles. In the other parts of the column, the pebbles were repacked randomly, and the convective heat transfer coefficient was measured at all the superficial inlet gas velocities studied, before moving the copper pebble probe to the next location in the same way, by unpacking and repacking the pebbles in the column. The superficial inlet gas velocities at which the measurements were carried out range from 0.02 m/s to 2 m/s, which correspond to  $994 < Re < 6625$ , covering both laminar and turbulent flow regimes.

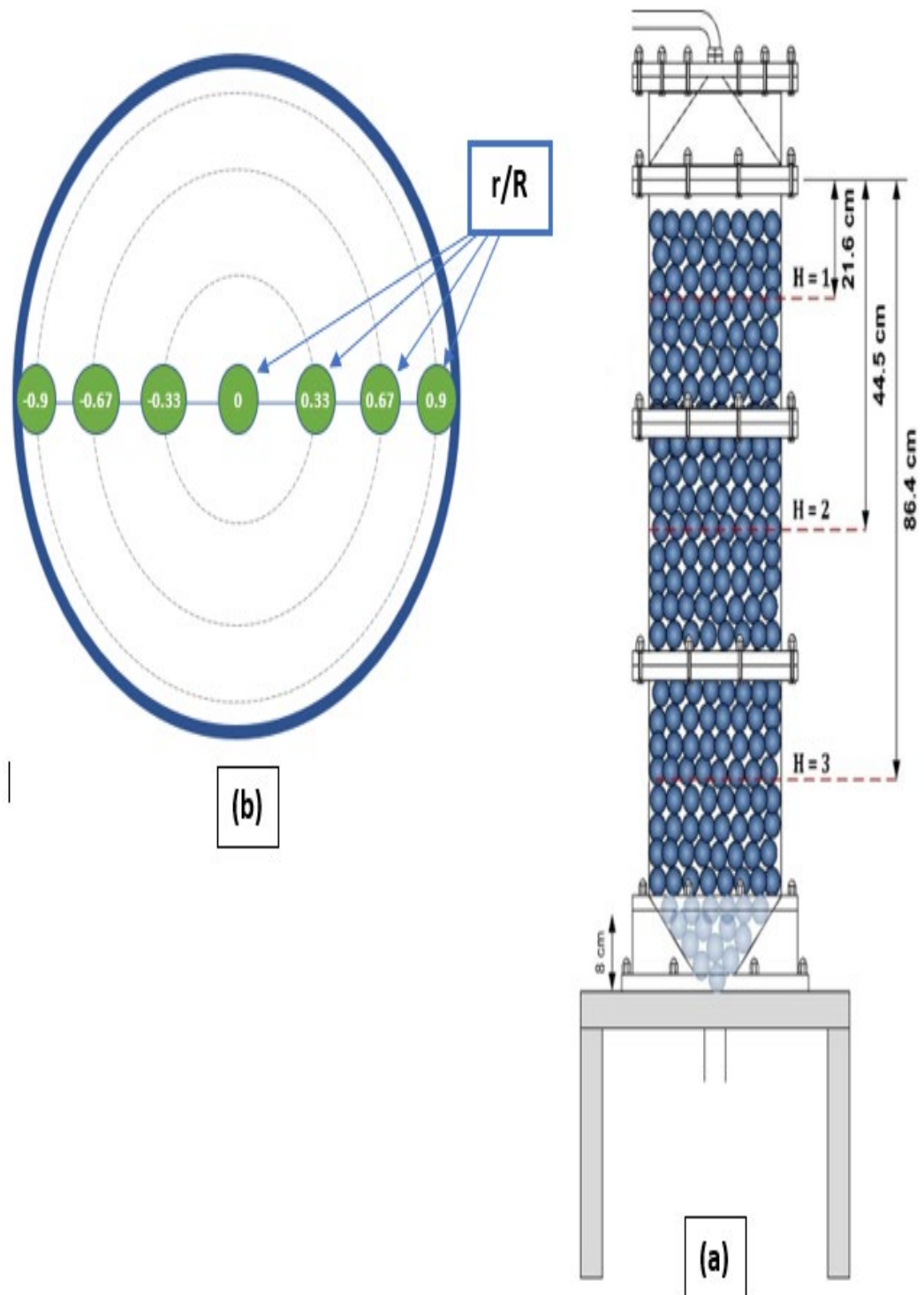


Figure 7. Schematic illustration showing a) axial levels and, b) radial positions where the measurements were taken.



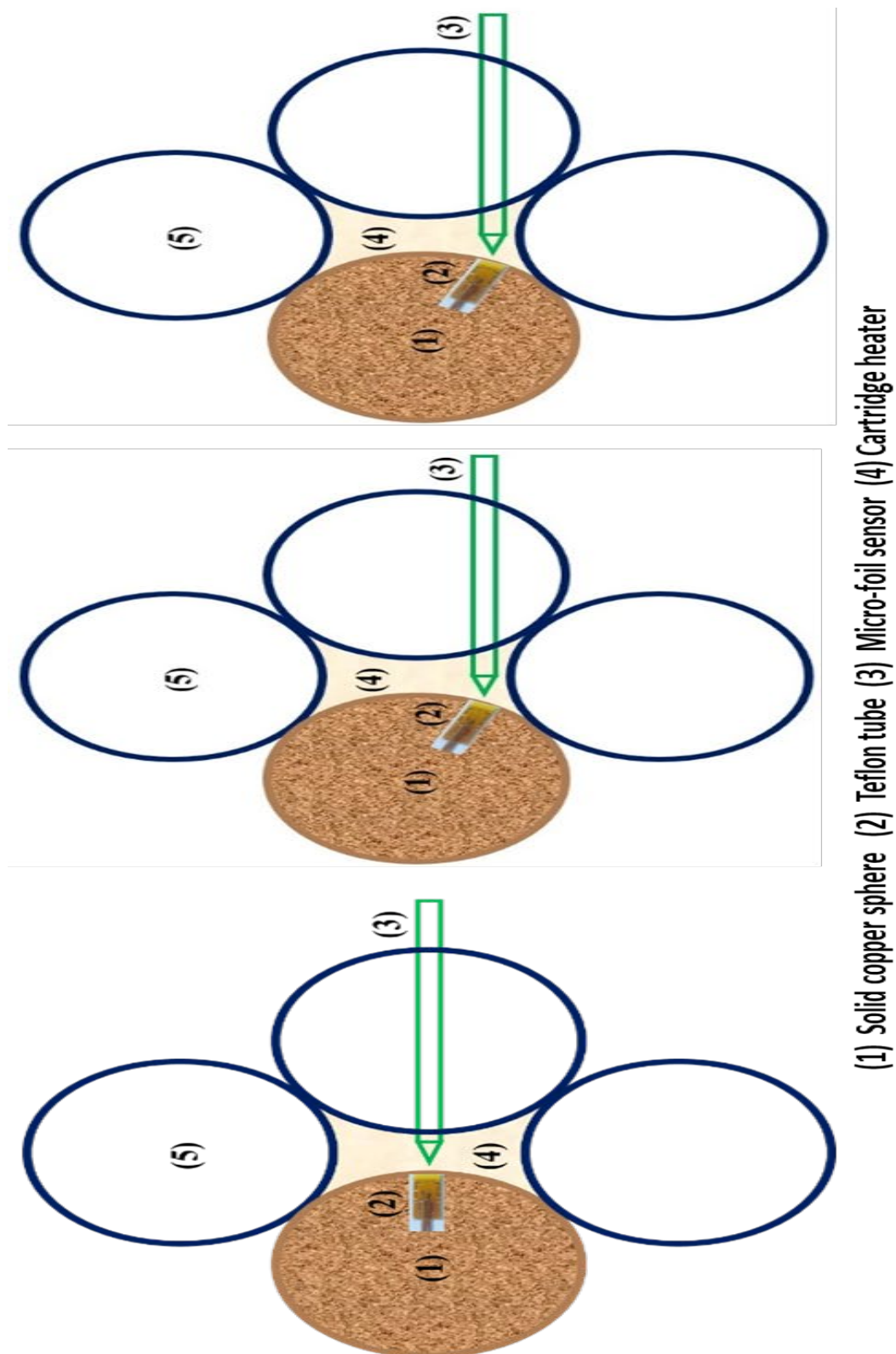


Figure 8. Schematic representation of the position of the three angular orientations of the copper probe pebble in the void.

## 5. RESULTS AND DISCUSSION

### 5.1. EFFECT OF THE GAS FLOW AND LOCATION INSIDE THE PBR'S CORE ON THE HEAT TRANSFER

The convective heat transfer coefficient was measured at three axial levels (top, middle, and bottom) and four radial locations ( $r/R = 0.0, \pm 0.33, \pm 0.67$ , and  $\pm 0.9$ ). The angular orientation of the pebble was varied three times at each radial and axial position, in order to measure the convective heat transfer at different positions in the void, and the thermocouple was moved accordingly in order to be aligned with the micro-foil sensor that is placed on the surface of the probe pebble, as shown in Figure 8. The superficial inlet velocity of the coolant gas (air) was also varied at each position ( $U_g = 0.3, 0.6, 1.2, 1.6$  and  $2$  m/s), covering both laminar and turbulent flow of the gas in the column. The heat local heat transfer measurements were repeated three times and the repeatability standard deviation was 0.22. Figures 9, 10, and 11 show the variation of the heat transfer coefficients based on the radial position, the superficial inlet gas velocity, and the angular orientation inside the void, at the top, middle and bottom of the column, respectively. It can be observed that, regardless of the axial level in the column and the angular orientation of the pebble inside the void, the heat transfer coefficient increases with the increase of the  $r/R$  value, meaning that the heat transfer due to forced convection is much higher near the wall compared to the center of the test column. This is further elucidated in Figure 12, where the heat transfer for each of the voids at the three axial levels of the column was plotted as a function of the superficial inlet velocity at the center of the reactor ( $r/R = 0$ ) and the near-wall region ( $r/R = 0.9$ ). It is apparent from Figure 12 that the heat transfer is much higher near the wall than in the center of the test column. This is owing to the difference in

the local actual gas velocities, which are much higher near the wall due to the effect of the wall-pebble contact that creates a much higher void fraction, compared to the center of the column and hence, the flow of the gas encounters less resistance in the near-wall region (Al Falahi and Al-Dahhan, 2016; Khane et al., 2017). On the other hand, at the center of the column, the pebbles are tightly packed due to the pebble-pebble contact and the weight of the pebbles, and hence, less void is available for the flow of the gas, which encounters a higher resistance leading to lower local actual velocities of the gas and eventually resulting in lower heat transfer coefficients in the center of the column (Al Falahi and Al-Dahhan, 2016; Khane et al., 2017). This effect is more pronounced when the pebble diameter is big, which is the case in this study (5 cm) and which approaches the actual size of the pebble in a real PBR (6 cm). Despite the low bed diameter to pebble diameter ratio (aspect ratio) of the set-up used in this study, the wall effect was still highlighted due to the large diameter of the pebbles, while the aspect ratio of a real PBR cannot be mimicked in a laboratory due to the unavailability of column that are large enough and the corresponding energy requirements for the flow of the gas, which are also currently unavailable.

The difference in the heat transfer coefficients between the center and the wall of the reactor is more graphically visible at high superficial inlet gas velocities, as the heat transfer coefficients at these high superficial inlet gas velocities are much higher, ranging between 108.84–125.65  $W/m^2K$  at  $U_g = 2 \text{ m/s}$  and  $r/R = 0.9$ , compared to a range of variation of 20.55–24.49  $W/m^2K$  at  $U_g = 0.3 \text{ m/s}$  and  $r/R = 0.9$ . However, this does not mean that this difference increases with the increase of the superficial inlet gas velocity. As a matter of fact, the difference in the heat transfer coefficients between the center and

the near-wall region of the reactor are higher at low superficial inlet gas velocities ( $U_g = 0.3 - 0.6 \text{ m/s}$ ), for which the heat transfer values are between 21.86% and 55.88% higher near the wall ( $r/R$ ) compared to the center of the column. At high superficial inlet gas velocities ( $U_g = 1.2 - 2 \text{ m/s}$ ), the heat transfer measurements near the wall are between 14.5% and 20.32% higher than at the center, which is a much lower difference when compared to the difference that was obtained at low superficial inlet gas velocities. Hence, it is obvious that the wall effect is reduced at high superficial inlet gas velocities when flow of the gas is turbulent ( $U_g = 1.2 - 2 \text{ m/s}$ ), compared to the laminar flow of the gas ( $U_g = 0.3 - 0.6 \text{ m/s}$ ). This can be attributed to the gas fluctuations and thermal mixing that increase with the increase of the turbulence of the flow of the gas, and hence, helping to homogenize the heat transfer across the diameter of the column.

The above-mentioned observations are the same regardless of the axial location in the bed in the pebble bed. However, the heat transfer coefficients do vary based on the axial location in the bed. The heat transfer coefficients are higher when moving from the top to the bottom of the reactor, as the heat transfer coefficient increased by 7.73-17.16% at the various superficial inlet gas velocities studied when moving from the top to the bottom of the reactor at the center of the bed ( $r/R = 0$ ), where the measurements were taken in the center of the void. A similar pattern was observed when moving from top of the reactor to the bottom section of the bed in the near-wall region ( $r/R = 0$ ), with a 7.75-16.1% increase in the heat transfer coefficient. However, this effect is only due to the flow of the gas, which is not equilibrated at the top of the bed ( $(H/D) = 0.72$ ) due to the height of the bed above it not being enough to allow for the flow of the gas to equilibrate. On the other hand, in the middle ( $(H/D) = 1.48$ ) and bottom ( $(H/D) = 2.88$ ) axial locations in the bed,

which are the fully developed regions of the bed, the height of the bed above these regions is sufficient to allow for the flow of the volumetric flow of the gas to equilibrate and hence the local heat transfer coefficients in these axial locations are very similar. Hence, the relationship between the heat transfer coefficients and the local gas velocities is established and experimentally proven in the fully developed region of the bed, where the flow of the gas is equilibrated and the structure of the packing in this region which is more homogenous and isotropic (Alshammari et al., 2023a, 2023b; Khane, 2014).

Figures 13, 14, and 15 elucidate the differences between the heat transfer coefficients based on the angular orientation of the pebble in the void, at different axial levels, in the center of the bed and in the region near the wall, under the different superficial inlet gas velocities studied. It is clear from the figures that the heat transfer coefficients are substantially lower when the measurements are taken at the upper position in the void compared to the center and bottom of the void. This is especially the case in the top axial level ( $(H/D)=0.72$ ) of the bed, where the heat transfer coefficients at the center of the void are between 16.26% and 49.88% higher than the heat transfer coefficients at the upper position in the void, at  $r/R = 0$ . This high difference in the local heat transfer coefficients between the upper and the middle location in the void is only the case in the top axial level of the bed, where the flow of the gas has not had enough height above it to equilibrate and the packing structure is not homogenous and isotropic as in the middle ( $(H/D)=1.48$ ) and bottom ( $(H/D)=2.88$ ) axial locations. However, at the near-wall region in the top axial level ( $(H/D)=0.72$ ), the difference in the heat transfer coefficients between the upper region of the void and the center of the void is not as pronounced, while the same pattern is observed with an increase between 11.55% and 18.41%. The lower heat transfer coefficients at the

upper position in the void are due to the low actual local velocities of the gas in those positions due to their vicinity to the pebbles that are above it, which limit the passage of the gas to the upper region of the void and reduce its local velocity. In the center and bottom of the void, however, the actual local velocities of the gas are higher due to the lower resistance to the flow of the gas by the pebbles above the void due to the relatively greater distance between these positions in the void and the pebbles that are above the void. This difference is less pronounced near the wall ( $r/R = 0.9$ ) due to the effect of the pebble-wall interaction, which is more uniform, compared to the non-uniform structure of the bed in the center ( $r/R = 0$ ) due to the inhomogeneity resulting from the packing of the pebbles and the pebble-pebble interactions. At the middle axial level of the bed ( $(H/D) = 1.48$ ), the increase of the heat transfer coefficients when passing from the upper to the center position in the void is between 3.37% and 11.44% at  $r/R = 0$ , and between 6.33% and 17.35% at  $r/R = 0.9$ . On the other hand, at the bottom axial level of the bed ( $(H/D) = 2.88$ ), the increase becomes even less significant with a maximum increase of 4.94% at  $r/R = 0$  and 5.01% at  $r/R = 0.9$ . The same pattern of variability is observed when moving from the center of the void to the bottom position in the void. When moving from the top axial level to the bottom axial level, the effect of the angular orientation of the probe pebble, and hence the effect of the position in the void at which the measurement was taken gradually becomes less significant. This is due to the enhancement of the uniformity of the flow of the gas when moving down the bed by the help of the packing and hence the differences between the measurements due to the position in the void becoming limited.

Figure 16 compares the heat transfer coefficients taken at the center of the void with the average heat transfer coefficients in the void based on three measurements along the

height of the void (upper, middle, and lower locations in the void). It is apparent from Figure 16 that the difference between the heat transfer coefficients in the center and the average heat transfer in the void increases when increasing the superficial inlet gas velocity in the top level of the column in both the center ( $r/R=0$ ) and the near-wall region ( $r/R=0.9$ ). At the top axial level, the difference in the heat transfer coefficients in the center and the average in the void increases from 1.88-2.64% to 5.86-8.17% at  $r/R=0$ , and from 0.71-4% to 1.42-4.7% at  $r/R=0.9$ , when passing from laminar to turbulent flow. At the middle level of the test column, these differences are lower, in the range of 1.32-4.31% at  $r/R=0$  and 0.18-3.62% at  $r/R=0.9$ . At the bottom level of the column, the difference becomes very insignificant ( $<1\%$ ) at both the center and the near-wall region. The deviation between the heat transfer coefficients in the center of the void and the average heat transfer in the void at the top level of the reactor are due to the non-uniformity of the flow of the gas, which could be due to the distributor at the top of the test column, where low pressure drop is created. The uniformity of the flow is enhanced as the gas flows down the bed of pebbles, which enhances the uniformity of the flow in the void. Based on this, the difference remains small, except at the top level and hence, it may not be necessary to take measurements at several locations in the void as one measurement in the center can be considered representative of the heat transfer coefficient in the void.

Figure 17 shows the convective heat transfer coefficients measured at the center of the void at the center of the bed ( $r/R=0$ ) and at the near wall region ( $r/R=0.9$ ), compared with the measurements reported in Alshammari et al., 2023b, at the same location at the top ( $(H/D)=0.72$ ), middle ( $(H/D)=1.48$ ), and bottom ( $(H/D)=2.88$ ) levels of the bed. It can be clearly seen that there is no visible difference between the results of the heat transfer

measurements collected in this study and the results of the measurement reported in the work of Alshammari et al., 2023b.

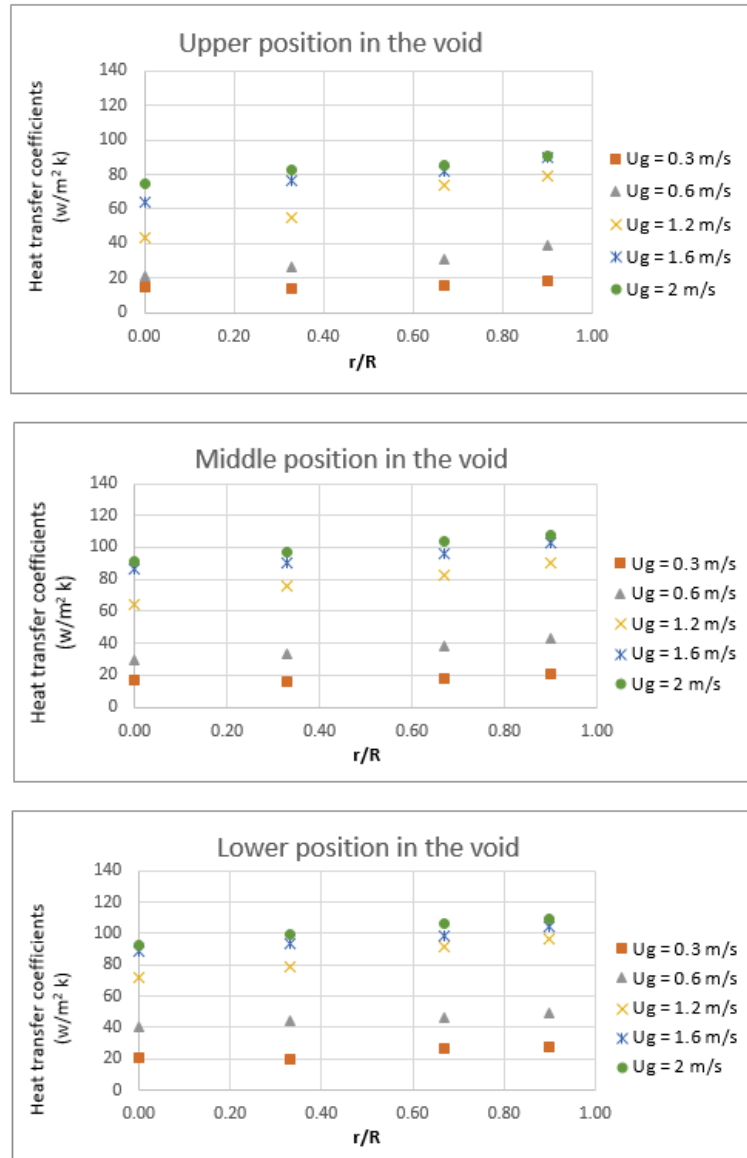


Figure 9. The variation of heat transfer coefficient depending on the radial position and the velocity of the flowing gas when the thermocouple probe is placed at three different positions in the void, at the top level of the bed ( $H/D = 0.72$ ).



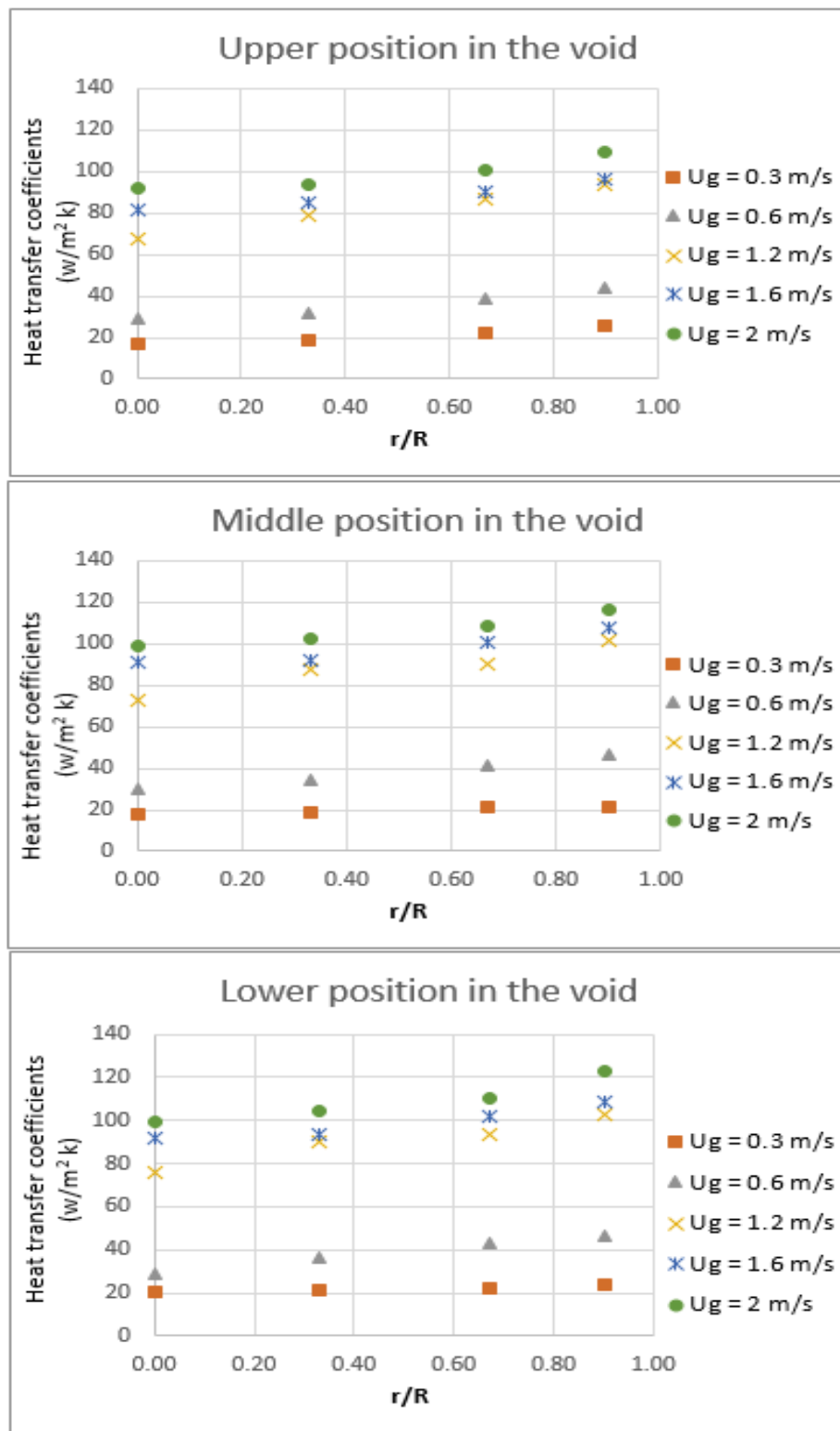


Figure 10. The variation of heat transfer coefficient depending on the radial position and the velocity of the flowing gas when the thermocouple probe is placed at three different positions in the void, at the middle level of the bed ( $H/D = 1.48$ ).

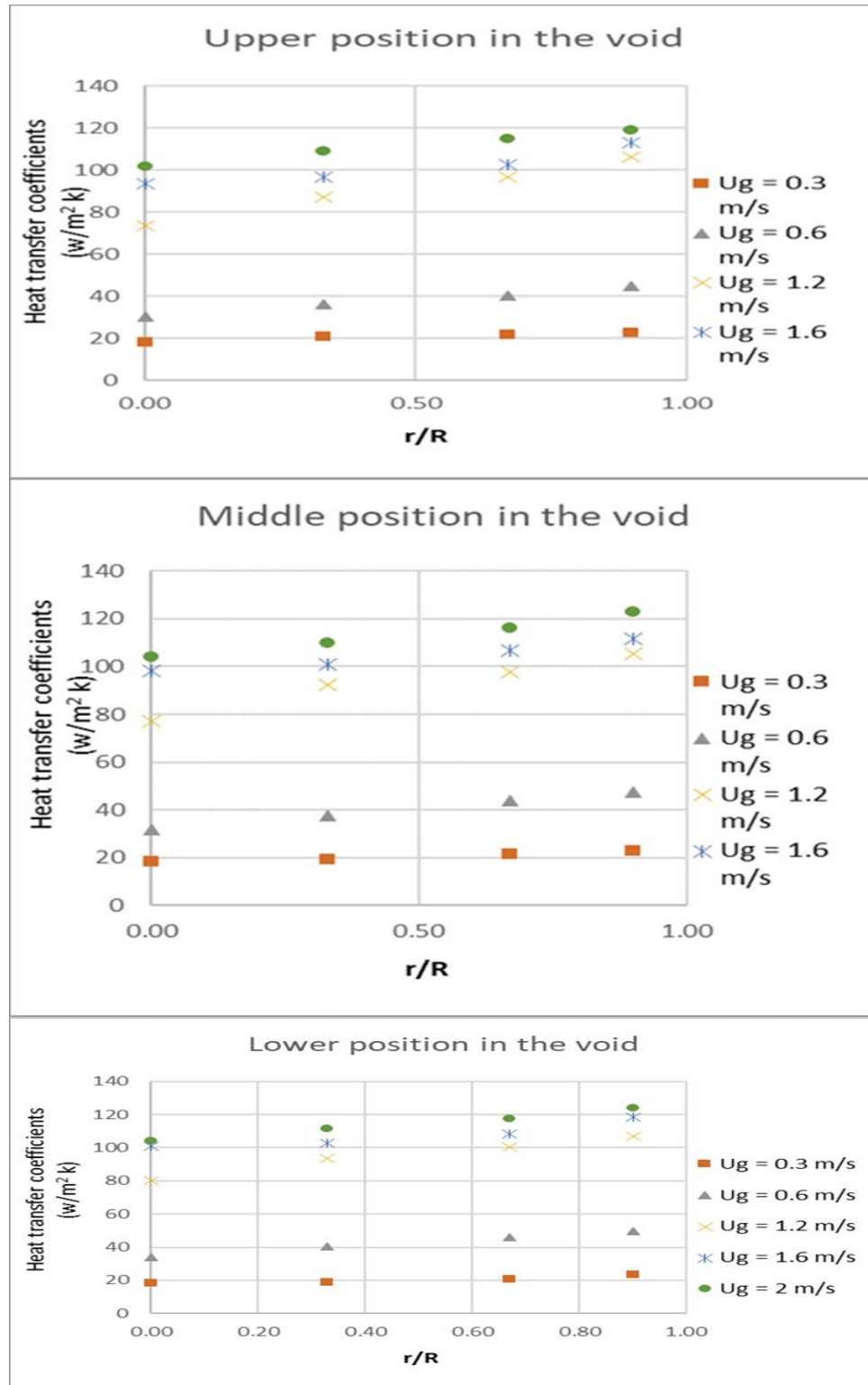


Figure 11. The variation of heat transfer coefficient depending on the radial position and the velocity of the flowing gas when the thermocouple probe is placed at three different positions in the void, at the lower level of the bed ( $H/D = 2.88$ ).

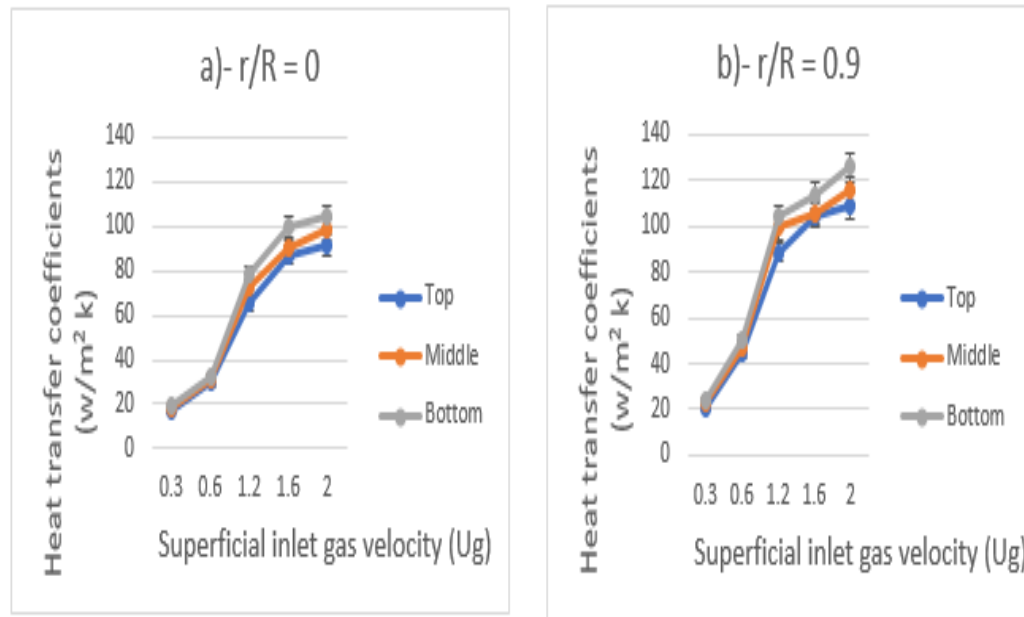


Figure 12. The variation of the local heat transfer coefficients as a function of the superficial inlet gas velocity at the three axial positions (Top ((H/D) = 0.72), Middle ((H/D) = 1.48), Bottom ((H/D) = 2.88)) in the center of the void at a)- r/R = 0 and b)- r/R = 0.9.

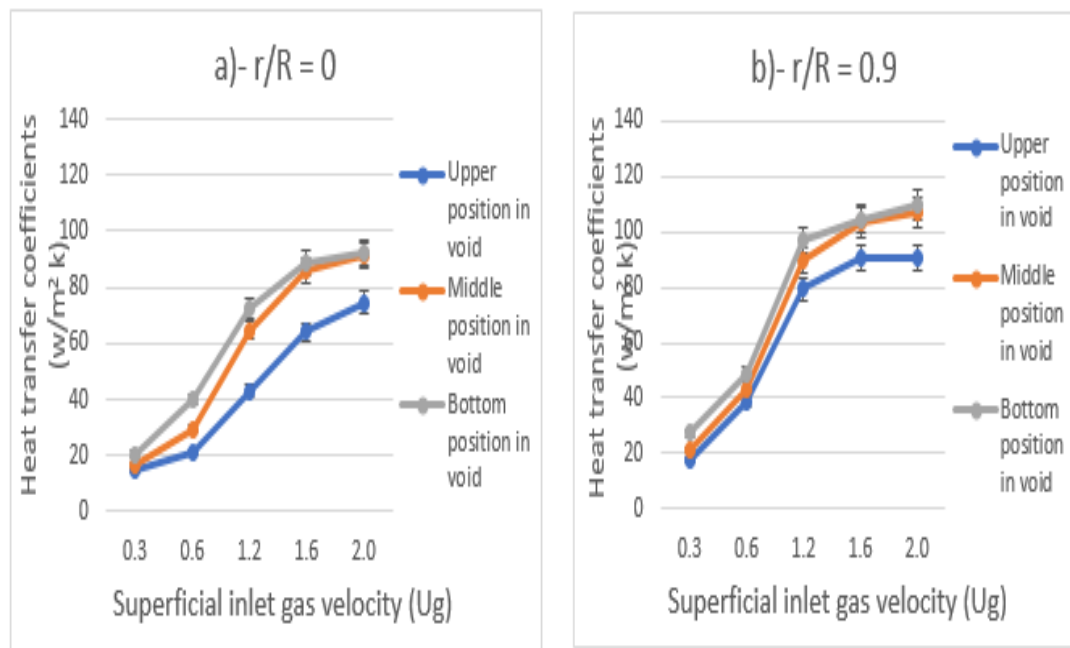


Figure 13. The variation of the heat transfer coefficients as a function of the superficial inlet gas velocity at the top axial level ((H/D) = 0.72) of the column for three different angular orientation of the pebble in the void at a)- r/R = 0 and b)- r/R = 0.9.

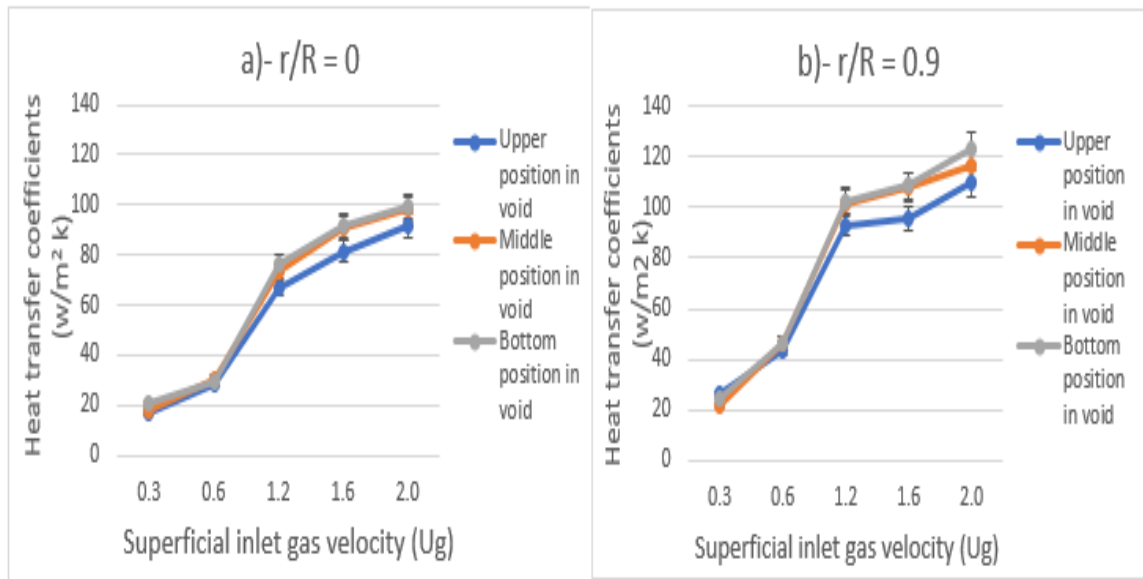


Figure 14. The variation of the heat transfer coefficients as a function of the superficial inlet gas velocity at the middle axial level ((H/D) = 1.48) of the column for three different angular orientation of the pebble in the void at a)- r/R = 0 and b)- r/R = 0.9.

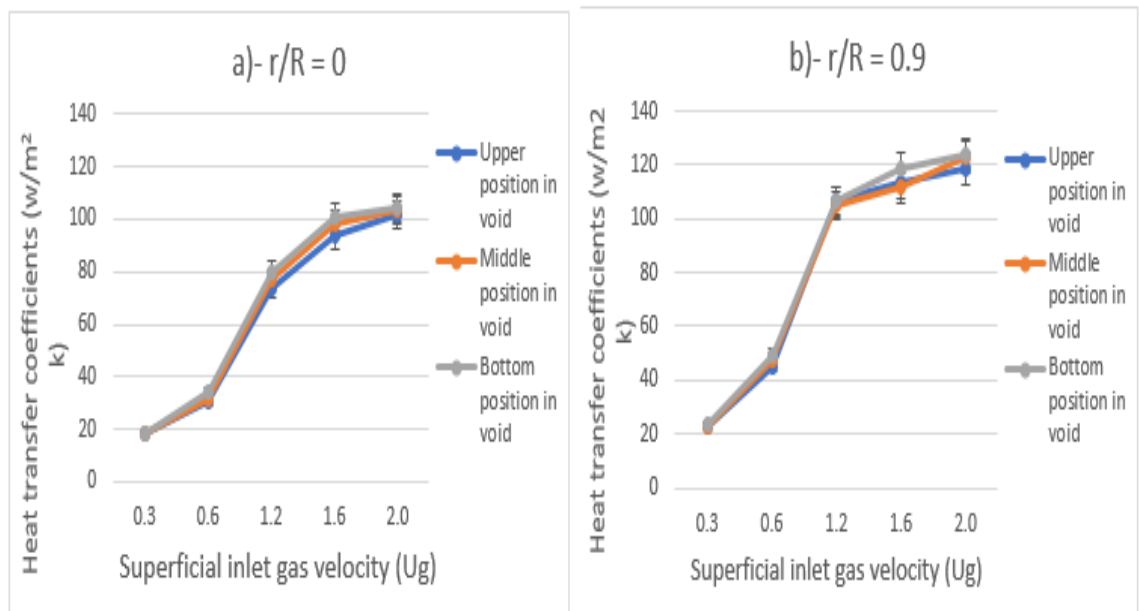


Figure 15. The variation of the heat transfer coefficients as a function of the superficial inlet gas velocity at the bottom axial level ((H/D) = 2.88) of the column for three different angular orientation of the pebble in the void at a)- r/R = 0 and b)- r/R = 0.9.

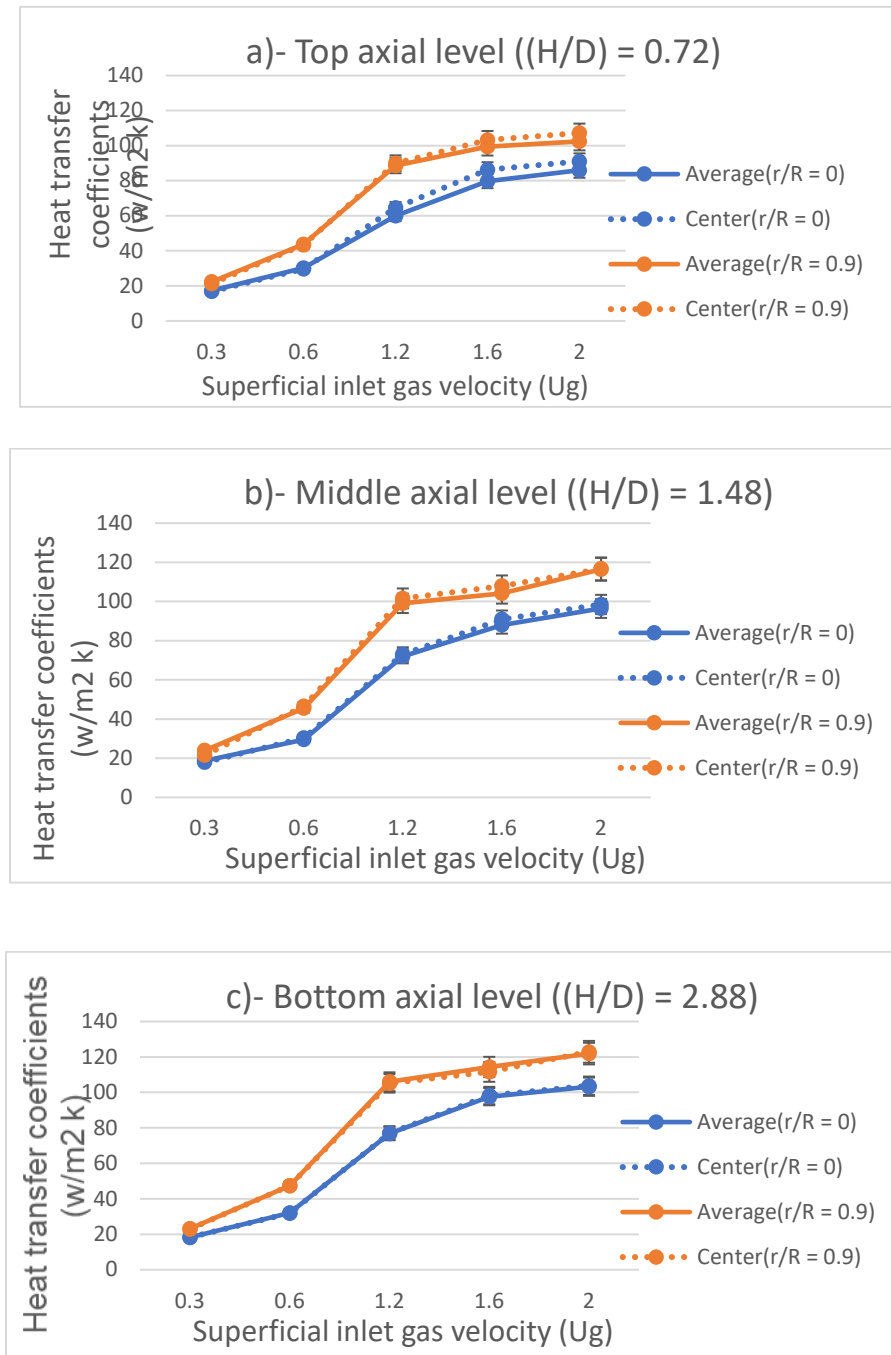


Figure 16. Comparison between the heat transfer coefficients in the center of the void and the average heat transfer coefficients in the void in the center ( $r/R = 0$ ) and the near-wall region ( $r/R = 0.9$ ) at a)- Top level ((H/D) = 0.72), b)- Middle level ((H/D) = 1.48), c)- Bottom level ((H/D) = 2.88).

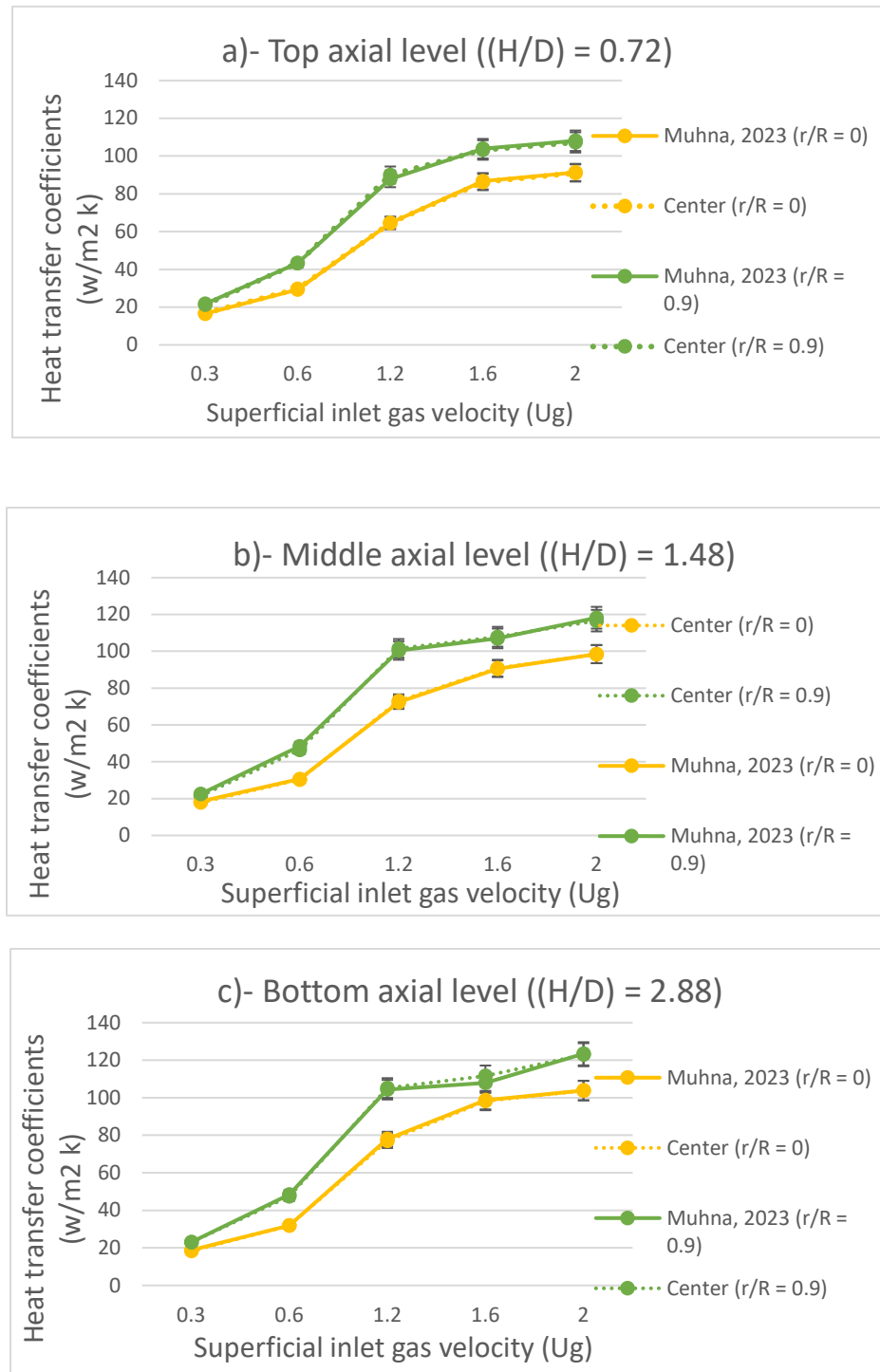


Figure 17. Comparison between the heat transfer coefficients in the center of the void and the average heat transfer coefficients in the void in the center ( $r/R = 0$ ) and the near-wall region ( $r/R = 0.9$ ) at Top level ((H/D) = 0.72), b)- Middle level ((H/D) = 1.48), c)- Bottom level ((H/D) = 2.88).

The average percentage difference between these the heat transfer measurements at the center of the bed ( $r/R=0$ ) in this study are only 0.75%, 1.15% and 0.96% different from the measurements of Alshammari et al., 2023b, at the top, middle and bottom of the bed, respectively. The same low difference are observed in the region near the wall ( $r/R= 0.9$ ), with the average percentage differences being 1.2%, 2.46% and 1.39% at the top, middle and bottom axial levels, respectively. This comparison proves that the technique that was used for measuring the local heat transfer coefficients in our work and in the work of Alshammari et al., 2023b has high reproducibility, hence provides highly reliable data quantitative data.

## **5.2. COMPARISON OF THE OVERALL HEAT TRANSFER INSIDE THE PBR WITH THE EMPIRICAL CORRELATIONS AVAILABLE IN THE LITERATURE**

Most of the studies available in the literature have based their proposed empirical correlation on insufficient experimental data, either directly measuring the overall convective heat transfer, or measuring the local convective heat transfer using techniques that are considered to provide unreliable data. This has led to the results of the various empirical correlations to be significantly different, owing to the different design conditions, operation conditions and the measurement techniques that were used to gather the required experimental data for the correlations.

In order to find the empirical correlations that would best describe the variation of the overall heat transfer for our design and operation conditions, the local heat transfer coefficients that were measured in our work were first arithmetically averaged in the void, then radially and axially averaged, in order to obtain the overall heat transfer coefficient,

which was then compared with the predictions of the empirical correlations for the superficial inlet gas velocities studied ( $U_g = 0.3, 0.6, 1.2, 1.6$  and  $2$  m/s). In these correlations, the overall heat transfer coefficients are expressed using the dimensionless Nusselt's number ( $Nu$ )(Eq.2), which is related to the dimensionless Reynold's number ( $Re$ ) and Prandtl number ( $Pr$ ), which are expressed in Eq 3 and Eq 4 respectively.

The details of the empirical correlations that are compared with experimental data can be found in Table 1.

Table 1. Empirical correlations for the overall convective heat transfer coefficient.

Authors	Empirical Correlation	Range of Application
(Ranz, 1952)	$Nu = 2 + 0.6Pr^{1/3}Re^{0.5}$	$Re \geq 100$ $0.6 \leq Pr \leq 400$
(Gupta et al., 1974)	$Nu = 2.876 \left( \frac{Pr^{1/3}}{\varepsilon} \right) + 0.3023 \left( \frac{Pr^{1/3}}{\varepsilon} \right) Re^{0.65}$	$10 \leq Re \leq 10^5$ $0.71 \leq Pr \leq 7.18$ $0.26 \leq \varepsilon \leq 0.935$
(Gnielinski, 1981, 1978)	$Nu = f_\varepsilon Nu_{sp}$ $f_\varepsilon = 1 + 1.5(1 - \varepsilon)$ $Nu_{sp} = 2 + \sqrt{Nu_{lam}^2 + Nu_{turb}^2}$ $Nu_{lam} = 0.664(\varepsilon)^{1/2} Pr^{1/3}$ $Nu_{turb} = \frac{0.037(Re/\varepsilon)^{0.8} Pr}{1 + 2.443 \left( \frac{Re}{\varepsilon} \right)^{-0.1} (Pr^{2/3} - 1)}$	$Re/\varepsilon \leq 2 \times 10^4$ $0.71 \leq Pr \leq 10^4$ $\varepsilon = 0.387$
(Wakao and S, 1982)	$Nu = 2 + 1.1Pr^{1/3}Re^{0.6}$	$15 \leq Re \leq 8500$ $\varepsilon = 0.4$
(KTA, 1983)	$Nu = 1.27 \left( \frac{Pr^{1/3}}{\varepsilon^{1.18}} \right) Re^{0.36} + 0.033 \left( \frac{Pr^{1/2}}{\varepsilon^{1.07}} \right) Re^{0.86}$	$100 \leq Re \leq 10^5$ $Pr = 0.7$ $0.36 \leq \varepsilon \leq 0.42$
(Achenbach, 1995)	$Nu = [(1.18Re^{0.58})^4 + (0.23(Re_h)^{0.75})^4]^{1/4}$ $Re_h = \frac{\rho \cdot V \cdot d_h}{\mu} = \frac{1}{(1 - \varepsilon)} Re$ $d_h = d \times \frac{\varepsilon}{1 - \varepsilon}$	$Re/\varepsilon \leq 7.7 \times 10^5$ $Pr = 0.71$ $\varepsilon = 0.387$
(Bird et al., 2002)	$Nu = 2.19 + Pr^{1/3}Re^{1/3} + 0.78Pr^{1/3}Re^{0.62}$	$1 \leq Re \leq 10^5$ $Pr > 0.70$



The averaged overall heat transfer is also compared with predictions of the pseudo-3D model that was developed by Alshammari et al., 2023b with a databank that was collected using the same measurement technique and the same experimental setup. The pseudo-3D model of Alshammari et al., 2023b is expressed as follows:

$$Nu = 5.25 \times (3.91 \ln(Re) - 25.9) \times \left(0.38 \frac{r}{R} + 1.9\right) \times \left(-0.11 \frac{H}{D} + 2.46\right) - 64.91 \left(\frac{Pr}{\varepsilon}\right)^{0.05} \quad (9)$$

This pseudo-3D model is applicable for  $993.78 \leq Re \leq 6625.2$ ,  $Pr = 0.74$  and  $\varepsilon = 0.397$  (Alshammari et al., 2023b).

In order to assess and quantify the difference between the experimental results and the predictions of the empirical correlations, the average absolute relative error (*AARE*) was calculated using the following Eq 10 (Ostertagová, 2012):

$$AARE = \frac{1}{N} \sum_{i=1}^{i=N} \frac{Nu_{predicted,i} - Nu_{experimental,i}}{Nu_{experimental,i}} \quad (10)$$

Figure plots Nusselt's number ( $Nu$ ) as function of the effective Reynold's number ( $Re_h$ ). It can be clearly seen that the predictions of the empirical correlations of Ranz, 1952; KTA, 1983 and Achenbach, 1995 are the furthest away from all the experimental points, hence the most different with high *AARE* values of 70.78%, 28.72% and 38.22%, respectively. The predictions of the correlation of Wakao and S, 1982 provide the closest estimation to the experimental data with an overall *AARE* of 19.17%, followed by Gupta et al., 1974 with an *AARE* of 20.74% and Gnielinski, 1978 with an *AARE* of 22.29%. These *AARE* are high due to the high deviation between the experimental values and the predictions of the correlation at laminar flow conditions ( $Re_h < 3000$ ). However, the

predictions at turbulent flow  $Re_h \geq 3000$  conditions are much closer to the experimental results with an *AARE* of 4.69% for the Gnielinski, 1978 correlation, 4.96% for the Gupta et al., 1974 correlation, 6.84% for the correlation of Bird et al., 2002 and 7.18% for the Wakao and S, 1982 correlation. These low *AARE* values indicate high prediction accuracy for these empirical correlation at turbulent flow conditions, considering the complexity of the heat transfer mechanism and the numerous factors involved. These prediction errors are due to the difference in the measurement techniques used and the different design and operation conditions.

As for the comparison with the pseudo-3D model that was developed by Alshammari et al., 2023b, its predictions of the overall heat transfer coefficients are most accurate compared to the other correlations that are found in the literature, with an *AARD* of 13.37%. The heat transfer predictions of this pseudo-3D model are most accurate at turbulent flow conditions with an *AARD* of 4.8%, compared to an *AARD* of 26.23% at laminar flow conditions.

However, this pseudo-3D model is only valid for the prediction of the local heat transfer coefficients at the center of the void, and not accounting for the variation of the heat transfer in the void, which can be better approximated by including more measurements at different locations in the void between the pebbles, which was done in this work. As for the other empirical correlations that are found in the literature, they are only applicable for the prediction of the overall heat transfer in a pebble bed reactor's core. Therefore, in the following subsection, we develop a polynomial regression model for the prediction of the local Nusselt's number and, hence, the local convective heat transfer coefficients within the range of the design and operation conditions investigated this work.

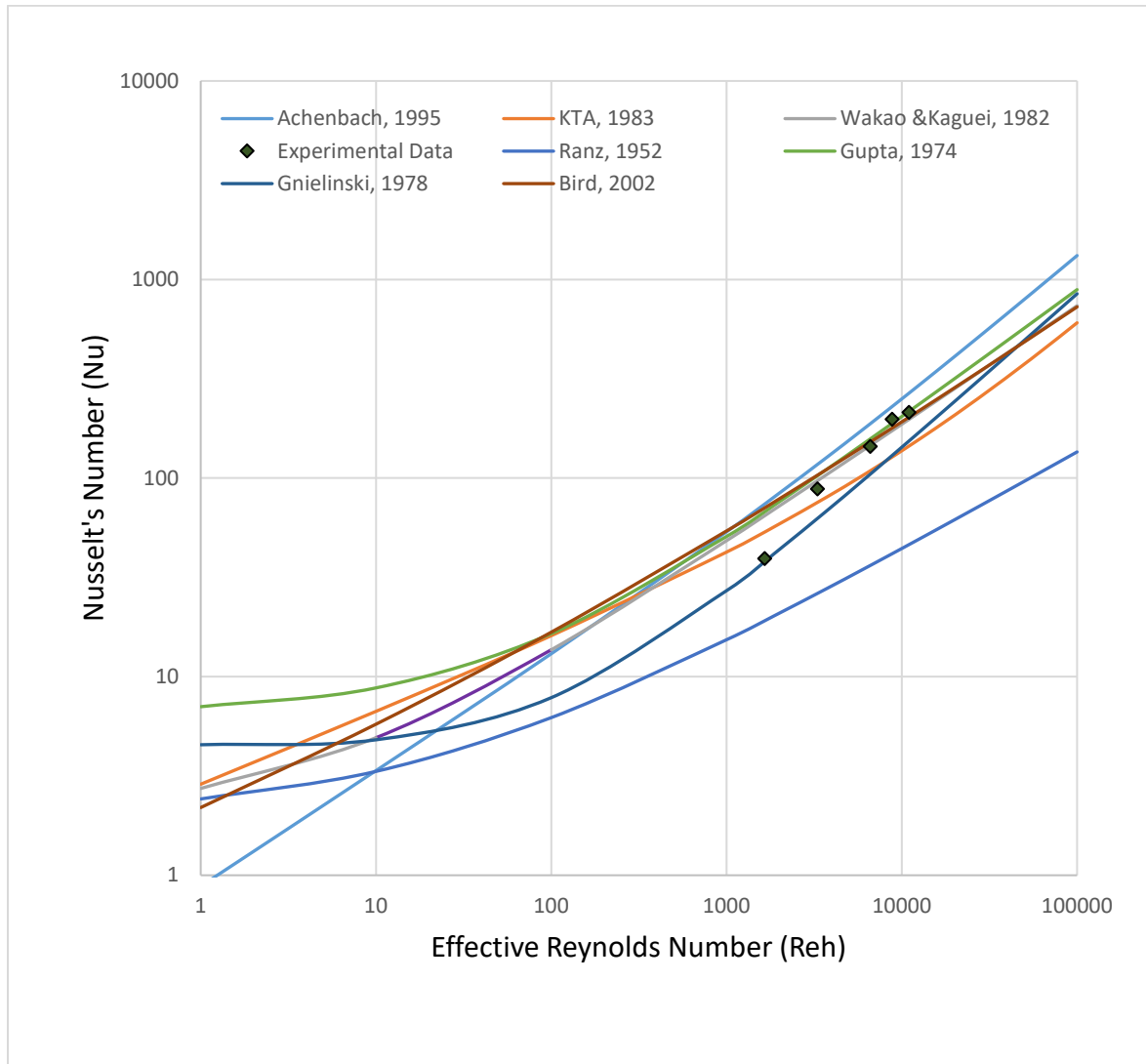


Figure 18. Comparison of the empirical correlations with the measured overall convective heat-transfer at the superficial inlet gas velocities studied (0.3 m/s to 2 m/s).

### 5.3. MODELING OF THE LOCAL HEAT TRANSFER COEFFICIENT IN A PBR

Polynomial regression is used for the modeling and prediction of various operation systems, in both research and the optimization of industrial processes. These models link the input operation parameters of a system with its output via a mathematical equation. If the relationship between the input operation parameters and the output of the system

includes some nonlinearity, quadratic terms are added to develop a second order polynomial model, which can account for the nonlinearity (Montgomery et al., 2013).

A second order polynomial model can be expressed as (Bas and Boyaci, 2007):

$$\hat{y} = \beta_0 + \sum_{j=1}^k \beta_j \cdot X_j + \sum_{j=1}^k \beta_{jj} \cdot X_j^2 + \sum_{i < j} \beta_{ij} \cdot X_i \cdot X_j \quad (11)$$

where  $\hat{y}$  is the predicted response,  $\beta_0$  is the intercept,  $\beta_j$  are the estimates of the main effects  $X_j$ ,  $\beta_{jj}$  are the estimates of the quadratic effects  $X_j^2$ ,  $\beta_{ij}$  are the estimates of the two-factor interactions  $X_i \cdot X_j$ .

These second order polynomial models provide an in-depth understanding of the effect of each of the input features on the output as well as the interaction between the input features. Two features are said to interact if the effect of one of the features on the response depends on the settings of another feature. The quadratic terms are included in the model to quantify the nonlinearity in the relationship between the input features and the output of the system (Bas and Boyaci, 2007).

For our study, in order to be able to assess and mathematically estimate the local heat transfer coefficients between the pebbles and the flowing gas inside the pebble bed reactor within the range of our experimental set-up, a second order polynomial model was developed for the prediction of Nusselt's number ( $Nu$ ). The parameters and their experimental range are shown in Table 2. The model development and data analysis were conducted using the JMP Pro 16 software (SAS, 2021).

Table 2. Parameters and their experimental range.

Parameters	Range of variation
Axial position ( $\frac{Z}{H}$ )	0.23 – 0.94
Radial position ( $\frac{r}{R}$ )	0 - 0.9
Axial position in the void ( $\frac{l}{L}$ )	- 0.9
Reynolds number	993.78 – 6625.2

The coefficients of the model were obtained using the normal equation as the optimization algorithm. The normal equation is expressed as follows (Montgomery et al., 2013):

$$X' \cdot X \cdot \beta = X' \cdot y \quad (12)$$

where  $X$  is the matrix of the input features of the model,  $X'$  is the transpose of  $X$ ,  $y$  is the response vector and  $\beta$  is the vector of the coefficients.

For our study, after eliminating the quadratic and interaction terms that have an insignificant effect on the variation of Nusselt's number ( $Nu$ ), the model Eq 13 can be expressed as follows:

$$\begin{aligned}
 Nu = & -62.50 + 60.1 \frac{Z}{H} + 52.7 \frac{l}{L} + 20.16 \frac{r}{R} + 0.057 Re \\
 & - 34.1 \left( \frac{Z}{H} \right)^2 - 19.79 \left( \frac{l}{L} \right)^2 - 10^{-6} Re^2 - 42.52 \frac{Z}{H} \cdot \frac{l}{L} \\
 & + 0.0086 \frac{Z}{H} \cdot Re + 0.0034 \frac{l}{L} \cdot Re + 0.0044 \frac{r}{R} \cdot Re
 \end{aligned} \quad (13)$$

The analysis of variance (Christensen, 2018), the lack of fit (Neill and Johnson, 1984) and the analysis of residuals (Kim, 2019) proved that the model was statistically validated and can be used for the prediction of the heat transfer coefficient (expressed as  $Nu$ ) within our experimental range.

To evaluate the accuracy of the model, the coefficient of determination  $R^2$  was calculated using the average absolute relative error ( $AARE$ ) was calculated using Eq.10.

$$R^2 = 1 - \frac{SSE}{SST} = 1 - \frac{\sum_{i=1}^N (y_i - \hat{y}_i)^2}{\sum_{i=1}^N (y_i - \bar{y})^2} \quad (14)$$

where  $SSE$  is the sum of the squares of the residuals,  $SST$  is the total sum of squares,  $y_i$  is the response for experiment  $i$ ,  $\hat{y}_i$  is the predicted response for experiment  $i$ ,  $\bar{y}$  is the arithmetic mean of the responses  $y_i$  and  $N$  is the number of experiments.

The  $R^2$  value was found to be equal to 0.9808, indicating that 98.08% of the variation of the heat transfer coefficient can be explained by the studied parameters. This high  $R^2$  value also indicates an excellent correlation between the experimental output and the predicted output, as shown in the goodness of fit plot (Figure ). The overall  $AARE$  value was found to be equal to 9.08%, which is less than 10%, indicating that the model provides excellent forecasting of the heat transfer coefficient within the studied experimental range, considering the complexity of the heat transfer mechanisms. The  $AARE$  value is even lower for the predictions at turbulent flow conditions, with an  $AARE$  of 4.11%, meaning that the model performs much better at turbulent flow conditions compared to laminar flow conditions for which the  $AARE$  is equal to 16.52%.

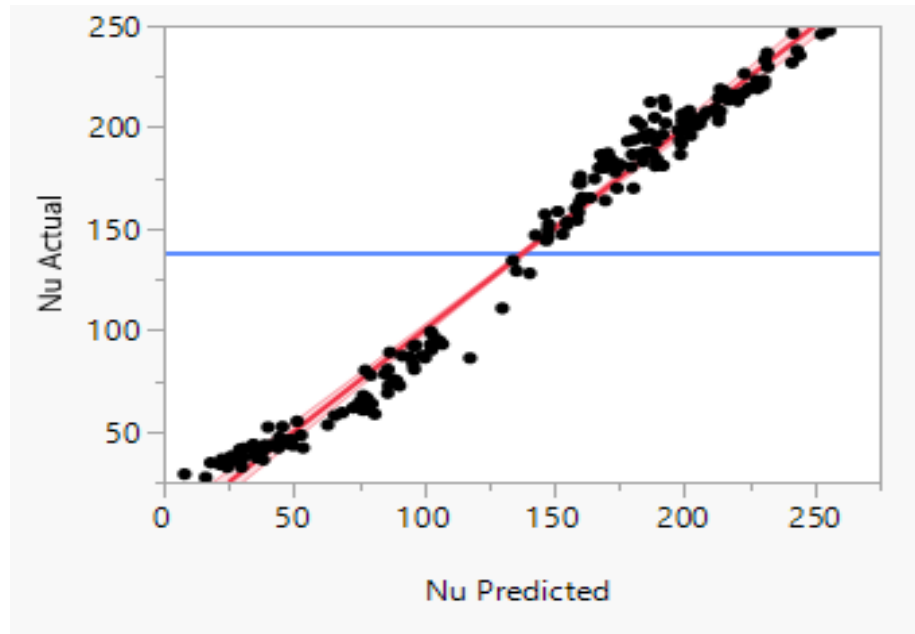













Figure 19. Goodness of fit plot.

Student's t-test was done in order to rank the terms of the model by their importance, and hence, by the significance of their influence on the variation of the heat transfer (Nusselt's number) (Neideen and Brasel, 2007). Student's t-test consists of a comparison between the  $t_{ratio}$  of each input feature with the  $t_{statistic}$  that is calculated based on the number of experiments and the degrees of freedom (Neideen and Brasel, 2007).

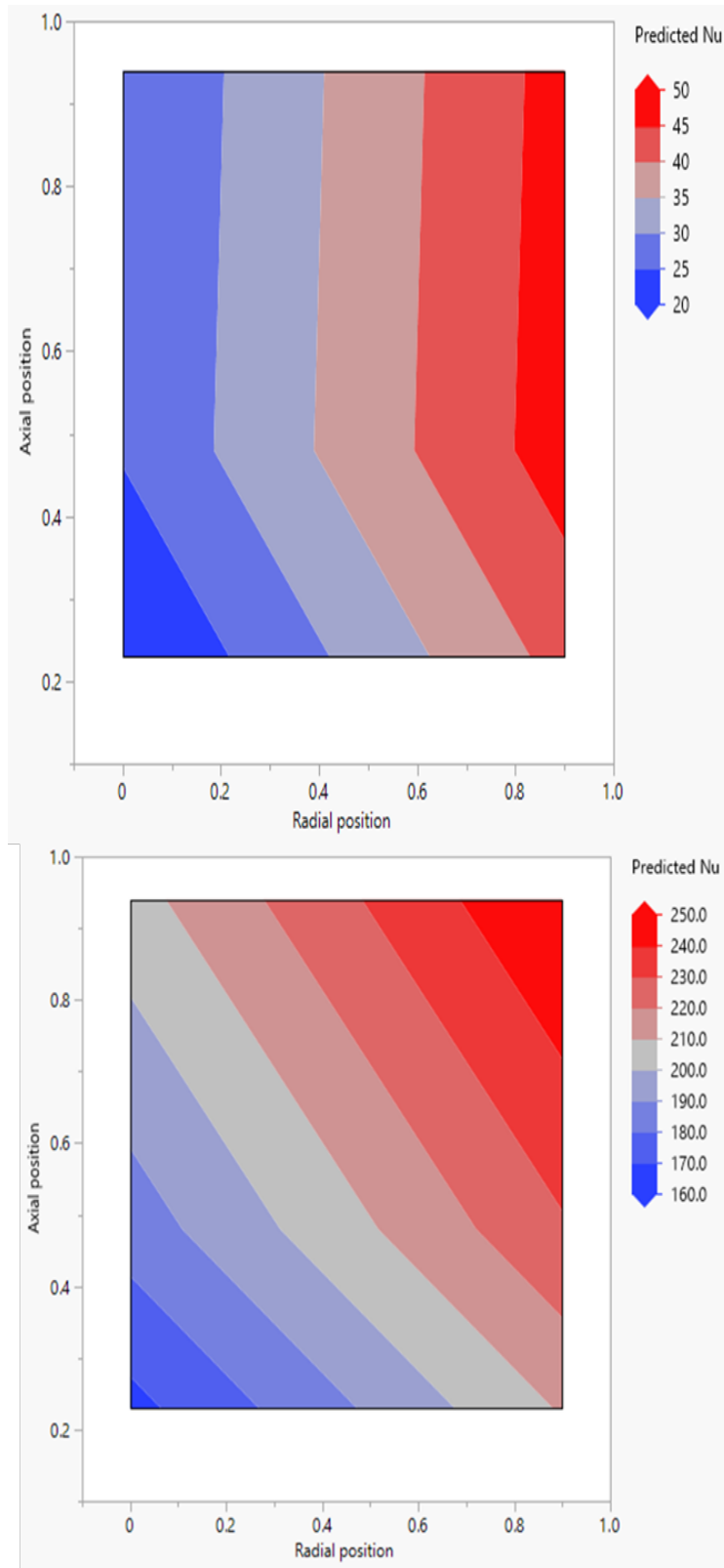
The results of student's t-test are shown in Table 3. The  $p_{value}$  of the terms of the model is too low, and hence to make the comparison between the terms easier, the *LogWorth* was calculated for each term as  $-\log_{10}(p_{value})$ . From Table 3, Reynold's number ( $Re$ ) has the most significant influence on the heat transfer coefficient, followed by the radial position ( $\frac{r}{R}$ ) due to the effect of the wall, followed by the axial level ( $\frac{H}{D}$ ) and the position in the void ( $\frac{l}{L}$ ), which depends on the angular orientation of the probe pebble.

The nature of the effect of each of the input features on Nusselt's number ( $Nu$ ) is better elucidated in Figure 20 which consists of contour plots that show the variation of  $Nu$  based on the axial position ( $\frac{H}{D}$ ) the radial position ( $\frac{r}{R}$ ) in the column, at laminar flow conditions ( $Re = 993.78$ ) and turbulent flow conditions ( $Re = 6625.2$ ). It is apparent that the range of variation of Nusselt's number is much higher when the flow of the gas is turbulent ( $Re = 6625.2$ ), and near the wall ( $\frac{r}{R} = 0.9$ ), as explained above.

Table 3. The results of student's t-test.

Term	Log Worth	Graphical Comparison of LogWorth	P-value
$Re$	140.591		0.00000
$Re^2$	43.271		0.00000
$\frac{r}{R}$	36.879		0.00000
$\frac{Z}{H}$	22.430		0.00000
$\frac{l}{L}$	17.358		0.00000
$\frac{Z}{H} \cdot Re$	10.185		0.00000
$\frac{Z}{H} \cdot \frac{l}{L}$	6.793		0.00000
$\frac{r}{R} \cdot Re$	4.227		0.00006
$\frac{l}{L} \cdot Re$	2.597		0.00253
$\left(\frac{Z}{H}\right)^2$	1.806		0.01564
$\left(\frac{l}{L}\right)^2$	1.326		0.04718





a)-  $Re = 993.78$

b)-  $Re = 6625.2$

Figure 20. Contour plots showing the variation of Nusselt's number (Nu) as a function of the axial lev l (Z/H) and the radial position (r/R) at a)-  $Re=993.78$  and b)-  $Re=6625.2$ .

Despite pebble bed reactors being operated at high superficial inlet gas velocities and hence at high turbulent flow conditions, this correlation is still useful for the estimation of the local convective heat transfer coefficients, represented by Nusselt's Number ( $Nu$ ), in the case of loss of flow accidents (LOFA) within the design and operating conditions of the experimental data. The *AARE* of this correlation is 4.55%.

Based on the above explanation, two separate polynomial regression correlations were developed based on the flow regime inside the pebble bed.

The first correlation is valid for laminar flow conditions ( $993.78 \leq Re \leq 1987.56$ ) and is expressed as follows (Eq5):

$$Nu = -0.44 + 7.238 \frac{H}{D} + 12.17 \frac{l}{L} - 10.28 \frac{r}{R} + 0.02 Re - 10.07 \frac{H}{D} \cdot \frac{l}{L} + 0.012 \frac{l}{L} \cdot Re + 0.02 \frac{r}{R} \cdot Re \quad (5)$$

The second model is valid for the estimation of the local convective heat transfer coefficients at high superficial inlet gas velocities, corresponding to high turbulence flow conditions ( $3975.12 \leq Re \leq 6625.2$ ), within the design and operating conditions of the experimental data. This correlation is expressed in the following (Eq.6) and it has an *AARE* of 2.69%:

$$Nu = -53.40 + 43.67 \frac{H}{D} + 94.88 \frac{l}{L} + 89.14 \frac{r}{R} + 0.038 Re - 5.5 \left(\frac{H}{D}\right)^2 - 38.36 \left(\frac{l}{L}\right)^2 - 2 \times 10^{-6} Re^2 - 16.58 \frac{H}{D} \cdot \frac{l}{L} - 0.008 \frac{r}{R} \cdot Re \quad (6)$$

## 6. CONCLUSION

The heat transfer coefficient is one of the main criteria by which the performance of the very high gas-cooled nuclear reactor is evaluated. In this study, the forced convective heat transfer coefficient between the pebbles and the coolant gas (air) that passes through the bed was investigated using an advanced technique that consisted of a probe pebble, a micro-foil sensor and a thermocouple probe. The measurements were taken at four radial locations ( $r/R = 0.0, \pm 0.33, \pm 0.67$ , and  $\pm 0.9$ ) along one diameter line at three axial levels ( $H_1 = 21.6$  cm,  $H_2 = 44.5$  cm,  $H_3 = 86.4$  cm from the top of the distributor) under various superficial inlet gas velocities ( $U_g = 0.3, 0.6, 1.2, 1.6$  and  $2$  m/s). At each location and under every superficial inlet gas velocity, the angular orientation of the pebble was changed in order to allow the measurement of the heat transfer at three vertical positions in the void ( $l/L = 0.1, 0.5$  and  $0.9$ ).

The local heat transfer coefficients varied significantly depending on the position inside the pebble bed and increased substantially with the increase of the coolant gas velocity. Additionally, the heat transfer coefficients were also found to be higher in the near-wall region, compared to the center of the reactor. This was attributed to the wall-pebble interactions, which provides lower resistance to the flow of the gas compared to the center of the reactor, where the pebbles are tightly packed, lowering the local actual velocity of the coolant gas.

The heat transfer coefficient was also found to be dependent on the position in the void as changing the angular orientation of the probe pebble in the void from top to bottom showed that the heat transfer coefficients are considerably higher in the center and bottom

of the void, compared to the top position, where being in vicinity of the pebbles from the top limits the passage of the coolant gas and its velocity.

The increase of the turbulence of the flow of the coolant gas was found to increase the heat transfer coefficient regardless of the location inside the reactor. However, this increase in turbulence also decreases the differences in the heat transfer coefficients obtained at different location, due to the increase of thermal mixing.

The local heat transfer coefficients obtained in this study were used to calculate the overall heat transfer in the reactor, which was compared with several correlations that are found in the literature. The comparison showed a relatively good agreement of the experimental data with the (Wakao and S, 1982), (Gupta et al., 1974) and (Bird et al., 2002) empirical correlations at turbulent flow conditions. A polynomial regression model was also developed for the prediction of the Nusselt's number based on the location inside the reactor and the flow conditions and it showed a very good agreement with the experimental data within the range of the design and operation conditions of this study.

The acquisition of accurate data of the local heat transfer inside a PBR, like in this study, is essential for the development of an in depth understanding of the reactor's performance and can be utilized as benchmark data for the validation of CFD simulations.

## NOMENCLATURE

<b>Symbol</b>	<b>Discretion</b>	<b>Unit</b>
HTC	Heat Transfer Coefficient.	(-)
PBR	Pebble Bed Reactor.	(-)
VHTGR	Very High Temperature Gas-Cooled Reactor.	(-)

TRISO	Tristructural-isotropic fuel particle.	(-)
LOFA	Loss Of Flow Accident.	(-)
CFD	Computational Fluid Dynamics	(-)
DEM	Discrete Element Method	(-)
mFReel	Multiphase Flows and Reactors Engineering and Education Laboratory	(-)
$h_i$	Instantaneous heat transfer coefficient	$\frac{W}{m^2 K}$
$h_{avg}$	Time-averaged heat transfer coefficient	$\frac{W}{m^2 K}$
$T_{s,i}$	Pebble surface temperature	$K$
$T_{b,i}$	Flowing air temperature	$K$
$q_i$	Local instantaneous heat flux	$W/m^2$
$\varepsilon$	Average void of the bed.	(-)
$U_g$	Superficial inlet gas velocity	$m/s$
$\frac{Z}{H}$	Axial position inside the column.	(-)
$\frac{l}{L}$	Axial position of the thermocouple probe in the void.	(-)
$\frac{r}{R}$	Radial position inside the experimental column.	(-)
$R^2$	Coefficient of determination	
AARE.	Average Absolute Relative Error.	

## REFERENCES

1. Abdulmohsin, R., 2013. Gas dynamics and heat transfer in a packed pebble-bed reactor for the 4th generation nuclear energy. Missouri University of Science and Technology.
2. Abdulmohsin, R.S., Al-Dahhan, M.H., 2015a. Characteristics of convective heat transport in a packed pebble-bed reactor. Nucl. Eng. Des. 284, 143–152. <https://doi.org/10.1016/j.nucengdes.2014.11.041>
3. Abdulmohsin, R.S., Al-Dahhan, M.H., 2015b. Characteristics of convective heat transport in a packed pebble-bed reactor. Nucl. Eng. Des. 284, 143–152. <https://doi.org/10.1016/j.nucengdes.2014.11.041>
4. Achenbach, E., 1995. Heat and flow characteristics of packed beds. Exp. Therm. Fluid Sci. 10, 17–27. [https://doi.org/10.1016/0894-1777\(94\)00077-L](https://doi.org/10.1016/0894-1777(94)00077-L)
5. Al-Juwaya, T., Ali, N., Al-Dahhan, M., 2019. Investigation of hydrodynamics of binary solids mixture spouted beds using radioactive particle tracking (RPT) technique. Chem. Eng. Res. Des. 148, 21–44. <https://doi.org/10.1016/j.cherd.2019.05.051>
6. Al-Juwaya, T., Ali, N., Al-Dahhan, M., 2017. Investigation of cross-sectional gas-solid distributions in spouted beds using advanced non-invasive gamma-ray computed tomography (CT). Exp. Therm. Fluid Sci. 86, 37–53. <https://doi.org/10.1016/j.expthermflusci.2017.03.029>
7. Al Falahi, F., Al-Dahhan, M., 2016. Experimental investigation of the pebble bed structure by using gamma ray tomography. Nucl. Eng. Des. 310, 231–246. <https://doi.org/10.1016/j.nucengdes.2016.10.009>
8. Al Falahi, F., Mueller, G., Al-Dahhan, M., 2018. Pebble bed nuclear reactor structure study: A comparison of the experimental and calculated void fraction distribution. Prog. Nucl. Energy 106, 153–161. <https://doi.org/10.1016/j.pnucene.2018.03.006>
9. Auwerda, G.J., Zhang, Y., Lathouwers, D., Kloosterman, J., 2011. Effect of Non-uniform Porosity Distribution on Thermohydraulics in a Pebble Bed Reactor, in: Proceedings of NURETH-14.
10. Bas, D., Boyaci, I.H., 2007. Modeling and optimization i: Usability of response surface methodology. J. Food Eng. 78, 836–845. <https://doi.org/10.1016/j.jfoodeng.2005.11.024>

11. Bird, B.R., Stewart, W.E., Lightfoot Edwin N., 2002. Transport Phenomena, 2nd Ed. ed, John Wiley & Sons Inc.
12. Christensen, R., 2018. Analysis of Variance, Design, and Regression. Anal. Variance, Des. Regres. <https://doi.org/10.1201/9781315370095>
13. De Beer, M., Du Toit, C.G., Rousseau, P.G., 2018. Experimental study of the effective thermal conductivity in the near-wall region of a packed pebble bed. Nucl. Eng. Des. 339, 253–268. <https://doi.org/10.1016/j.nucengdes.2018.09.014>
14. Dominguez-ontiveros, E.E., Estrada-perez, C., Hassan, Y.A., 2008. Measurements of Flow Modification by particle Deposition Inside a Packed Bed Using Time-Resolved PIV, in: Proceedings of the 4th International Topical Meeting on High Temperature Reactor Technology. pp. 1–7.
15. Fenech, H., n.d. Heat Transfer and Fluid Flow in Nuclear Systems, 1981st ed. Pergamo Press.
16. Gnielinski, V., 1981. Equations for the Calculation of Heat and Mass Transfer during Flow through Stationary Spherical Packings at Moderate and High Peclet Numbers. Int. Chem. Eng. 21, 378–383.
17. Gnielinski, V., 1978. Formula for Calculating the Heat and Mass Transfer In Through Flow of a Fixed Bed at Medium and Large Peclet. Process-Technology 12, 363–366.
18. Goodjohn, A.J., 1991. Summary of Gas-Cooled reactor programs. Energy 16, 79–106. [https://doi.org/10.1016/0360-5442\(91\)90089-5](https://doi.org/10.1016/0360-5442(91)90089-5)
19. Gupta, S.N., Chaube, R.B., Upadhyay, S.N., 1974. Fluid-Particle and Heat Transfer Beds. Chem. Eng. 29, 839–843.
20. Hassan, Y.A., Dominguez-Ontiveros, E.E., 2008. Flow visualization in a pebble bed reactor experiment using PIV and refractive index matching techniques. Nucl. Eng. Des. 238, 3080–3085. <https://doi.org/10.1016/j.nucengdes.2008.01.027>
21. Hu, Y., Wang, J., Yang, J., Mudawar, I., Wang, Q., 2019. Experimental study of forced convective heat transfer in grille-particle composite packed beds. Int. J. Heat Mass Transf. 129, 103–112. <https://doi.org/10.1016/j.ijheatmasstransfer.2018.09.103>
22. Kadak, A.C., 2005. A future for nuclear energy: Pebble bed reactors. Int. J. Crit. Infrastructures 1, 330–345. <https://doi.org/10.1504/IJCIS.2005.006679>

23. Kagumba, M., Al-Naseri, H., Al-Dahhan, M.H., 2019. A new contact time model for the mechanistic assessment of local heat transfer coefficients in bubble column using both the four-optical fiber probe and the fast heat transfer probe-simultaneously, *Chemical Engineering Journal*. Elsevier B.V. <https://doi.org/10.1016/j.cej.2018.12.046>
24. Kaviany, M., 1995. *Principles of Heat Transfer in Porous Media*, Mechanical Engineering Series. Springer, New York.
25. Khane, V., Taha, M.M., Mueller, G.E., Al-Dahhan, M.H., 2017. Discrete element method-based investigations of granular flow in a pebble bed reactor. *Nucl. Technol.* 199, 47–66. <https://doi.org/10.1080/00295450.2017.1324729>
26. Khane, V.B., 2014. *Experimental and Computational Investigation of Flow of Pebbles in a Pebble Bed Nuclear Reactor*. Missouri University of Science and Technology.
27. Kim, H.-Y., 2019. Statistical notes for clinical researchers: simple linear regression 3 – residual analysis. *Restor. Dent. Endod.* 44, 1–8. <https://doi.org/10.5395/rde.2019.44.e11>
28. Koster, A., Matzner, H.D., Nicholisi, D.R., 2003. PBMR design for the future. *Nucl. Eng. Des.* 222, 231–245. [https://doi.org/10.1016/S0029-5493\(03\)00029-3](https://doi.org/10.1016/S0029-5493(03)00029-3)
29. KTA, 1983. *Reactor Core Design of High-Temperature Gas-Cooled Reactors Part 2 : Heat Transfer in Spherical Fuel Elements*. Saf. Stand. Nucl. Saf. Stand. Com. 3102.2, 1–5.
30. Lee, J.Y., Lee, S.Y., 2009. Flow visualization in the scaled up pebble bed of high temperature gas-cooled reactor using particle image velocimetry method. *J. Eng. Gas Turbines Power* 131, 1–4. <https://doi.org/10.1115/1.3098417>
31. Li, H., Prakash, A., 1997. Heat Transfer and Hydrodynamics in a Three-Phase Slurry Bubble Column. *Ind. Eng. Chem. Res.* 36, 4688–4694. <https://doi.org/10.1021/ie9701635>
32. Liu, L., Deng, J., Zhang, D., Wang, C., Qiu, S., Su, G.H., 2020. Experimental analysis of flow and convective heat transfer in the water-cooled packed pebble bed nuclear reactor core. *Prog. Nucl. Energy* 122. <https://doi.org/10.1016/j.pnucene.2020.103298>



33. Liu, L., Zhang, D., Li, L., Yang, Y., Wang, C., Qiu, S., Su, G.H., 2018. Experimental investigation of flow and convective heat transfer on a high-Prandtl-number fluid through the nuclear reactor pebble bed core. *Appl. Therm. Eng.* 145, 48–57. <https://doi.org/10.1016/j.applthermaleng.2018.09.017>
34. Meyer, M.K., Fielding, R., Gan, J., 2007. Fuel development for gas-cooled fast reactors. *J. Nucl. Mater.* 371, 281–287. <https://doi.org/10.1016/j.jnucmat.2007.05.013>
35. Montgomery, D.C., Peck, E.A., Vining, G.G., 2013. *Introduction to Linear Regression Analysis*. John Wiley & Sons, Inc.
36. Nabielek, H., Kühnlein, W., Schenk, W., Heit, W., Christ, A., Ragoss, H., 1990. Development of advanced HTR fuel elements. *Nucl. Eng. Des.* 121, 199–210. [https://doi.org/10.1016/0029-5493\(90\)90105-7](https://doi.org/10.1016/0029-5493(90)90105-7)
37. Nazari, M., Jalali Vahid, D., Saray, R.K., Mahmoudi, Y., 2017. Experimental investigation of heat transfer and second law analysis in a pebble bed channel with internal heat generation. *Int. J. Heat Mass Transf.* 114, 688–702. <https://doi.org/10.1016/j.ijheatmasstransfer.2017.06.079>
38. Neideen, T., Brasel, K., 2007. Understanding Statistical Tests. *J. Surg. Educ.* 64, 93–96. <https://doi.org/10.1016/j.jsurg.2007.02.001>
39. Neill, J.W., Johnson, D.E., 1984. Testing For Lack Of Fit In Regression - A Review. *Commun. Stat. - Theory Methods* 13, 485–511. <https://doi.org/10.1080/03610928408828696>
40. Ostertagová, E., 2012. Modelling using polynomial regression. *Procedia Eng.* 48, 500–506. <https://doi.org/10.1016/j.proeng.2012.09.545>
41. Ranz, W.E., 1952. Friction and Transfer Coefficients for Single Panicles and Packed Beds. *Chem. Eng. Prog.* 48, 247–253.
42. Rimkevičius, S., Uspuras, E., 2008. Experimental investigation of pebble beds thermal hydraulic characteristics. *Nucl. Eng. Des.* 238, 940–944. <https://doi.org/10.1016/j.nucengdes.2007.08.001>
43. Rimkevicius, S., Vilemas, J., Uspuras, E., 2006. Experimental investigation of heat transfer and flow mixing in pebble beds. *Heat Transf. Eng.* 27, 9–15. <https://doi.org/10.1080/01457630600793939>
44. SAS, I. inc, 2021. JMP.

45. Schröder, E., Class, A., Krebs, L., 2006. Measurements of heat transfer between particles and gas in packed beds at low to medium Reynolds numbers. *Exp. Therm. Fluid Sci.* 30, 545–558. <https://doi.org/10.1016/j.expthermflusci.2005.11.002>
46. Taha, M.M., Said, I.A., Usman, S., Al-Dahhan, M.H., 2018. Natural convection inside heated channel of a facility representing prismatic modular reactor core. *AIChE J.* 64, 3467–3478. <https://doi.org/10.1002/aic.16185>
47. Wakao, N., S, K., 1982. *Heat and Mass Transfer in Packed Beds*. Gordon and Breach Science Publishers Ltd., Paris.
48. Wu, C., Al-Dahhan, M.H., Prakash, A., 2007. Heat transfer coefficients in a high-pressure bubble column. *Chem. Eng. Sci.* 62, 140–147. <https://doi.org/10.1016/j.ces.2006.08.016>
49. Wu, Z., Lin, D., Zhong, D., 2002. The design features of the HTR-10. *Nucl. Eng. Des.* 218, 25–32. [https://doi.org/10.1016/S0029-5493\(02\)00182-6](https://doi.org/10.1016/S0029-5493(02)00182-6)
50. Yamoah, S., Akaho, E.H.K., Ayensu, N.G.A., Asamoah, M., 2012. Analysis of fluid flow and heat transfer model for the pebble bed high temperature gas cooled reactor. *Res. J. Appl. Sci. Eng. Technol.* 4, 1659–1666.

## SECTION

### 3. CONCLUSIONS

The first paper investigated the local velocity of the gas flowing within the pebble bed reactor (PBR). For the first time, a sophisticated hot wire anemometry (HWA) technique was used, which was supported with a novel probe-protector case that protected the probe, allowing the measurements to be gained at various locations in a long pebble bed with a pebble diameter of 5 cm and an aspect ratio of 6. A second-order polynomial correlation was developed to predict the local gas velocity at the fully developed region of the bed within the experimental range. Thus, the work obtained new benchmark data with high-accuracy results for local gas velocities inside the PBR.

The second paper involved an investigation of the local heat transfer coefficients between the pebbles and the coolant gas in a PBR using a sophisticated measurement technique that consists of a heated pebble probe, a micro-foil heat flux sensor flushed mounted on the surface of the heated pebble probe, and a thermocouple in the center of bed void in front the sensor. Therefore, local heat transfer coefficients were measured at various axial, radial, and angular locations with superficial gas velocities covering both laminar and turbulent flow conditions. Furthermore, a pseudo-3D correlation was developed and found to provide accurate predictions, with an averaged absolute relative error (AARE) of 3.33% at high Reynolds numbers of our operation and design conditions.

In the third paper, the effect of increasing the effect of location inside the pebble bed while orienting the probe pebble angularity during interaction with the coolant gas. An advanced technique consisting of a probe pebble, a micro-foil sensor, and a thermocouple

probe was used to obtain accurate measurements of the local heat transfer coefficients. A second-order polynomial model using dimensionless parameters such as Nusselt's number (Nu) from experimental data was then compared with the empirical correlations available in the literature. Therefore, the accurate data of gas velocity measurements of local heat transfer obtained in this study can serve as benchmark data for validating numerical models such as CFD simulations coupled with heat transfer calculations.

## BIBLIOGRAPHY

- I. M. Daniel, O. Ishai, I. M. Daniel, and I. Daniel, *Engineering mechanics of composite materials*. Oxford university press New York, 1994.
- Koster, A., Matzner, H. D., and Nicholsi, D. R., (2003). "PBMR design for the future." *Nuclear Engineering and Design* 222: 231–245.
- Abdulmohsin, R. (2013). Gas dynaimcs and heat transfer in a packed pebble-bed reactor for the 4th generation nuclear energy. PhD, Missouri University S&T.
- Mahmoud, Taha (2017) Experimental investigations of natural circulation in a separate-and-mixed effects test facility mimicking prismatic modular reactor (PMR) core PhD, Missouri University S&T.
- Aung, W. (1972). "Fully developed laminar free convection between vertical plates heated asymmetrically." *International Journal of Heat and Mass Transfer* 15(8): 1577-1580.
- Aung, W., L. S. Fletcher and V. Sernas (1972). "Developing laminar free convection between vertical flat plates with asymmetric heating." *International Journal of Heat and Mass Transfer* 15(11): 2293-2308.
- Badr, H. M., M. A. Habib, S. Anwar, R. Ben-Mansour and S. A. M. Said (2006). "Turbulent natural convection in vertical parallel-plate channels." *Heat and Mass Transfer/Waerme- und Stoffuebertragung* 43(1): 73-84.
- Bejan, A. and J. L. Lage (1990). "Prandtl number effect on the transition in natural convection along a vertical surface." *Journal of Heat Transfer* 112(3): 787-790.
- Celataa, G. P., F. Dannibale, A. Chiaradia and M. Cumo (1998). "Upflow turbulent mixed convection heat transfer in vertical pipes." *International Journal of Heat and Mass Transfer* 41(24): 4037-4054
- Beck, J. M., Pincock, L. F., (2011). High Temperature Gas-Cooled Reactors Lessons Learned Applicable to the Next Generation Nuclear Plant, Idaho National Laboratory.
- Jackson, R. B., E. Smith and B. G. Woods (2009). FLUENT modeling for heat transfer in upper plenum of VHTR. Transactions of the American Nuclear Society.

- Jaluria, Y. and B. Gebhart (1974). "On transition mechanisms in vertical natural convection flow." *Journal of Fluid Mechanics* 66: 309-337.
- Doug Chapin, S. K., and Jim Nestell (2004). *The very high temperature reactor: A technical summary*, MPr Associates, Inc.

## VITA

Muhna Nazal Alshammari was born in Saudi Arabia. He earned his bachelor's degree in 2008 from the University of Toledo, OH. in Electrical Engineering. Augst, 2014, he received his master's degree in nuclear engineering from Missouri University of Science and Technology (Missouri S&T). He continued at Missouri S&T to pursue his Doctor Philosophy (Ph.D.) in nuclear engineering. He was funded by King Abdulaziz City for Science and Technology (KACST) in Saudi Arabia. His research involved experimentally investigation of heat transfer and local gas dynamics in a pebble bed very high-temperature nuclear reactor using advanced measurement techniques heat. In May 2023 he received a Ph.D. in nuclear engineering from Missouri S&T. He worked in several companies such as ARAMCO, ABB, and lates in KACST.